



Universidad de Navarra

Facultad de Farmacia y Nutrición

Departamento de Tecnología y Química Farmacéuticas

TESIS DOCTORAL

**Development of three-dimensional biomaterials
containing stem cells and neurotrophic factors
for brain repair in Parkinson's disease**

Pablo Vicente Torres Ortega

Pamplona, 2021



Universidad de Navarra

Facultad de Farmacia y Nutrición

Departamento de Tecnología y Química Farmacéuticas

TESIS DOCTORAL

Development of three-dimensional biomaterials containing stem cells and neurotrophic factors for brain repair in Parkinson's disease

Trabajo presentado por Pablo Vicente Torres Ortega para aspirar al grado de

Doctor en Farmacia por la Universidad de Navarra

Fdo. Pablo Vicente Torres Ortega

Pamplona, 2021



Universidad de Navarra

Facultad de Farmacia y Nutrición

Departamento de Tecnología y Química Farmacéuticas

Doña **MARÍA BLANCO PRIETO**, Catedrática de la Universidad de Navarra y Profesora Investigadora del Departamento de Tecnología y Química Farmacéuticas y Doña **ELISA GARBAYO ATIENZA**, Profesora contratada doctora de la Universidad de Navarra y Profesora Investigadora del Departamento de Tecnología y Química Farmacéuticas,

Certifican:

Que el presente trabajo, titulado “Development of three-dimensional biomaterials containing stem cells and neurotrophic factors for brain repair in Parkinson's disease”, presentado por PABLO VICENTE TORRES ORTEGA para optar al grado de Doctor en Farmacia, ha sido realizado bajo su dirección en el Departamento de Tecnología y Química Farmacéuticas de la Universidad de Navarra. Considerando finalizado el trabajo autorizan su presentación a fin de que pueda ser juzgado y calificado por el Tribunal correspondiente.

Y para que así conste, firman la presente:

Prof. María Blanco Prieto

Prof. Elisa Garbayo Atienza

Pamplona, 14 de Octubre de 2021

Las investigaciones realizadas en el presente trabajo se han desarrollado gracias a la financiación recibida a través del Gobierno de Navarra (2019_66_NAB9).

Asimismo, agradezco al Ministerio de Educación y Formación profesional por la beca predoctoral para la formación de profesorado universitario (FPU17/01212) y a la Asociación de Amigos de la Universidad de Navarra por la ayuda predoctoral para la elaboración de la tesis y la obtención del grado de doctor.

A mis padres, María del Rosario y José María.

AGRADECIMIENTOS

Me gustaría aprovechar estas líneas para expresar mi más sincero agradecimiento a todas las personas que han hecho posible esta tesis doctoral. En primer lugar, quisiera agradecer a la Universidad de Navarra y a la Facultad de Farmacia y Nutrición la oportunidad de realizar esta tesis doctoral en el Departamento de Tecnología y Química Farmacéuticas. Gracias a la Asociación de Amigos de la Universidad de Navarra, al Ministerio de Universidades y al Gobierno de Navarra por la ayuda económica recibida durante estos años de formación.

Gracias a mis directoras de tesis, María Blanco y Elisa Garbayo, por el tiempo y la confianza depositada en mí, por transmitirme su entusiasmo por la ciencia y por su comprensión e inestimable ayuda. Ha sido un honor trabajar junto a vosotras. Gracias a los profesores Eduardo Ansorena, Cristian Smerdou, Jacobo Paredes, Javier Aldazabal, Daniel Plano, Charo Luquín y Carmen Sanmartin por vuestra disponibilidad, colaboración, asesoramiento y por todo lo que me habéis enseñado. Mi agradecimiento, también, a la unidad de Neuroproteómica clínica de Navarrabiomed, y especialmente a Enrique Santamaría por la ayuda prestada.

Gracias a los doctores y profesores del Departamento de Tecnología y Química farmacéuticas: Dra. Conchita Tros, Dr. Juan Manuel Irache, Dr. Iñaki Fernández de Trocóniz, Dra. M^a Jesús Garrido, Dr. Silvia Vela, Dr. Fernando Martínez, Dña. María Huici, Dra. Socorro Espuelas y Dra. Maribel Calvo.

Gracias a Diego, Nico, Ricardo, Aymara, Tania, Sara, Rubén, Paula, Souhaila, Alejandro, Hugo, Jaime, Maite y Carmen, por esos ratos de café tan divertidos y entrañables. Gracias también a Alba, Cristina, Raquel, Esther, Cristian, Jorge y Silvia por contribuir día a día a crear a un entorno de trabajo agradable, amigable y ejemplar. Gracias Hugo por tu sentido del humor y por haberme hecho la vida más fácil en el laboratorio. Gracias a mis compañeros de grupo, Laura, Carlos y Souhaila por vuestra ayuda, por vuestro apoyo, y por poder haber compartido junto a vosotros este duro camino.

Gracias a mis grandes amigos, Pablo, Javi Mateo, Perico, Enrique, Gonzalo, Edu, Juancar y Aurelio por su apoyo y por haberme ayudado a crecer como persona en momentos importantes de mi vida.

Gracias a mi familia. A mi compañera de viaje, Lucía, por su apoyo incondicional, su paciencia y su cariño, por hacerme sonreír cada día y estar siempre a mi lado.

A mi abuela Antonia, que desde el cielo me cuida y me da la fuerza necesaria para superarme cada día. A mis hermanos José María y Macarena, por estar siempre a mi lado.

Gracias a mis padres, porque es gracias a ellos por quienes estoy aquí y soy quien soy, por su cariño y comprensión, no hay suficientes palabras para mostraros mi agradecimiento.

De corazón,

Gracias a todos.

“Lo esencial es invisible a los ojos”

Antoine de Saint-Exupéry

LIST OF PUBLICATIONS

- I. P. V. Torres-Ortega, L. Saludas, A. S. Hanafy, E. Garbayo, M. J. Blanco-Prieto. Micro- and nanotechnology approaches to improve Parkinson's disease therapy, *Journal of Controlled Release*. 2019;201–213. <https://doi.org/10.1016/j.jconrel.2018.12.036>
- II. P. V. Torres-Ortega, I. Martínez-Valbuena, G. Martí-Andrés, A. S. Hanafy, M. R. Luquin, E. Garbayo, M. J. Blanco-Prieto, Nanobiotechnology in Neurodegenerative Diseases. Springer International Publishing. 2019, pp. 177–208. https://doi.org/10.1007/978-3-030-30930-5_7.
- III. P. V. Torres-Ortega, C. Smerdou, E. Ansorena, M. C. Ballesteros-Briones, E. Martisova, E. Garbayo, M. J. Blanco-Prieto, Optimization of a GDNF production method based on Semliki Forest virus vector. *European Journal Pharmaceutical Sciences*. 2021, 159, 105726. <https://doi.org/10.1016/j.ejps.2021.105726>.
- IV. P. V. Torres-Ortega, D. Plano, J. Paredes-Puente, J. Aldazabal, Rosario-Luquin, C. Sanmartin, M. J. Blanco-Prieto, E. Garbayo. Encapsulation of hMSCs and hGDNF in a novel injectable nanoreinforced-hydrogel to improve cell replacement therapy in Parkinson's Disease. (Under review).
- V. P. V. Torres-Ortega, L. Saludas, J. Eneko, C. Rodríguez-Nogales, E. Garbayo, M. J. Blanco-Prieto, Nanoparticles for Brain Drug Delivery. *Jenny Stanford Publishing*. 2021, pp.189-210. <https://doi.org/10.1201/9781003119326>.

TABLE OF CONTENTS

ABBREVIATIONS	1
FOREWORD.....	5
Hydrogel-based therapies for neural protection and functional rewiring in Parkinson’s Disease.....	5
INTRODUCTION	15
Nanobiotechnology in Parkinson’s Disease	17
Micro- and nanotechnology approaches to improve Parkinson’s Disease therapy	55
HYPOTHESIS AND OBJECTIVES	95
CHAPTER 1	99
Optimization of a GDNF production method based on Semliki Forest virus vector	101
CHAPTER 2	123
Transcriptome analysis of hiPS-DANs after hGDNF stimulation	125
Encapsulation of hMSCs and hGDNF in a novel injectable nanoreinforced-hydrogel to improve cell replacement therapy in Parkinson’s Disease	145
GENERAL DISCUSSION	187
CONCLUSIONS	223
ANNEXES	227
ANNEX 1	229

ABBREVIATIONS

AD	Alzheimer's disease
APS	Atypical parkinsonism syndrome
ATCC	American Type Culture Collection
BBB	Brain-blood barrier
BDNF	Brain-derived neurotrophic factor
bFGF	Basic fibroblast growth factor
BHK-21	Baby hamster kidney cell line
BPN	Brain-penetrating nanoparticles
BSCB	Blood-spinal barrier
CD	Cyclodextrin
CD-Tos	6- <i>O</i> -monotosyl-6-deoxy- β -cyclodextrin
CHO	Chinese hamster ovary cells
CNS	Central nervous system
COMT	Catechol-O-methyltransferase
CQD	Carbon quantum dots
CSF	Cerebrospinal fluid
CT	Computed Tomography
CTS	Chitosan
DAns	Dopaminergic neurons
DaT	Dopamine transporter
DLS	Dynamic light scattering
DMSO	Dimethyl sulfoxide
DPA	Dendrigraft poly-L-lysine-polyethyleneglycol-angiopep
DRT	Dopamine replacement therapy
EPO-FC	Erythropoietin fusion protein
FBS	Fetal bovine serum
FDA	Food and drug administration
FUS	Focused ultrasound
GBD	Global Burden of Disease

GFP	Green fluorescent protein
GLNs	Gelatin nanostructured lipid carriers
GMO	Glyceryl monooleate
GMP	Good manufacturing practice
GSEA	Gene Set Enrichment Analysis
HA	Hyaluronic acid
HA-HG	Hyaluronic Hydrogel
HG	Hydrogel
hGDNF	Human Glial Cell Line-derived Neurotrophic Factor
hiPS-DAns	Dopaminergic neurons derived from human induced pluripotent stem cells
hMSCs	Human Mesenchymal Stem Cells
HRP	Horseradish peroxidase
HUVECs	Human umbilical cord endothelial cells
IGFBPs	Insulin like growth factor binding proteins
IMR	Immunomagnetic reduction
LBs	Lewy bodies
LPS	Lipopolysaccharide
MAO-B	Monoamine oxidase isoform B
MAPK	Mitogen-activated protein kinase
MBs	Microbubbles
MPs	Microparticles
MPTP	1-methyl-4-phenyl-1,2,3,6-tetrahydropyridine
MRI	Magnetic Resonance Imaging
nBSA	Native bovine serum albumin
NFH	Non-Fe Hemin
NGF	Nerve growth factor
NIPAm-AA	N-isopropylacrylamide derivative
NLC	Nanostructured lipid carrier
NTFs	Neurotrophic factors
NPs	Nanoparticles
NTA	Nanoparticle Tracking Analysis
PAA	Poly(amidoamine)
PD	Parkinson's Disease

PDD	Parkinson disease dementia
PDI	Polydispersity index
PEG	Polyethylene glycol
PLA	Poly(lactide)
PLGA	Poly-lactic-co-glycolic acid
PLK2	Polo like kinase 2
PLs-GDNF-MBs	GDNF plasmid-loaded PEGylated liposomes
PMPC	Poly(2-methacryloyloxyethyl) phosphorylcholine
PNIPAM	Poly(N-isopropylacrylamide)
PS80	Polysorbate 80
PVA	Polyvinyl alcohol
ROS	Reactive species oxygen
RW	Residual weight
SA-NC	Schisantherin A
SD	Standard deviation
SEM	Scanning electron microscope
sFIDA	Surface-based fluorescence intensity distribution analysis assay
SFV	Semliki forest virus
ShRNA	Short hairpin RNA
SiRNA	Synuclein small interfering RNA
SLN	Solid lipids nanoparticles
SP	Substance P
SPIONs	Superparamagnetic iron oxide nanoparticles
SUMO	Small ubiquitin-related modifier
TAT	Transactivator of transcription
TEA	Triethylamine
TH	Tyrosine hydroxylase
TROMS	Total recirculation One-Machine System
Ts₂O	<i>p</i> -toluensulfonic anhydride
VEGF	Vascular endothelial growth factor
6-OHDA	6-hydroxydopamine
[¹²³I]MIBG-SPECT	Iodine-123–labeled metaiodobenzylguanidine single-photon emission computed tomography
[¹⁸F] FDG-PET	¹⁸ F-fluorodeoxyglucose positron emission tomography

FOREWORD

Hydrogel-based therapies for neural protection and functional rewiring in Parkinson's disease

Parkinson's disease (PD) has an enormous impact on society and is considered one of the commonest and most important neurodegenerative diseases in the world. According to the last Global Burden of Disease, Injuries, and Risk Factors Study (GBD), neurological disorders are now the leading source of disability globally and PD was the fastest growing in prevalence, disability and deaths, from 1990 to 2015 (1). This neurodegenerative disorder is characterized by the progressive loss of dopaminergic neurons in the substantia nigra pars compacta and the abnormal accumulation and aggregation of α -Synuclein in the form of Lewy bodies (LBs) (2–4) (Figure 1). The discovery of new drugs and advanced therapies able to halt PD progression represents an uphill battle for modern medicine (5,6). The latest advances in protein and stem cell therapies have led to a growing interest in their potential as disease-modifying therapies for PD (7). However, the development of these therapies is still in its infancy with some challenges requiring further investigation.

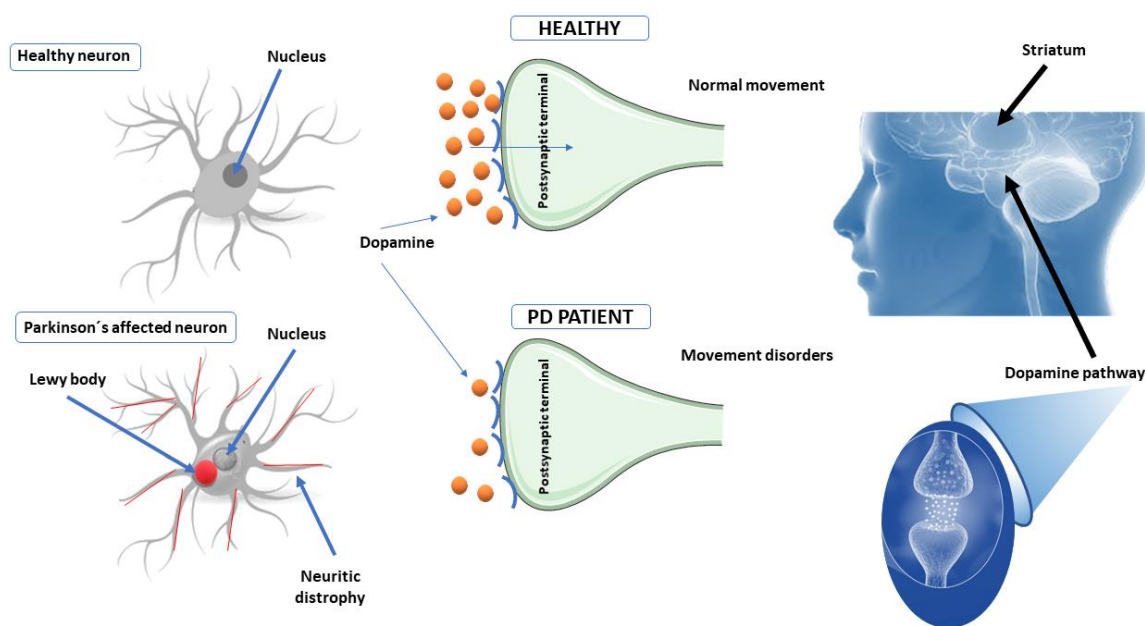


Figure 1. Normal and Parkinson's disease-affected neuron. Impaired dopamine metabolism, presence of LBs and neuritic dystrophy in Parkinson's disease-affected neurons.

Cell transplant-based treatments provide an enormous potential for the management of PD (8). In this context, cell implantation through a systemic intravascular route (intravenous or intra-arterial) has been proposed in several animal models and brain injury patients (8). Systemic administration is feasible and less invasive than cerebral implantation. However, this route is hampered by the limited mobilization of therapeutic cells from the blood towards the brain tissue (8). Particularly, the central nervous system

FOREWORD

(CNS) is separated from the circulating blood by two highly selective barriers: the blood-brain barrier (BBB) and the blood-spinal barrier (BSCB). These barriers are formed by tight junctions between the extracellular membranes of endothelial cells and astrocytes. Under normal physiological conditions, few molecules can passively pass from the circulating blood to the CNS extracellular fluid (9). As a result, only a small number of cells reaches the brain and crosses the BBB.

Brain implantation, albeit the most invasive approach, is the most promising strategy. This route offers the possibility of grafting therapeutic cells directly onto the lesioned area (8,10–12). However, such strategies have shown reduced engraftment temporality, poor cell survival rate, as well as dispersal to regions far from the area of interest, which limits therapeutic effect (8,13). They pose a number of challenges for various reasons:

- The injury to the brain tissue implies a hostile microenvironment for the brain itself and the cell graft limiting its survival to a few weeks after implantation (8,11,12).
- The scarcity or absence of survival factors, coupled with cell death signals triggered by reactive astrocytes, microglia and peripheral leukocytes, is capable of extending the brain tissue injury to perilesional areas (8).

On the other hand, therapeutic proteins, cytokines and growth factors have also been administered directly into the injured zone to enhance the stimulation of endogenous and exogenous stem cells (5,14). However, this approach is limited by a deficient control of drugs/factors kinetics at effective doses after cerebral administration and low survival/engraftment of transplanted cells (5).

These handicaps could be overcome through “advanced biomaterials” that provide a structural and functional matrix with stiffness modules in the range of the soft tissues such as the brain (8). The latest advances in biomaterial technologies support the regeneration of a range of tissues (15,16). Between new techniques and advances in biomaterial design, hydrogels (HGs) open new therapeutic strategies thanks to their ability to promote neuronal alignment, neuronal growth, and brain repair (17).

Importantly, exogenous stem cells and various drugs/compounds could be simultaneously included in these scaffolds to achieve functional recovery (18,19).

Specifically, HGs provide a natural aqueous environment, which is very attractive for controlled drug delivery of proteins, but also as a scaffold to deliver cells (20). Furthermore, HGs can be functionalized with different molecules to tailor and improve their mechanical properties according to specific applications (e.g., stimuli-responsive, degradable, highly or lightly crosslinked, higher or lower stiffness, etc) (20). Notably, these biomaterials can be made under mild reaction conditions without disrupting the encapsulated agents (20). In this sense, different natural and synthetic hydrogels have been explored for cell/drug delivery applications into the brain, including hyaluronan (HA), chitosan, collagen, silk fibroin, isopropylacrylamide, methylcellulose, alginate, Matrigel, poly-lactic-co-glycolic acid (PLGA) or polyethylene glycol (PEG) (5,21,22). Each material presents its advantages and disadvantages. However, none of these composites fulfils all the properties of a tissue substitute. Under these circumstances, it seems more likely that the production of tissue substitutes that meet all clinical requirements will come from scaffolds made from a combination of natural and synthetic biopolymers (23). Inherently, these systems take advantage of the cross-linked HG layer to allow the diffusion of small molecules and solutes, excluding larger molecules, such as antibodies and proteases. This particularity of HGs is especially relevant to avoid immunological rejection and/or degradation of biological agents (5). In parallel, the 3D structure allows the flow of oxygen/nutrients. Moreover, their porous structure creates a restrictive barrier against inflammatory cells present in the injured area. Together, these properties contribute to improve the survival of the grafted cells and to promote functional rewiring in damaged areas (Figure 2) (5). Previous studies in PD animal models position drug and cell delivery approaches as highly promising strategies (5,18,19). In the PD framework, neurotrophic factors (NTFs), such as the brain-derived neurotrophic factor (BDNF) or the glial cell line-derived neurotrophic factor (GDNF) together with embryonic stem cell-derived dopaminergic neurons (DAns), have been included in HGs of different nature obtaining satisfactory results (5,18,24). Therefore, HGs vehicles, in which proteins and cells can be combined, could be powerful systems for brain tissue repair (20).

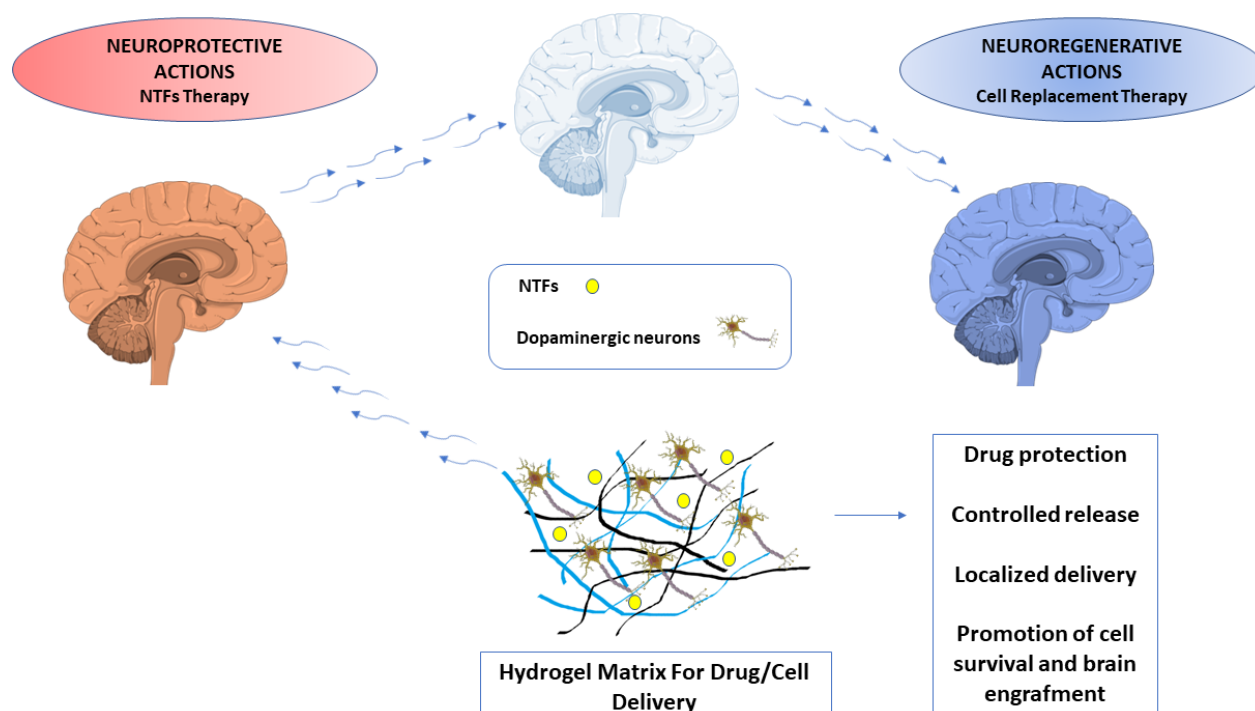


Figure 2. Hydrogel scaffolds for drug/cell delivery in the brain. Advantages of simultaneous encapsulation of NTFs and dopaminergic neurons on HGs and its potential actions.

In this PhD thesis, we aimed to develop a therapeutic tool in which NTFs, cell replacement therapies and drug delivery systems (nanoparticles (NPs) and HGs) are combined to bring about significant improvements in the treatment of the second most common neurodegenerative disease.

Therapeutical management of PD is predominantly focused on controlling motor symptoms and there is no gold standard treatment strategy. Consequently, the medical treatment is tailored to each patient, based on the severity of their symptoms and the adverse effects associated with their medication. Unfortunately, the available therapies provide temporary relief of symptoms but are unable to reverse and halt the disease progression (3,25).

In the light of this situation, this thesis addresses the development of a PD-modifying therapy where stem cells and hGDNF are included in a nanoparticle-modified HG. To this end, the following challenges were investigated:

- 1) The production of clinical-grade therapeutic hGDNF to provide appropriate post-translational modifications and to solve the safety issues related to the immune response (Chapter 1).
- 2) The assessment of hGDNF potential to modulate the gene expression profile of two cell types with potential for clinical use in PD: Dopaminergic neurons derived from human induced pluripotent stem cells (hiPS-DANs) and human mesenchymal stem cells (hMSCs). (Chapter 2)
- 3) The development and characterization of an original drug delivery system for brain tissue engineering, where hGDNF and hMSCs are rationally combined into a nanoreinforced HG for their simultaneous administration into the brain (Chapter 2).

In the introduction, some of the most encouraging nanotechnology advances for PD application are summarized and discussed. First, the etiology and the pathological hallmarks of PD are described and the limitations of current diagnostic and treatment strategies are discussed. Then, a comprehensive review of the latest nanotechnology advances for both the diagnosis and treatment of PD is provided. In the second part, different micro- and nanotechnology systems that have been explored to date for the administration of potential drugs for PD therapy are presented, including antioxidant molecules, neurotrophic factors, and gene therapies. Particular attention paid to the nature of particles, the delivery route and the therapeutic agent. Finally, the current limitations and challenges of micro and nanotechnologies for PD therapy are discussed. The experimental section is divided into two chapters. The first experimental section presents a novel biphasic temperature cultivation protocol to improve the expression of hGDNF with a high degree of purity and a specific glycosylation pattern.

In these experiments, an RNA vector was electroporated into the baby hamster kidney cell line (BHK-21) and the electroporated cells were incubated at 37°C or 33°C with 5% CO₂. A significant improvement in cell survival and hGDNF expression was demonstrated with the increase in the temperature from 33°C to 37 °C during the “shut-off period”. In consonance, this protocol led to the production of almost 3-fold more hGDNF when compared to the previously described methods.

FOREWORD

Subsequently, in the second chapter, the potential of hGDNF to induce changes in the transcriptome of two cell types with potential for clinical use in PD (hiPS-DANs and hMSCs) was evaluated. The observed effects suggest that this neurotrophic factor can stimulate the expression of genes involved in neuronal plasticity and neurogenesis in both cell types. Next, the neurotrophic factor was successfully encapsulated in polymeric NPs to be subsequently included in a HA-HG modified with adamantane (AD) and cyclodextrin (CD). In this section, the mechanical properties of this scaffold were investigated. Then, the neural compatibility of the system was studied on PC12 cells and its compatibility with the hMSCs cell line was explored. Regarding mechanical properties, the developed biomaterial demonstrated shear-thinning and self-healing features. Moreover, the NPs incorporation into the HG allowed a more sustained hGDNF release profile, as well as a significant reduction of drug release at two weeks (25% vs 36%). Importantly, this scaffold provided an ideal environment for PC12 and hMSCs. In summary, the suitable strength, excellent self-healing properties and good biocompatibility make this HG a good candidate to administer drugs and cells for brain repair applications.

Finally, a comprehensive perspective on the different hypotheses set forth in this thesis as well as their scientific contribution to the brain regenerative field is provided in the General Discussion. Overall, this thesis reflects cutting-edge trends in brain regeneration and neuroprotection in the PD arena, harnessing the enormous potential of drug delivery systems and cell replacement therapies to overcome the current challenges in the field.

REFERENCES

1. Ray Dorsey E, Elbaz A, Nichols E, Abd-Allah F, Abdelalim A, Adsuar JC, et al. Global, regional, and national burden of Parkinson's disease, 1990–2016: a systematic analysis for the Global Burden of Disease Study 2016. *Lancet Neurol.* 2018;17(11):939–53.
2. Gómez-Benito M, Granado N, García-Sanz P, Michel A, Dumoulin M, Moratalla R. Modeling Parkinson's Disease With the Alpha-Synuclein Protein. *Front Pharmacol.* 2020 Apr 23;11.
3. Torres-Ortega PV, Martínez-Valbuena I, Martí-Andrés G, Hanafy AS, Luquin MR, Garbayo E, et al. Nanobiotechnology in Parkinson's Disease. In: *Nanobiotechnology in Neurodegenerative Diseases*. Springer International Publishing; 2019. p. 177–208.
4. Del Rey NLG, Quiroga-Varela A, Garbayo E, Carballo-Carbajal I, Fernández-Santiago R, Monje MHG, et al. Advances in parkinson's disease: 200 years later. *Front Neuroanat.* 2018 Dec 14;12:113.
5. Fernandez-Serra R, Gallego R, Lozano P, González-Nieto D. Hydrogels for neuroprotection and functional rewiring: A new era for brain engineering. *Neural Regen Res.* 2020 May 1;15(5):783–9.
6. Torres-Ortega PV, Saludas L, Hanafy AS, Garbayo E, Blanco-Prieto MJ. Micro- and nanotechnology approaches to improve Parkinson's disease therapy. *J Control Release.* 2019 Feb 10;295:201–13.
7. Sakthiswary R, Raymond AA. Stem cell therapy in neurodegenerative diseases: From principles to practice. *Neural Regen Res.* 2012 Aug 15;7(23):1822–31.
8. González-Nieto D, Fernández-García L, Pérez-Rigueiro J, Guinea G V., Panetsos F. Hydrogels-assisted cell engraftment for repairing the stroke-damaged brain: Chimera or reality. *Polymers (Basel).* 2018 Feb 13;10(2).
9. Khaing ZZ, Thomas RC, Geissler SA, Schmidt CE. Advanced biomaterials for repairing the nervous system: What can hydrogels do for the brain? *Mater Today.* 2014 Sep 1;17(7):332–40.
10. Wang Y, Zhao Z, Rege S V., Wang M, Si G, Zhou Y, et al. 3K3A-activated protein C stimulates postischemic neuronal repair by human neural stem cells in mice. *Nat Med.* 2016 Sep 1;22(9):1050–5.
11. Tuladhar A, Morshead CM, Shoichet MS. Circumventing the blood-brain barrier: Local delivery of cyclosporin A stimulates stem cells in stroke-injured rat brain. *J Control Release.* 2015 Aug 5;215:1–11.
12. Mora-Lee S, Sirerol-Piquer MS, Gutiérrez-Pérez M, Gomez-Pinedo U, Roobrouck VD, López T, et al. Therapeutic Effects of hMAPC and hMSC Transplantation after Stroke in Mice. *PLoS One.* 2012 Aug 31;7(8):e43683.
13. Wang Y, Tan H, Hui X. Biomaterial scaffolds in regenerative therapy of the central nervous system. *Biomed Res Int.* 2018;2018.

FOREWORD

14. Bondarenko O, Saarma M. Neurotrophic Factors in Parkinson's Disease: Clinical Trials, Open Challenges and Nanoparticle-Mediated Delivery to the Brain. *Front Cell Neurosci.* 2021 Jun 2;15:178.
15. Langer R, Vacanti J. Advances in tissue engineering. *J Pediatr Surg.* 2016 Jan 1;51(1):8–12.
16. Saludas L, Pascual-Gil S, Prósper F, Garbayo E, Blanco-Prieto M. Hydrogel based approaches for cardiac tissue engineering. *Int J Pharm.* 2017 May 25;523(2):454–75.
17. Cangellaris O V., Gillette MU. Biomaterials for enhancing neuronal repair. In: *Frontiers in Materials.* Frontiers Media S.A.; 2018. p. 21.
18. Wang TY, Bruggeman KF, Kauhausen JA, Rodriguez AL, Nisbet DR, Parish CL. Functionalized composite scaffolds improve the engraftment of transplanted dopaminergic progenitors in a mouse model of Parkinson's disease. *Biomaterials.* 2016 Jan;74:89–98.
19. Carballo-Molina OA, Sánchez-Navarro A, López-Ornelas A, Lara-Rodarte R, Salazar P, Campos-Romo A, et al. Semaphorin 3C Released from a Biocompatible Hydrogel Guides and Promotes Axonal Growth of Rodent and Human Dopaminergic Neurons. *Tissue Eng Part A.* 2016;22(11–12):850–61.
20. Pérez-Luna V, González-Reynoso O. Encapsulation of Biological Agents in Hydrogels for Therapeutic Applications. *Gels.* 2018 Jul 11;4(3):61.
21. Potjewyd G, Moxon S, Wang T, Domingos M, Hooper NM. Tissue Engineering 3D Neurovascular Units: A Biomaterials and Bioprinting Perspective. *Trends Biotechnol.* 2018 Apr 1;36(4):457–72.
22. Kornev VA, Grebenik EA, Solovieva AB, Dmitriev RI, Timashev PS. Hydrogel-assisted neuroregeneration approaches towards brain injury therapy: A state-of-the-art review. *Comput Struct Biotechnol J.* 2018 Jan 1;16:488–502.
23. Reddy MSB, Ponnamma D, Choudhary R, Sadasivuni KK. A comparative review of natural and synthetic biopolymer composite scaffolds. *Polymers (Basel).* 2021 Mar 30;13(7):1105.
24. Ucar B, Humpel C. Therapeutic efficacy of glial cell-derived neurotrophic factor loaded collagen scaffolds in ex vivo organotypic brain slice Parkinson's disease models. *Brain Res Bull.* 2019 Jul 1;149:86–95.
25. Bloem BR, Okun MS, Klein C. Parkinson's disease. *Lancet.* 2021 Jun 12;397(10291):2284–303.

INTRODUCTION

Nanobiotechnology in Parkinson`s Disease

Pablo Vicente Torres-Ortega¹, Iván Martínez-Valbuena^{2,5}, Gloria Martí-Andrés^{2,5}, Amira Sayed Hanafy^{3,4}, María Rosario Luquin^{2,5} Elisa Garbayo^{1,5*}, María José Blanco-Prieto^{1,5*}

¹Department of Pharmaceutical Technology and Chemistry, Faculty of Pharmacy and Nutrition, Universidad de Navarra, C/ Irunlarrea 1, 31008 Pamplona, Spain

²Department of Neurology and Neurosciences, Centro de Investigación Médica Aplicada and Clínica Universidad de Navarra, Pamplona, Spain.

³Department of Pharmaceutics and Pharmaceutical Technology, Faculty of Pharmacy and Drug Manufacturing, Pharos University in Alexandria (PUA), Alexandria, Egypt

⁴Department of Pharmacy, Ludwig-Maximilians-Universität München, Munich, Germany

⁵Instituto de Investigación Sanitaria de Navarra, IdiSNA, C/ Irunlarrea 3, 31008 Pamplona, Spain

* Corresponding authors at: Department of Pharmaceutical Technology and Chemistry, Faculty of Pharmacy and Nutrition, Universidad de Navarra, C/Irunlarrea 1,31008 Pamplona, Spain.

E-mail addresses: egarbayo@unav.es (E. Garbayo), mjblanco@unav.es (M.J. Blanco-Prieto).

Springer International Publishing, 2019: pp. 177–208.

Micro- and nanotechnology approaches to improve parkinson's disease therapy

Pablo Vicente Torres-Ortega^{1,2}, Laura Saludas^{1,2}, Amira Sayed Hanafy³, Elisa Garbayo^{1,2,*}
and María José Blanco-Prieto^{1,2,*}

¹ Department of Pharmaceutical Technology and Chemistry, Faculty of Pharmacy and Nutrition, Universidad de Navarra, C/ Irunlarrea 1, 31008 Pamplona, Spain

² Instituto de Investigación Sanitaria de Navarra, IdiSNA, C/ Irunlarrea 3, 31008 Pamplona, Spain

³ Department of Pharmaceutics and Pharmaceutical Technology, Faculty of Pharmacy and Drug Manufacturing, Pharos University in Alexandria (PUA), Alexandria, Egypt

* Corresponding authors at: Department of Pharmaceutical Technology and Chemistry, Faculty of Pharmacy and Nutrition, Universidad de Navarra, C/Irunlarrea 1,31008 Pamplona, Spain.

E-mail addresses: egarbayo@unav.es (E. Garbayo), mjblanco@unav.es (M.J. Blanco-Prieto).

Journal of controlled Release (2019). 295: 201-213

Impact Factor: 9.776

10/275 in PHARMACOLOGY & PHARMACY (Q1)

HYPOTHESIS AND **OBJECTIVES**

Hypothesis and Objectives

The brain administration of neuroprotective drugs and stem cells is probably the only therapeutic modality that offers a potential ‘cure’ for neurodegenerative diseases. However, these therapies are still largely in the research and development phase. Drug and cell delivery approaches have been tested in preclinical and clinical studies aiming to repair brain damage. Unfortunately, the short half-life of administered drugs and the poor cell survival rate are serious obstacles that limit their potential effect.

The initial premise of this thesis is that the combination of neurotrophic factors, stem cells and drug delivery systems (nanoparticles and hydrogels) could achieve substantial progress for the clinical management of Parkinson’s Disease by offering optimal survival and delivery of therapeutic agents.

On this basis, the main objective of this doctoral thesis was to design and develop a tissue engineering approach that combines glial cell line-derived neurotrophic factor and stem cells in a nanoparticle-modified hydrogel for application in Parkinson’s Disease.

To that end, the following partial objectives were set:

1. To optimize the production of the glial cell line-derived neurotrophic factor and evaluate its purity and biological activity.
2. To evaluate the potential of glial cell line-derived neurotrophic factor to induce changes in the transcriptome of dopaminergic neurons derived from human induced pluripotent stem cells and human mesenchymal stem cells and to assess the suitability of their combination for the treatment of Parkinson’s Disease.
3. To develop and characterize an advanced drug delivery system for brain tissue engineering, where the glial cell line-derived neurotrophic factor and human mesenchymal stem cells are rationally combined into a nanoreinforced hydrogel for their simultaneous administration into the brain.

CHAPTER 1

Optimization of a GDNF production method based on Semliki Forest virus vector

Pablo Vicente Torres-Ortega ^(1,2) Cristian Smerdou ^(2,4), Eduardo Ansorena ^(2,3), María Cristina Ballesteros-Briones ^(2,4), Eva Martisova ^(2,4), Elisa Garbayo ^{(1,2)*}, María J. Blanco-Prieto ^{(1,2)*}.

¹ Department of Pharmaceutical Technology and Chemistry, Faculty of Pharmacy and Nutrition, Universidad de Navarra, C/ Irunlarrea 1, 31008 Pamplona, Spain

² Navarra Institute for Health Research, IdiSNA, C/ Irunlarrea 3, 31008 Pamplona, Spain

³ Department of Biochemistry and Genetics, School of Sciences, University of Navarra, Pamplona, Spain

⁴ Division of Gene Therapy and Regulation of Gene Expression, Cima Universidad de Navarra, Av. Pío XII 55, 31008, Pamplona, Spain

* Corresponding authors at: Department of Pharmaceutical Technology and Chemistry, Faculty of Pharmacy and Nutrition, Universidad de Navarra, C/Irunlarrea 1, 31008 Pamplona, Spain.

E-mail addresses: egarbayo@unav.es (E. Garbayo), mjblanco@unav.es (M.J. Blanco-Prieto).

European Journal of Pharmaceutical Sciences (2021). 159: 1-7

Impact Factor: 4.384

86/275 in PHARMACOLOGY & PHARMACY (Q1)

Abstract

Human glial cell line-derived neurotrophic factor (hGDNF) is the most potent dopaminergic factor described so far, and it is therefore considered a promising drug for Parkinson's disease (PD) treatment. However, the production of therapeutic proteins with a high degree of purity and a specific glycosylation pattern is a major challenge that hinders its commercialization. Although a variety of systems can be used for protein production, only a small number of them are suitable to produce clinical-grade proteins. Specifically, the BHK-21 cell line has shown to be an effective system for the expression of high levels of hGDNF, with appropriate post-translational modifications and protein folding. This system, which is based on the electroporation of BHK-21 cells using a Semliki Forest virus (SFV) as expression vector, induces a strong shut-off of host cell protein synthesis that simplifies the purification process. However, SFV vector exhibits a temperature-dependent cytopathic effect on host cells, which could limit hGDNF expression. The aim of this study was to improve the expression and purification of hGDNF using a biphasic temperature cultivation protocol that would decrease the cytopathic effect induced by SFV. Here we show that an increase in the temperature from 33°C to 37°C during the "shut-off period", produced a significant improvement in cell survival and hGDNF expression. In consonance, this protocol led to the production of almost 3-fold more hGDNF when compared to the previously described methods. Therefore, a "recovery period" at 37°C before cells are exposed at 33°C is crucial to maintain cell viability and increase hGDNF expression. The protocol described constitutes an efficient and highly scalable method to produce highly pure hGDNF.

Keywords: GDNF; Biphasic growth, BHK cells, Semliki Forest Virus; Shut-off; Parkinson's Disease.

1. Introduction

Glial cell line-derived neurotrophic factor (GDNF) is one of the most important neurotrophic factors present in the nervous system (1,2). Our current knowledge attributes to hGDNF special relevance in the development, maintenance and function of a variety of neurons and glial cells, suggesting an important role in halting the progression of Parkinson's Disease (PD) (1,3). The ability of this neurotrophic factor to increase dopaminergic neuron survival *in vitro* encouraged several *in vivo* studies (4–8) and even clinical trials focused on halting PD progression (9–11). However, the therapeutic potential of hGDNF, as a glycosylated protein, will largely depend on the possibility of administering a protein with a glycosylation pattern similar to the native one (12). For this reason, some clinical studies carried out using the non-glycosylated hGDNF produced in *E. coli* reported the development of antibodies against the protein, which may represent a safety issue (9,13). The production of proteins in mammalian cell lines appears to be more appropriate since they allow the expression of functionally relevant and active proteins, as these systems can provide post-translational modifications (14,15). To date, despite the drawbacks described here, most of the procedures developed for hGDNF expression have used prokaryotic organisms, highlighting *E. coli* (13,16,17).

As an alternative, alphaviruses have been engineered as expression vectors due to their ability to induce the expression of proteins at very high levels in mammalian cells. Among the alphaviruses, those based on Semliki Forest virus (SFV) allow a high degree of expression of topologically diverse proteins (18). More specifically, the electroporation of BHK-21 with this SFV self-replicating RNA has previously demonstrated to be a high efficiency system for the expression of hGDNF (19). This system presents the additional advantage that it induces a very strong inhibition of host-cell protein synthesis (shut-off). After the establishment of the shut-off, which takes place between four and eight hours post-electroporation, most protein synthesis becomes vector-specific, facilitating the subsequent purification of heterologous proteins expressed from the SFV vector (19,20). Among other factors, the incubation temperature of host cells presents important effects on the level and duration of recombinant protein expression in SFV infected mammalian cell lines, being optimal at 33°C (21). Moreover, the cytotoxic effect on host cells caused by SFV vectors could be influenced by the temperature employed during incubation (22). Several studies have obtained higher productivity in other cell lines using biphasic temperature protocols (23–25), but until now it had not been studied in our expression

system. Therefore, this study investigates the effect of a biphasic temperature culture protocol (37°C-33°C) on the expression of hGDNF using an SFV vector in BHK cells. Our findings demonstrate that the increase of the temperature during the shut-off period from 33°C to 37°C, with the incubation maintained at 33°C during the post-shut-off period, led to a significant improvement in cell viability. In addition, a three-fold increase in hGDNF expression was observed compared to previously established conditions (19). We have thus improved a method to purify hGDNF by increasing the culture temperature during the shut-off stage. This procedure, which could be scaled up using higher-capacity incubation systems, would allow the production of higher levels of hGDNF, offering an attractive system for the production of this and other recombinant proteins.

2. Material and methods

2.1 Cell lines

Baby hamster kidney (BHK-21) and rat adrenal PC12 cells were purchased from American Type Culture Collection (ATCC). BHK-21 cells were cultured in BHK-21 Glasgow MEM supplemented with 5% fetal bovine serum (FBS), 10% tryptose phosphate broth, 2 mM glutamine, 20 mM HEPES, 100 µg/mL streptomycin and 100 U/mL penicillin (BHK complete). BHK-21 cells were incubated in a humidified atmosphere with 5% CO₂, at 37°C, and kept ≤ 24 h before electroporation so they were actively growing on the day of electroporation. Rat PC12 cells were cultured on collagen I-coated plate (Invitrogen, Waltham, MA) in D-MEM supplemented with 5% horse heat-inactivated serum, 10% FBS, 100 µg/mL streptomycin and 100 U/mL penicillin.

2.2 hGDNF expression by BHK-21 cells transfected with the SFV-hGDNF vector and shut-off analysis

Plasmid pSFV-hGDNF was constructed as described before (19). The plasmid was linearized with *SpeI* and used as the template for RNA synthesis using SP6 polymerase (New England Biolabs, Ipswich, MA) as previously described (26). Briefly, linearized DNA was purified using a PCR purification kit (Qiagen, Germany) and quantified using an ND-1000 Spectrophotometer (NanoDrop Technologies, Wilmington, DE). Then, 1.5 µg of linearized pSFV-hGDNF DNA were incubated for 1 h at 37°C in SP6 buffer (40 mM Tris-HCl pH 7.9, 6 mM MgCl₂, 1 mM DTT and 2 mM spermidine) supplemented with 1 mM (m⁷G(5')ppp(5')G) (New England Biolabs, Ipswich, MA), 2 mM DTT, 1 mM rNTP mix, 4.5 µl of RNase inhibitor (Promega, Madison, WI), and 0.5 µl of SP6 RNA polymerase (New England Biolabs, Ipswich, MA) in a final volume of 50 µl. This

reaction yielded approximately 50 µg of RNA. 25 reactions were performed to obtain 1250 µg of SFV-hGDNF RNA. Each reaction was confirmed by gel electrophoresis. For each electroporation, 25 µg of *in vitro* synthesized RNA were mixed with 10^7 BHK-21 cells in a volume of 0,8 ml of PBS and electroporated in a 0.4 cm cuvette by giving two consecutive pulses at 850 V and 25 µF in a Bio-Rad electroporator (Hercules, CA). Cells from two electroporations were mixed in 10 ml of BHK-21 complete medium, seeded on a T75 flask (Greiner Bio-One, Kremsmünster, Austria) and incubated at 37°C or 33°C with 5% CO₂. After 8 h (shut-off period) medium was removed, cells were washed twice with 10 ml of PBS (Gibco, Waltham, MA), and 10 ml of BHK-21 complete medium without FBS were added to each flask. Cells were then incubated at 33°C for 24h (post-shut-off period), and then supernatants were collected for Western blot analysis. Quantification of hGDNF present in the supernatants was determined by ELISA (Invitrogen, Waltham, MA) following the manufacturer's instructions.

2.3 Optimization of incubation temperatures in host cells

To study the influence of the incubation temperature on the expression system, electroporated cells were seeded on 6-well plates (1.5 ml/dish) (Corning, Lowell, MA) and incubated at 37°C or 33°C with 5% CO₂. After 8 h (shut-off period) medium was removed, cells were washed twice with 2 ml of PBS, and 2 ml of BHK-21 complete medium without FBS was added to each well. 24 h later (post-shut-off period) supernatants were collected and the quantity of hGDNF expressed was quantified by ELISA. The effect of temperature on cell viability after the shut-off and post shut-off period was also evaluated. Briefly, four 96-well culture plates (Corning) were seeded with 50 µl/dish of electroporated cells and completed up to 200 µl with medium. Plates were incubated at 37°C or 33°C with 5% CO₂. For the plates intended for cell viability analysis after 24h (post-shut-off period), the medium was removed at 8 h, and the cells were washed twice with 200 µl of PBS. Then, 200 µl of BHK-21 complete medium without FBS was added to each well. The viability was determined after shut-off period and post-shut-off period using MTS included in the CellTiter 96[®] AQueous Non-Radioactive Cell Proliferation Assay (Promega, Madison, WI) according to the manufacturer's recommendations.

2.4 Western blot analysis

SDS-PAGE was performed on NuPAGE™ 4-12% Bis-Tris Protein Gels (Invitrogen, Waltham, MA) under reducing conditions. Proteins were transferred for 2 h onto

nitrocellulose membranes (Invitrogen, Waltham, MA) and the membrane was incubated with blocking solution containing 5% non-fat dry milk in PBS for 2 h, followed by incubation with anti-GDNF or anti-insulin like growth factor binding proteins (IGFBPs) 4 or 5 (Santa Cruz Biotechnology, Dallas, TX) diluted 1:2000 in blocking solution overnight at 4 °C. After washing with PBS, a horseradish peroxidase (HRP) conjugated sheep polyclonal antiserum against mouse IgG (GE Healthcare-Amersham, UK) diluted in blocking solution (1:2000) was added for 2 h. Detection was achieved with LumiLight Plus Reagent (Roche, Switzerland). Band densities were analyzed using the software Image Studio Lite 5.2.

2.5 Production and purification of hGDNF

A total of 5.8×10^8 BHK-21 cells were electroporated with 1.25 mg of SFV-hGDNF RNA synthesized *in vitro* as previously described (50 electroporations of 10^7 BHK-21 cells with 25 ug of RNA each) (19). Electroporated cells were pooled, resuspended in BHK-21 complete medium, and distributed in 25 flasks of T75 (Greiner Bio-One). After the expression process described in section 2.2, supernatants from all flasks (250 ml) were collected, centrifuged at 1000 g for 5 min to remove cell debris, and filtered through a 0.22 μm filter. 1 ml of SP-Sepharose™ Fast Flow resin (GE Healthcare) was packed into a disposable column (Bio-Rad), which was washed with 1.5 M NaCl in phosphate buffer (PB, 10 mM phosphate pH 7.4) and equilibrated with 150 mM NaCl in PB. The supernatant was transferred through the column and the resin was washed with 10 column volumes (CV) of 150 mM NaCl in PB. Finally, bounded protein was eluted in a single step with 10 CV of 0.5 M NaCl in PB. The presence of the protein was confirmed by western blot and the quantity of purified protein was determined by ELISA. The expression process was assessed under the two experimental conditions investigated (shut-off period: 33°C vs 37°C) and then compared. The purity of the sample was assessed by SDS-PAGE followed by Coomassie blue staining.

2.6 *In vitro* bioactivity assay

The bioactivity of purified hGDNF was proven by a PC-12 neurite outgrowth assay as previously described (27). Briefly, PC12 cells were plated on collagen-coated plates at low density (2000 cells/cm²) and cells were treated 24 h later with 100 ng/ml of hGDNF purified from the supernatant of BHK-21 cells. The neurite outgrowth was analyzed after 10 days of incubation.

2.7 Statistical analysis

All the results were expressed as the mean \pm standard deviation (SD). Data obtained from MTS and ELISA assays were statistically analyzed using a Paired-samples t-test by using Graphpad prism Version-6.0 software. The t-test of paired samples was conducted to compare cell survival and hGDNF expression of the biphasic temperature protocol with the conventional protocol. All samples were assayed in triplicate. Values were considered statistically significant when $p < 0.05$.

3. Results and discussion

3.1 Optimization of hGDNF expression in BHK-21 cells after electroporation with SFV-hGDNF RNA vector

SFV vectors can induce a strong shut-off of host cell protein synthesis in mammalian cells, which is one of the major advantages of this system (28). This ability is exploited here to produce hGDNF, since it is the most abundant protein present in the supernatant of transfected cells and can be purified by a simple ion-exchange chromatography. The shut-off allows the inhibition of host-cell proteins such as IGFBP-4 and IGFBP-5, with physical-chemical similarity with hGDNF, and whose subsequent purification would limit the yield of the process (19,29). To express hGDNF, we first *in vitro* transcribed SFV-hGDNF RNA obtaining a total amount of 1250 μg of RNA, which was electroporated into BHK-21 cells (10^7 BHK-21 cells for each electroporation with 25 μg of RNA). Several cell culture parameters can influence the level of expression and the quality of the recombinant protein. In this regard, the cell incubation temperature is an essential factor in the level and duration of recombinant protein expression. In the last few years, many studies have supported the idea that exposure of cell cultures to mild hypothermia during the phase of expression of the specific protein leads to increased productivity. However, in most cases, the molecular mechanisms governing the production of specific proteins under mild hypothermia are currently unknown (25). One study investigated the influence of the incubation temperature (33°C vs 37°C) in two rodent cell lines, BHK-21 and CHO infected with an SFV vector expressing luciferase (21). The luciferase expression levels were much higher in both cells lines when cultured at 33°C compared to 37°C, with a 10-20-fold increase in luciferase expression at 50 h post-infection (21). The effect of mild hypothermia on the specific productivity of other proteins such as r-protein or erythropoietin fusion protein (Epo-Fc) in CHO cell culture has also been explored, reporting higher productivity (24,25). For example, the final Epo-

CHAPTER 1

Fc concentration was increased around 2.5-fold when the cell culture temperature was decreased from 37°C to 33.5°C (24). As mentioned, our expression system consists of two phases: the shut-off period and the post-shut-off period. In this sense, our group had previously analyzed the levels of hGDNF expression from SFV by testing different time and temperature combinations during the shut-off and post-shut-off stages. Moreover, the time required to complete shut-off stage was also determined (19). The highest hGDNF expression levels were obtained with the combination of an 8 h shut-off period at 33°C followed by a 24 h post-shut-off period at 33°C. Overall, it was concluded that the shut-off period required at least 8 h regardless of the temperature used. The exposure to mild hypothermia during both phases ensured a very high hGDNF expression level with no detection of contaminating proteins. Thus, our expression system seems to be strongly dependent on the incubation temperature of BHK-21 cells after electroporation (21) and it is known that SFV vector exhibits a temperature-dependent cytopathic effect on host cells (22). However, the possibility of using different temperatures for the shut-off and post-shut-off periods was not investigated in that study. The use of a biphasic temperature system has been previously explored by Lin *et al.* in HEK-293S cells transfected with a green fluorescent protein (GFP) plasmid (23). A decrease of temperature up to 33°C, was an effective way to increase protein expression, but only when the transfected culture was allowed to “recover” at 37°C overnight (23). Additionally, it is well known that the temperature at which cells are incubated is also one of the most important factors for cell growth, being usually optimal at 37°C (30). Incubations at lower temperatures have been related to poor cell growth (31,32). In this context, we hypothesized that the performance of shut-off at 37°C might stimulate higher cell viability and also, an enhanced hGDNF expression during the post-shut-off period. Therefore, we decided to test if increasing the shut-off temperature to 37°C could improve hGDNF expression in BHK-21 cells. To evaluate this hypothesis, we studied BHK-21 cell viability and hGDNF expression using

the biphasic temperature protocol (37°C for the shut-off period and 33°C for the post-shut-off period) (**Fig. 1**).

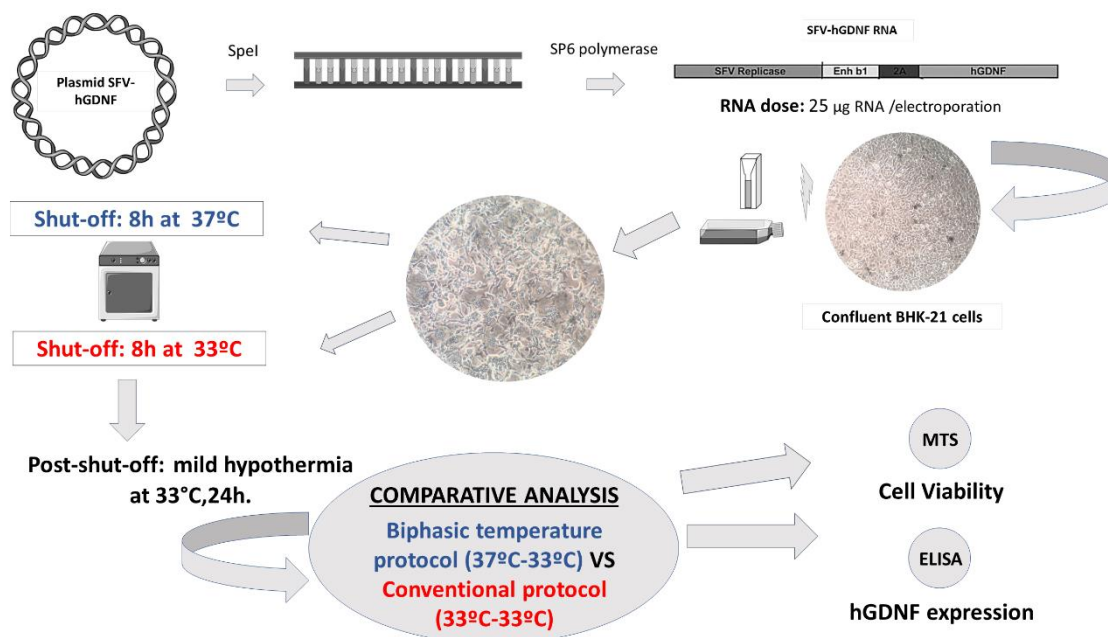


Figure 1. Schematic representation of the biphasic temperature protocol for hGDNF expression. The plasmid containing SFV-hGDNF was linearized with Spe I and used to transcribe in vitro the vector RNA, using SP6 polymerase. SFV-hGDNF RNA was electroporated into BHK-21 cells. Electroporated cells were incubated at 37°C or 33°C with 5% CO₂. After 8 h (shut-off period), cells were exposed to mild hypothermia at 33°C for 24h (post-shut-off period). Cell viability was determined after the shut-off period and post-shut-off period using MTS. Quantification of hGDNF present in the supernatants was determined by ELISA.

CHAPTER 1

The same parameters were analyzed using the conventional protocol in which the whole process is performed at 33°C. Cell viability was evaluated by MTS after shut-off and post-shut-off periods for both protocols showing that cell survival was significantly lower when both periods of incubation were performed at 33°C (**Fig. 2**).

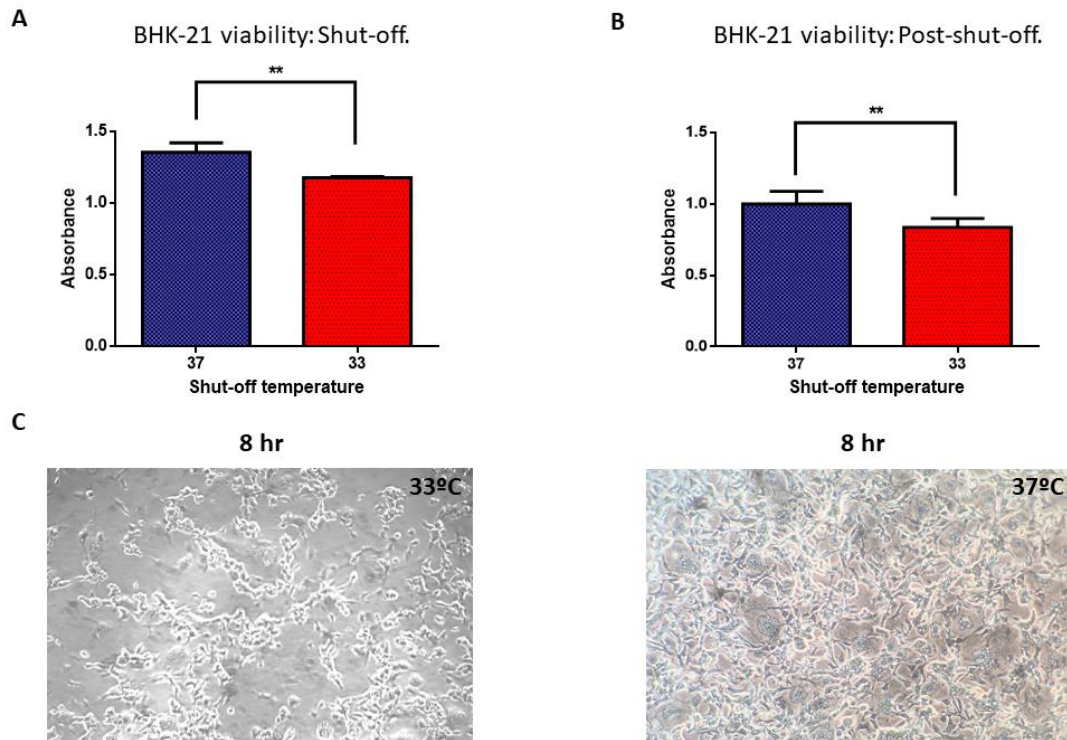


Figure 2. Analysis of cell viability after the shut-off and post shut-off period. Cells used for the assays were electroporated with SFV-hGDNF RNA and incubated at 37°C or 33°C (N=4) during the shut-off period. **A**) Cell viability in BHK-21 cells that grew at 37°C (blue bar), as compared with 33°C (red bar) after the shut-off period **B**) Cell survival in BHK-21 cells that were incubated at 37°C (blue bar), as compared with 33°C (red bar) after the post-shut-off period. Cell survival was significantly increased with biphasic temperature protocol (**, $p < 0.01$, Paired t test). The data are shown as the mean \pm SD. **C**) Representative images of cells after shut-off period at 33°C (left) or 37°C (right) taken with a phase-contrast microscope. Magnification: 40x

Thus, when the shut-off was performed at 33°C, the absorbance detected by MTS, which is directly proportional to the number of living cells in culture was significantly lower compared to its performance at 37°C (**Table 1**).

Table 1. Optimization of incubation temperature for hGDNF production using SFV system

Number of electroporations	µg RNA/ electroporation	Shut-off temperature	Post shut-off temperature	µg hGDNF / ml of supernatant	*Absorbance detected in MTS after shut-off	*Absorbance detected in MTS after post shut-off
4	25	37°C	33°C	5.49 ± 1.33	1.35 ± 0,06	0.99 ± 0.09
4	25	33°C	33°C	4.38 ± 0.47	1.17 ± 0.01	0.83 ± 0.06

*Data of absorbance and hGDNF expression were presented as means ± standard deviation (SD).

hGDNF quantification by ELISA showed that its expression was significantly increased by 20% ($p < 0.05$) when the shut-off period was carried out at 37°C (**Table 1**). Likewise, the higher expression level achieved with the biphasic temperature protocol (37°C-33°C) was confirmed when performing the same experiment with a larger number of electroporations (50 electroporations) under the two experimental conditions investigated (shut-off period: 33°C vs 37°C) (Table 2). In this higher scale experiment, an average hGDNF expression level of 3.12 ± 1.17 µg/ml was obtained following the biphasic temperature protocol (37°C-33°C), reaching a total amount of 780 µg of GDNF in 250 ml. By contrast, only 1.21 ± 0.14 µg hGDNF/ml and a total amount of 300 µg of GDNF in 250 ml were obtained using the conventional protocol. According to these results, the new protocol proposed here represents a considerable improvement in hGDNF expression of almost 3-fold compared to previously established conditions (19) (**Table 2**).

Table 2. hGDNF expression on a larger scale applying different temperatures during shut-off.

Number of electroporations	µg of RNA/ electroporation	Shut-off temperature	Post shut-off temperature	µg of hGDNF/ml of supernatant	Total hGDNF protein expression	ml of supernatant
50	25	37°C	33°C	3.12 ± 1.17	780 µg	250
50	25	33°C	33°C	1.21 ± 0.14	300 µg	250
*100	25	33 °C	33°C	-----	741 µg	570

*Data extracted from Ansorena et al (19)

Accordingly, culturing mammalian cells at low temperature is an established method to maintain cell viability while at the same time inhibiting their growth. This inhibition is

associated with G1-phase cell cycle arrest, which has been positively correlated with increased protein productivity (21,23,33–35). In agreement with that observed with other expression systems, the mild hypothermia achieved at 33°C is suitable to obtain a high expression level during the post-shut-off stage when using the SFV system (21,23,34,35). However, in contrast to other studies performed with SFV vectors in BHK-21 cells, the use of low temperature after RNA transfection was not optimal for hGDNF expression (21,36). In our case, maintaining a higher temperature (37°C) during the shut-off period was important to increase hGDNF expression, since it increased cell viability. Although it had been assumed that the same temperature should be applied during the two phases following electroporation, we have shown that this is not optimal. Therefore, our results demonstrate that the conditions used during the initial shut-off period are of great importance for hGDNF expression during the post-shut-off period.

3.2 Shut-off of host cell protein synthesis analysis

As mentioned before, SFV RNA vector replication leads to a strong shut-off of host cell protein synthesis and after a few hours, most protein synthesis becomes vector-specific (37–39). To determine the efficiency of this effect in BHK-21 cells under the biphasic temperature culture protocol, the supernatants from 24 h post-shut-off electroporated cells were analyzed by western blot with specific antibodies for cellular proteins IGFBP-4, IGFBP-5 and hGDNF. The presence of these proteins was analyzed because IGFBP-4 and IGFBP-5 are also secreted by this cell line (19), representing a technical problem for hGDNF purification due to the high physicochemical similarity with hGDNF. The analysis of the supernatants from electroporated cells only showed the presence of

hGDNF as previously described by Ansorena et al (19), indicating that the shut-off had been highly efficient (**Fig. 3A**).

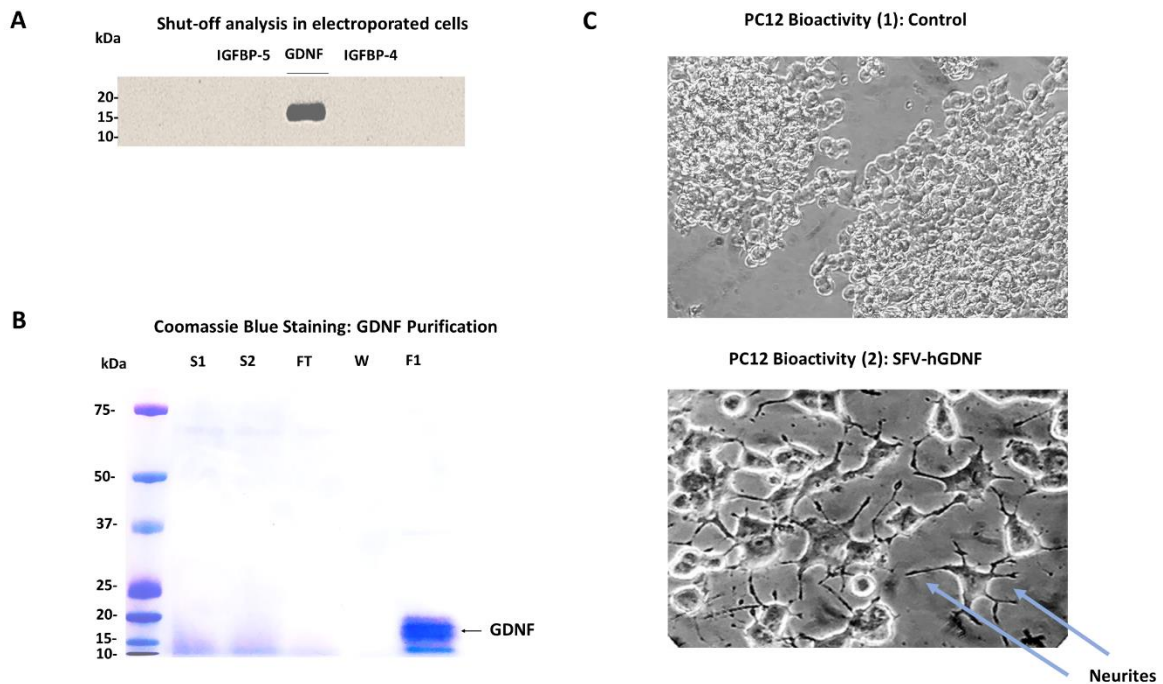


Figure 3. Analysis of the shut-off efficiency and bioactivity of purified hGDNF. **A**) Shut-off analysis in electroporated cells: After post-shut-off period, the medium was collected and analyzed by Western blot with antibodies specific for hGDNF, IGFBP-5 and IGFBP-4. **B**) Coomassie Blue Staining; S1 and S2: supernatant samples; FT: flow-through; W: column wash; F1: eluate with 0.5 M NaCl; **C**) Analysis of hGDNF activity in vitro. PC12 cells were incubated for 10 days with 100 ng/ml of hGDNF purified from the supernatant of BHK-21 cells transfected with SFV-hGDNF vector. Control cells were incubated without hGDNF. Representative images were taken with a phase-contrast microscope on day 10. Magnification: 20x (1) and 40x (2).

3.3 hGDNF purification by cation exchange chromatography

The purification strategy of recombinant proteins is crucial, and a chromatographic approach is usually required to meet the purity requirements, which sometimes are higher than 99% in the biopharmaceutical industry (40). We applied an ion-exchange chromatography, which allowed hGDNF purification in a single chromatographic step. The pH of the sample and buffers used were adjusted to 7.4. The use of an adequate buffer is fundamental for the maintenance of the biological activity of a protein (41) since it will prevent changes in pH that could irreversibly affect its folding, solubility, and function (42,43). In the present protocol, we have optimized the pH working conditions, employing a phosphate buffer at pH 7.4 for the purification of hGDNF by ion-exchange chromatography, which has a more physiological pH than the method previously

described (19). Considering the theoretical isoelectric point of our protein ($pI=9.4$), this pH could allow a greater attraction of hGDNF to the cation exchange column for subsequent elution. All the purified protein was found in the first fraction of elution with 0.5 M NaCl buffer (**Fig. 3B**). Quantification of purified protein by ELISA showed a total amount of 483 μg of hGDNF, obtained from 250 ml of medium, with a recovery yield of 62%, similar to previous reports (19). Therefore, pH modification did not affect the final yield of the chromatographic step. The analysis of the elution fractions by SDS-PAGE followed by Coomassie Blue staining showed the presence of several bands at different molecular weights. This complex pattern has been observed previously and corresponds to the different degrees of glycosylation present in hGDNF expressed by BHK-21 cells (**Fig. 3B**) (19). Likewise, purity analysis show that it is possible to obtain highly pure hGDNF through a biphasic temperature protocol and the application of a single chromatographic step.

3.4 Activity of purified hGDNF

Having demonstrated that this protocol is highly efficient for the production of glycosylated hGDNF, we next evaluated the bioactivity of the purified protein. Neurite outgrowth assay in the PC12 cell line has been widely used as a model of neuronal differentiation and to evaluate the activity of neurotrophic factors (44). Neurite extension was confirmed in PC12 cells after 10 days of culture (**Fig. 3C**). These results indicate that recombinant hGDNF produced using the biphasic protocol remains biologically active.

4. Future prospects and conclusion

Mammalian cells such as CHO and BHK-21 cells are ideal expression systems to produce recombinant proteins with features closer to their endogenous versions and potentially less immunogenic. However, working with mammalian cell expression systems, increasing protein production with fewer resources and shorter times remains a major challenge (45). In this case, the key aspect that we used to optimize a previously described method of hGDNF production was the temperature of incubation periods after electroporation. The use of a biphasic temperature protocol (37°C-33°C) led to a considerable (3-fold) improvement in hGDNF expression compared to previously established conditions. The first phase of this culture protocol, in addition to allowing the shut-off of host cell proteins synthesis, is also considered as a recovery period that allows cell viability to be maintained before the cells are exposed to mild hypothermia at 33°C in the second stage. Furthermore, this change allows the expression of a highly pure and

bioactive protein, potentially reducing the production costs, since it is possible to produce a greater amount of hGDNF using a smaller number of electroporations and a lower amount of RNA. Even though the quantity of hGDNF produced at a small scale in this study was sufficient for our objective, it would be very interesting to scale-up hGDNF production using this expression system (46–48). The ideal situation would be to adapt this method to a process able to handle large volumes of cells with suitable bioreactors. While on a laboratory scale, the SFV vector has been widely used to obtain sufficient amounts of recombinant proteins for different studies, the use of large volumes in bioreactors is mainly limited by the transient expression of the vector due to its cytotoxic character, the inhibition of host cell proteins and RNA-based expression (49). In recent years, many studies have focused on the development of vectors with a less cytopathic character. However, the complexity of controlling the duration of the protein expression remains a major limitation (48–51). On the other hand, cell electroporation is a discontinuous procedure, which could represent a limitation for scaling-up our method. In this regard, recent advances have led to higher throughputs by continuous electroporation using modified microfluidic devices. In fact, continuous cell electroporation has been successfully used to transfer DNA and mRNA into several cell lines (52–54) and it could be easily applied to our expression system. With this technology, it would be possible to process larger volumes of cells and to produce higher amounts of hGDNF during shorter times.

To conclude, this study opens up the possibility of using a biphasic protocol that increases cell culture temperature during the shut-off period to improve hGDNF expression. We have shown the importance of a “recovery period” at 37°C to maintain BHK-21 viability before exposing the cells to mild hypothermia at 33°C. Furthermore, our results provide additional important information for the future development of large-scale hGDNF production using SFV vectors in the mammalian cell line BHK-21. Moreover, the system described in this study could be extendable to the expression of different therapeutic proteins.

Acknowledgements

P. Torres thanks the Spanish Ministry of Education (Programa FPU (FPU17/01212)) and Government of Navarra (2019_66_NAB9). E. Garbayo is supported by a “Ramon y Cajal Fellowship (RYC2018-025897-I). MCBB received a Fundación Echébano fellowship. This work was partially supported by the following grants: Instituto Salud Carlos III

CHAPTER 1

financed with Feder Funds PI17/01859, Gobierno de Navarra. Departamento de Salud 64/2019 (co-financed at 50% by the European Regional Development Fund through the FEDER Operational Program 2014-2020 of Navarra: “European Union”).

CRedit authorship contribution statement

Pablo Vicente Torres Ortega: Validation, Formal analysis, Investigation, Writing - original draft. **Cristian Smerdou:** Conceptualization, Writing – Review and Editing, Supervision. **Eduardo Ansorena:** Writing – Review and Editing, Supervision. **María Cristina Ballesteros-Briones:** Investigation. **Eva Martisova:** Investigation. **Elisa Garbayo:** Conceptualization, Writing – Review and Editing, Supervision. **María J. Blanco-Prieto:** Conceptualization, Resources, Writing – Review and Editing, Supervision, Funding acquisition.

Conflict of interest

The authors declare that they have no conflict interests.

References

1. Lin L, Doherty D, Lile J, Bektesh S, Collins F. GDNF: a glial cell line-derived neurotrophic factor for midbrain dopaminergic neurons. *Science* (80-). 1993 May 21;260(5111):1130–2.
2. Pöyhönen S, Er S, Domanskyi A, Airavaara M. Effects of neurotrophic factors in glial cells in the central nervous system: Expression and properties in neurodegeneration and injury. Vol. 10, *Frontiers in Physiology*. Frontiers Media S.A.; 2019.
3. Torres-Ortega PV, Saludas L, Hanafy AS, Garbayo E, Blanco-Prieto MJ. Micro- and nanotechnology approaches to improve Parkinson’s disease therapy. *J Control Release*. 2019 Feb 10;295:201–13.
4. Garbayo E, Ansorena E, Lanciego JL, Blanco-Prieto MJ, Aymerich MS. Long-term neuroprotection and neurorestoration by glial cell-derived neurotrophic factor microspheres for the treatment of Parkinson’s disease. *Mov Disord*. 2011 Aug 15;26(10):1943–7.
5. Garbayo E, Ansorena E, Lana H, Carmona-Abellan M del M, Marcilla I, Lanciego JL, et al. Brain delivery of microencapsulated GDNF induces functional and structural recovery in parkinsonian monkeys. *Biomaterials*. 2016 Dec 1;110:11–23.
6. Herrán E, Requejo C, Ruiz-Ortega JA, Aristieta A, Igartua M, Bengoetxea H, et al. Increased antiparkinson efficacy of the combined administration of VEGF- and GDNF-loaded nanospheres in a partial lesion model of Parkinson’s disease. *Int J Nanomedicine*. 2014;9(1):2677–87.
7. Garbayo E, Montero-Menei CN, Ansorena E, Lanciego JL, Aymerich MS, Blanco-Prieto MJ. Effective GDNF brain delivery using microspheres-A promising strategy for Parkinson’s disease. *J Control Release*. 2009 Apr 17;135(2):119–26.
8. Salvatore MF, Gerhardt GA, Dayton RD, Klein RL, Stanford JA. Bilateral effects of unilateral GDNF administration on dopamine- and GABA-regulating proteins in the rat nigrostriatal system. *Exp Neurol*. 2009 Sep;219(1):197–207.
9. Slevin JT, Gash DM, Smith CD, Gerhardt GA, Kryscio R, Chebrolu H, et al.

CHAPTER 1

- Unilateral intraputamenal glial cell line-derived neurotrophic factor in patients with Parkinson disease: Response to 1 year of treatment and 1 year of withdrawal. *J Neurosurg.* 2007 Apr;106(4):614–20.
10. Whone A, Luz M, Boca M, Woolley M, Mooney L, Dharia S, et al. Randomized trial of intermittent intraputamenal glial cell line-derived neurotrophic factor in Parkinson's disease. *Brain.* 2019;142(3):512–25.
 11. Gash DM, Gerhardt GA, Bradley LH, Wagner R, Slevin JT. GDNF clinical trials for Parkinson's disease: a critical human dimension. *Cell Tissue Res.* 2020 Oct 1;382(1):65–70.
 12. Gupta SK, Shukla P. Glycosylation control technologies for recombinant therapeutic proteins. *Appl Microbiol Biotechnol.* 2018 Dec 1;102(24):10457–68.
 13. Lang AE, Gill S, Patel NK, Lozano A, Nutt JG, Penn R, et al. Randomized controlled trial of intraputamenal glial cell line-derived neurotrophic factor infusion in Parkinson disease. *Ann Neurol.* 2006 Mar;59(3):459–66.
 14. Hunter M, Yuan P, Vavilala D, Fox M. Optimization of Protein Expression in Mammalian Cells. *Curr Protoc Protein Sci.* 2019 Feb 1;95(1).
 15. Piccinini E, Kalkkinen N, Saarma M, Runeberg-Roos P. Glial cell line-derived neurotrophic factor: Characterization of mammalian posttranslational modifications. *Ann Med.* 2013 Feb;45(1):66–73.
 16. Chen ZY, Sun JX, Li JH, He C, Lu CL, Wu XF. Preparation of recombinant human GDNF by baculovirus expression system and analysis of its biological activities. *Biochem Biophys Res Commun.* 2000;273(3):902–6.
 17. Huang BR, Ma XM. Expression of neurotrophic factors such as GDNF in the *E. coli* system. *Methods Mol Biol.* 2001;169:101–14.
 18. Lundstrom K. Expression of mammalian membrane proteins in mammalian cells using Semliki Forest virus vectors. *Methods Mol Biol.* 2010;601:149–63.
 19. Ansorena E, Casales E, Aranda A, Tamayo E, Garbayo E, Smerdou C, et al. A simple and efficient method for the production of human glycosylated glial cell line-derived neurotrophic factor using a Semliki Forest virus expression system.

- Int J Pharm. 2013;440(1):19–26.
20. Ansorena E, Garbayo E, Lanciego JL, Aymerich MS, Blanco-Prieto MJ. Production of highly pure human glycosylated GDNF in a mammalian cell line. *Int J Pharm.* 2010 Jan 29;385(1–2):6–11.
 21. Schlaeger EJ, Lundstrom K. Effect of temperature on recombinant protein expression in Semliki Forest virus infected mammalian cell lines growing in serum-free suspension cultures. *Cytotechnology.* 1998;28(1–3):205–11.
 22. Lundstrom K, Abenavoli A, Malgaroli A, Ehrenguber MU. Novel Semliki Forest virus vectors with reduced cytotoxicity and temperature sensitivity for long-term enhancement of transgene expression. *Mol Ther.* 2003 Feb 1;7(2):202–9.
 23. Lin CY, Huang Z, Wen W, Wu A, Wang C, Niu L. Enhancing protein expression in HEK-293 cells by lowering culture temperature. *PLoS One.* 2015;10(4).
 24. Kaisermayer C, Reinhart D, Gili A, Chang M, Aberg PM, Castan A, et al. Biphasic cultivation strategy to avoid Epo-Fc aggregation and optimize protein expression. *J Biotechnol.* 2016 Jun 10;227:3–9.
 25. Becerra S, Berrios J, Osses N, Altamirano C. Exploring the effect of mild hypothermia on CHO cell productivity. Vol. 60, *Biochemical Engineering Journal.* Elsevier; 2012. p. 1–8.
 26. Liljeström P, Garoff H. Expression of Proteins Using Semliki Forest Virus Vectors. *Curr Protoc Mol Biol.* 1995 Jan 1;29(1):16.20.1-16.20.16.
 27. Garbayo E, Ansorena E, Lanciego JL, Aymerich MS, Blanco-Prieto MJ. Purification of bioactive glycosylated recombinant glial cell line-derived neurotrophic factor. *Int J Pharm.* 2007 Nov;344(1–2):9–15.
 28. Berglund P, Sjöberg M, Garoff H, Atkins GJ, Sheahan BJ, Liljeström P. Semliki Forest Virus Expression System: Production of Conditionally Infectious Recombinant Particles. *Bio/Technology.* 1993;11(8):916–20.
 29. Hsu D, Olefsky JM. Characterization of insulin-like growth factor (IGF) binding proteins and their role in modulating IGF-I action in BHK cells. *J Biol Chem.* 1992;267(35):25576–82.

CHAPTER 1

30. Akram Q. Optimization of Physico-chemical Factors for Augmenting Biomass Production of Baby Hamster Kidney Cells (BHK-21) in Roller Bottle. *Int J Agric Biol.* 2014;16.
31. Watanabe I, Okada S. Effects of temperature on growth rate of cultured mammalian cells (L5178Y). *J Cell Biol.* 1967;32(2):309–23.
32. Neutelings T, Lambert CA, Nusgens B V., Colige AC. Effects of Mild Cold Shock (25°C) Followed by Warming Up at 37°C on the Cellular Stress Response. Stoecklin G, editor. *PLoS One.* 2013 Jul 23;8(7):e69687.
33. Kumar N, Gammell P, Meleady P, Henry M, Clynes M. Differential protein expression following low temperature culture of suspension CHO-K1 cells. *BMC Biotechnol.* 2008 Apr 22;8(1):42.
34. Yoon SK, Song JY, Lee GM. Effect of low culture temperature on specific productivity, transcription level, and heterogeneity of erythropoietin in Chinese hamster ovary cells. *Biotechnol Bioeng.* 2003 May 5;82(3):289–98.
35. Kaufmann H, Mazur X, Fussenegger M, Bailey JE. Influence of low temperature on productivity, proteome and protein phosphorylation of CHO cells. *Biotechnol Bioeng.* 1999 Jun 5;63(5):573–82.
36. Fernández-Núñez EG, de Rezende AG, Puglia ALP, Leme J, Boldorini VLL, Caricati CP, et al. Transient expression of rabies virus G-glycoprotein using BHK-21 cells cultured in suspension. *Biotechnol Lett.* 2015 Jun 16;37(6):1153–63.
37. Strauss JH, Strauss EG. The alphaviruses: Gene expression, replication, and evolution. *Microbiol Rev.* 1994 Sep;58(3):491–562.
38. McInerney GM, Kedersha NL, Kaufman RJ, Anderson P, Liljeström P. Importance of eIF2 α Phosphorylation and Stress Granule Assembly in Alphavirus Translation Regulation. *Mol Biol Cell.* 2005 Aug;16(8):3753–63.
39. Rivas H, Schmaling S, Gaglia M. Shutoff of Host Gene Expression in Influenza A Virus and Herpesviruses: Similar Mechanisms and Common Themes. *Viruses.* 2016 Apr 16;8(4):102.
40. Owczarek B, Gerszberg A, Hnatuszko-Konka K. A Brief Reminder of Systems of

- Production and Chromatography-Based Recovery of Recombinant Protein Biopharmaceuticals. *Biomed Res Int.* 2019;2019.
41. Ugwu SO, Apte SP. The Effect of Buffers on Protein Conformational Stability. *Pharm Technol.* 2004;
 42. Ritchie C. Protein Purification. *Mater Methods.* 2012 Jan 1;2.
 43. Zhang C-Y, Wu Z-Q, Yin D-C, Zhou B-R, Guo Y-Z, Lu H-M, et al. A strategy for selecting the pH of protein solutions to enhance crystallization. *Acta Crystallogr Sect F Struct Biol Cryst Commun.* 2013 Jul 1;69(7):821–6.
 44. Chaurasiya ND, Shukla S, Tekwani BL. A Combined In Vitro Assay for Evaluation of Neurotrophic Activity and Cytotoxicity. *SLAS Discov.* 2017;22(6):667–75.
 45. Lalonde ME, Durocher Y. Therapeutic glycoprotein production in mammalian cells. *J Biotechnol.* 2017 Jun 10;251:128–40.
 46. Núñez EGF, Jorge SAC, Astray RM, de Rezende AG, da Costa BLV, Monteiro DCV, et al. Semliki forest virus as a vector: Pros and cons for its use in biopharmaceuticals production. *Brazilian Arch Biol Technol.* 2013 Sep;56(5):859–66.
 47. Lundstrom K. Semliki Forest virus vectors for large-scale production of recombinant proteins. *Methods Mol Med.* 2003;76:525–43.
 48. Aranda A, Bezunartea J, Casales E, Rodriguez-Madoz JR, Larrea E, Prieto J, et al. A quick and efficient method to generate mammalian stable cell lines based on a novel inducible alphavirus DNA/RNA layered system. *Cell Mol Life Sci.* 2014;71(23):4637–51.
 49. Casales E, Aranda A, Quetglas JI, Ruiz-Guillen M, Rodriguez-Madoz JR, Prieto J, et al. A novel system for the production of high levels of functional human therapeutic proteins in stable cells with a Semliki Forest virus noncytopathic vector. *N Biotechnol.* 2010 May 31;27(2):138–48.
 50. Casales E, Rodriguez-Madoz JR, Ruiz-Guillen M, Razquin N, Cuevas Y, Prieto J, et al. Development of a new noncytopathic Semliki Forest virus vector providing

CHAPTER 1

- high expression levels and stability. *Virology*. 2008 Jun 20;376(1):242–51.
51. Schott JW, Morgan M, Galla M, Schambach A. Viral and synthetic RNA vector technologies and applications. Vol. 24, *Molecular Therapy*. Nature Publishing Group; 2016. p. 1513–27.
 52. Lissandrello CA, Santos JA, Hsi P, Welch M, Mott VL, Kim ES, et al. High-throughput continuous-flow microfluidic electroporation of mRNA into primary human T cells for applications in cellular therapy manufacturing. *Sci Rep*. 2020 Dec 22;10(1):18045.
 53. Yoo BS, Im DJ, Ahn MM, Park SJ, Kim YH, Um TW, et al. A continuous droplet electroporation system for high throughput processing †. *Cite this Anal*. 2018;143:5785.
 54. Bhattacharjee N, Horowitz LF, Folch A. Continuous-flow multi-pulse electroporation at low DC voltages by microfluidic flipping of the voltage space topology. *Appl Phys Lett*. 2016 Oct 17;109(16):163702.

CHAPTER 2

Transcriptome analysis of hiPS-DANs after hGDNF stimulation

Pablo Vicente Torres-Ortega ^(1,2), Rosario Luquin ^(2,3), Elisa Garbayo ^(1,2), María J. Blanco-Prieto ^(1,2)

¹ Department of Pharmaceutical Technology and Chemistry, Faculty of Pharmacy and Nutrition, Universidad de Navarra, C/ Irunlarrea 1, 31008 Pamplona, Spain

² Navarra Institute for Health Research, IdiSNA, C/ Irunlarrea 3, 31008 Pamplona, Spain

³ Department of Neurology and Neurosciences, Clínica Universidad de Navarra, Pamplona, C/ Pío XII 36, 31008 Pamplona, Spain.

*Corresponding authors at: Department of Pharmaceutical Technology and Chemistry, Faculty of Pharmacy and Nutrition, Universidad de Navarra, C/Irunlarrea 1,31008 Pamplona, Spain.

E-mail addresses: egarbayo@unav.es (E. Garbayo), mjblanco@unav.es (M.J. Blanco-Prieto).

Abstract

Dopaminergic neurons derived from human induced pluripotent stem cells (hiPS-DANs) represent one of the most promising sources for cell replacement therapy in Parkinson's Disease (PD). However, the grafting efficiency after transplantation remains insufficient, which limits the therapeutic efficacy of dopamine (DA) cell replacement. The co-administration of glial cell line-derived neurotrophic factor (hGDNF) and hiPS-DANs has emerged as a powerful strategy to enhance the survival, plasticity, and efficient integration of dopaminergic neuron grafts. However, the mechanisms underlying these therapeutic effects remain poorly understood.

In the present study, the transcriptomic changes that hGDNF produces on hiPS -DANs were investigated to achieve a greater understanding of the mechanisms that enhance their functional integration. In the short term (day 1), the upregulation of some MAPK signaling pathway-related genes such as APP and EPHB1 genes and the positive regulation of several genes involved in processes such as axon ensheathment, synaptic transmissions and secretory function were found. The gene expression profile induced by hGDNF after 7-days of treatment demonstrated a positive regulation of survival and plasticity of DANs. Furthermore, the hGDNF stimulation promoted the DA biosynthesis through the regulation of the genes TH, WNT3, EN1 and FGF20. Remarkably, hGDNF could regulate the plasticity and survival of hiPS-DANs via the MAPK pathway. Overall, our findings demonstrate that hGDNF is a promising therapeutic agent to enhance the integration and biological functions of cell grafts based on hiPS-DANs.

1. Introduction

Parkinson's disease (PD) is the second most common progressive neurodegenerative disease worldwide (1). It is characterized by the selective loss of dopaminergic neurons (DANs) in the substantia nigra pars compacta (SNpc) (2,3). Dopamine (DA) replacement therapy and deep brain stimulation (DBS) are currently the main alternatives for symptomatic PD therapy (4,5). However, patients experience motor fluctuations and , which is non-responsive to levodopa in the later stages (6). On the other hand, DBS does not appear to be a feasible option owing to associated complications such as postoperative neuropsychiatric complications, including suicide, postoperative depression, postoperative euphoria, and/or hypomania, and it remains a symptomatic therapy (7). Since the neurodegenerative process that occurs in PD is caused by the selective and gradual degeneration of mesencephalic DA (mesDA) neurons (8), the transplantation of DANs in this brain region could contribute to brain repair (9).

In this arena, dopaminergic neurons derived from human induced pluripotent stem cells (hiPS-DANs) are a promising source for cell replacement therapy. Their use represents a breakthrough over fetal cells due to their wide availability, standardized manufacture, ability to be cryopreserved and increased purity (9). Overall, these advantages could contribute to the standardization of cell replacement studies (9). However, the low cell survival found after implantation limits their therapeutic efficacy (4,10,11). As a possible solution, some studies have demonstrated that glial cell line-derived neurotrophic factor (hGDNF) might promote DANs survival (12–15). Therefore, the co-administration of stem cells and hGDNF has recently been proposed as a powerful approach to enhance dopaminergic neuron (DA) graft survival, plasticity and functional integration (10,11,16). Nevertheless, the mechanisms underlying this interaction remain poorly understood and more mechanistic studies are required to clarify the pathways that promote the efficient integration of hiPS-DANs grafts.

In this study we investigate the transcriptomic changes that hGDNF produce on hiPS-DANs to promote the functional integration of DANs graft. A significant enrichment of different functional categories such as the locomotor behavior, the growth of neurites, the number of neurons or the growth of axons among others were noticed between days 1 and 7. Moreover, the transcriptional changes during hGDNF stimulation had an important influence on DA biosynthesis through the regulation of the genes TH, WNT3, EN1 and FGF20, involved in DA metabolism. Importantly, hGDNF could modulate the plasticity

CHAPTER 2

and survival of DANs via the MAPK pathway. Overall, these changes support the use of GDNF to improve DANs graft survival and contribute to a deeper understanding of the mechanisms by which improvements in the integration and biological functions occurred.

2. Materials and methods

2.1 In vitro cell viability

Briefly, hiPS-DANs (Cellular Dynamics) were seeded in 96-well culture plates at a density of 2×10^4 cells per well and cultured according to the manufacturer protocol (Cellular Dynamics) with or without GDNF (100 ng/ml). Presto Blue was performed at day 1, 3 and 7 after post-treatment. Briefly, 10 μ l of the Presto Blue solution was added to each well and the plate was incubated for 3 h in the dark at 37°C. The absorbance of each sample was measured at 570 nm as the experimental wavelength and 600 nm as the reference or normalization wavelength. The cell viability was evaluated by the equation:

$$\text{Cell viability (\%)} = (OD_{hGDNF \text{ treatment}} - OD_{blank}) / (OD_{control} - OD_{blank}) \times 100\%$$

2.2 RNA-seq

hiPS-DANs were seeded in 96-well plates (1,000 cells per well) and cultured according to the manufacturer protocol (Cellular Dynamics) with or without hGDNF (100ng/ml) for 1, 3 and 7-days. Bulk RNAseq was performed following MARS-seq protocol adapted for bulk RNAseq (17,18) with minor modifications. Briefly, hiPS-DANs were resuspended in 100 μ l of Lysis/Binding Buffer (Ambion, Waltham, USA), vortexed and stored at -80°C until further processing. Poly-A RNA was reverse-transcribed using poly-dT oligos carrying a 7 nt-index. Pooled samples were subjected to linear amplification by IVT. The resulting aRNA was fragmented and dephosphorylated. Ligation of partial Illumina adaptor sequences (18) was followed by a second reverse-transcription reaction. Full Illumina adaptor sequences were added during final library amplification. RNA-seq libraries quantification was done with Qubit 3.0 Fluorometer (Life Technologies, Waltham, USA) and size profiles were examined using Agilent's 4200 TapeStation System. Libraries were sequenced in an Illumina NextSeq 500 at a sequence depth of 10 million reads per sample.

2.3 RNA-Seq Data Analysis

RNA sequencing data analysis was performed using the following workflow: (1) the quality of the samples was verified using FastQC software

(<https://www.bioinformatics.babraham.ac.uk/projects/fastqc/>); (2) the alignment of reads to the mouse genome (hg38) was performed using STAR (19); (3) gene expression quantification using read counts of exonic gene regions was carried out with featureCounts (20); (4) the gene annotation reference was Gencode v38 (21); and (5) differential expression statistical analysis was performed using R/Bioconductor (22).

First, gene expression data were normalized with edgeR (23) and voom (24). After quality assessment and outlier detection using R/Bioconductor (22), a filtering process was performed. Genes with reading counts lower than 6 in more than 50% of the samples of all the studied conditions were considered as not expressed in the experiment under study. LIMMA (24) was used to identify the genes with significant differential expression between experimental conditions. Genes were selected as differentially expressed using a p-value cut off $p < 0.01$. Further functional and clustering analyses and graphical representations were performed using R/Bioconductor (20) and clusterProfiler (25). The results were compared with a previously published experiment (11) using Gene Set Enrichment Analysis (GSEA) (25,26).

3. Results and discussion

3.1 *In vitro* cell viability and cell morphology post-hGDNF-treatment.

A Presto Blue assay was performed to examine hiPS-DANs viability after hGDNF treatment (100 ng/ml). The treatment with hGDNF showed a trend to increase cell viability (Figure 1A), although no significant differences were detected. Thus, the hiPS-DANs are terminally differentiated cells and therefore, lack the proliferation ability (27–29). Regarding cell morphology, hiPS-DANs showed the typical neuron morphology (Figure 1B).

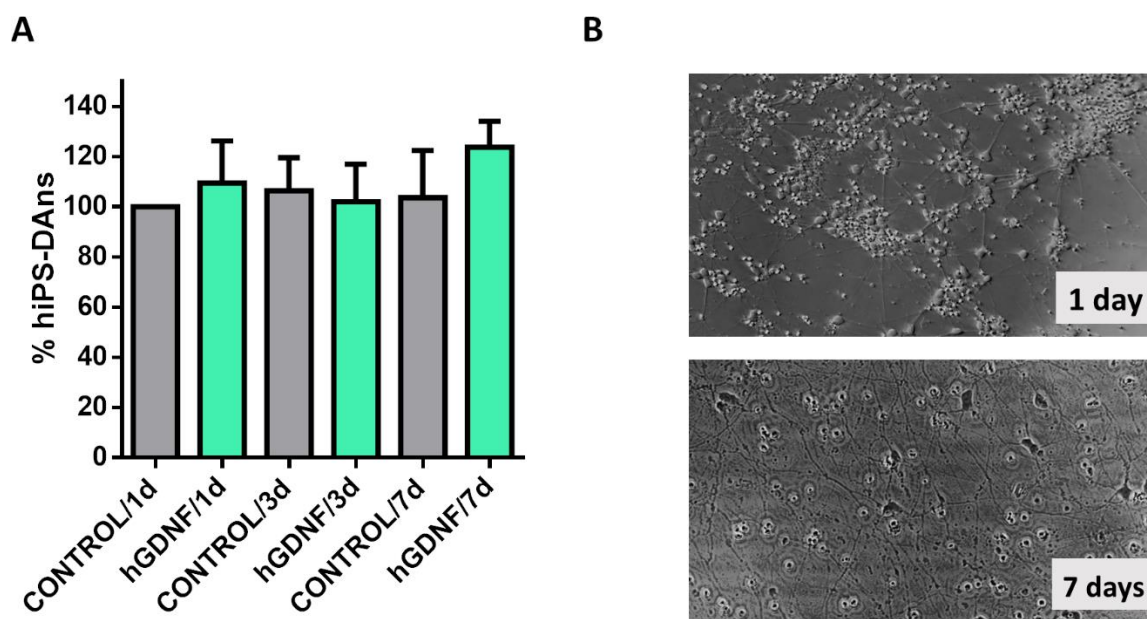


Figure 1. Cell survival of hiPS-DANs treated with hGDNF (A) and representative images of 1-day post hGDNF-treatment and 7-days post hGDNF-treatment showing the typical morphology of DANs (B).

3.2 hGDNF modulates hiPS-DANs gene expression

We next investigated the therapeutic potential of combining hiPS-DANs with hGDNF analyzing their transcriptome after treatment with the neurotrophic factor by RNA-seq. Our experimental design involved four biological replicates of hiPS-DANs cultured and treated with 100 ng/ml of hGDNF during 1, 3 and 7 days.

The whole-genome profile analysis revealed a remarkable potential of hGDNF to induce relevant changes in the gene expression profile of hiPS-DANs. First, we plotted the overlap between the datasets at different time points (1, 3 and 7 days) to show the changes in the transcriptome during hGDNF stimulation (Figure 2A). The greatest overlap occurred on day 1 and day 7, with 55 differentially expressed genes (Figure 2A). Interestingly, among the differentially expressed genes, hGDNF promoted DA biosynthesis through the regulation of TH gene expression, which was differentially expressed both at 1-day and 7-days post-hGDNF treatment. In addition, a significant enrichment of several functional categories was observed between days 1 and 7 (Figure 2B). In particular, the locomotor behavior pathway was significantly enriched. This is highly relevant and therefore, our data support the motor improvements previously seen in preclinical models of PD following hGDNF-treatment (6). Additionally, other pathways and biofunctions significantly enriched after hGDNF stimulation are represented in Figure 2C. We noticed that the major enrichment of pathways occurred on

day 1 and day 7, but not at day 3. Therefore, since the hGDNF effects on gene expression were not particularly relevant at day 3, these data were not considered for further analyses (Figure 2C).

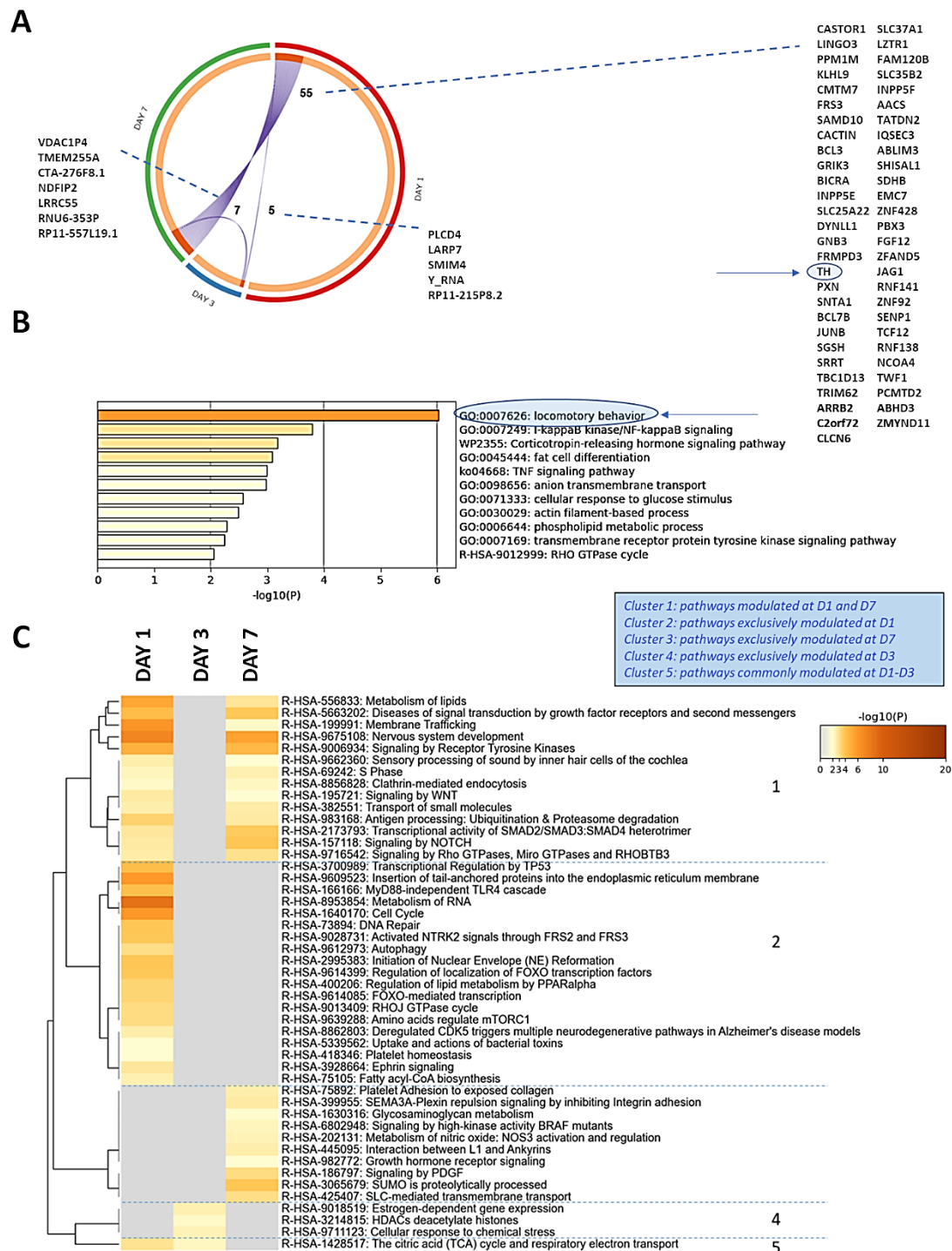


Figure 2. hGDNF modulates hiPS-DANs gene expression. (A) Circos-plot representing the overlap across datasets (Criteria: p-value < 0.01). (B) Significantly enriched functional categories corresponding to the commonly deregulated transcriptome between D1 and D7. (C) Functional clustering of pathways and biofunctions significantly enriched during GDNF stimulation of hiPS-DANs. The heatmap cells are

coloured by their p-values; grey cells indicate the lack of enrichment for that term in the corresponding transcript dataset. This analysis only integrates outputs from Reactome knowledgebase.

3.2.1 Gene expression profile of hiPS-DANs: 1-day post hGDNF-treatment

Having shown that hGDNF modulates hiPS-DANs gene expression, our results were compared with a previously published paper in which the viral delivery of hGDNF promoted the functional integration of DANs graft outcomes in a rodent model of PD (11). In this study, a transcriptome analysis was performed to investigate hGDNF effect on gene expression and DA metabolism within the graft finding 31 differentially expressed genes (11). In the short term (day 1), 6 genes (TH, ITGA3, CALB1, EGR1, SYTL5 and DUSP6) overlapped with their model. Remarkably, the initial administration of 100 ng/ml hGDNF induced a negative regulation of the TH gene in DANs, possibly as a compensatory mechanism in healthy dopaminergic cells (30,31). In addition, down-regulation of the ITGA3 gene, which may be involved in nerve cell formation, was identified (32). CALB1, a gene with a potential neuroprotective role (33,34), and EGR1, which is involved in neuronal plasticity (11) were also up-regulated at day 1 (Figure 3A). Next, a selective search for differentially expressed genes was performed in the following functional categories: MAPK, DA, Axon Ensheathment, Synaptic Transmission, Hormone and Secretion. Transcriptomic analysis reveals upregulation of some MAPK signalling pathway-related genes such as APP, which is involved in neuron projection maintenance (35,36), and EPHB1 involved in axon guidance (Figure 3B) (37,38). Specifically, hGDNF was implicated in the positive regulation of several genes involved in processes such as Axon ensheathment (EPB41L3, ID4, SBF2 and NSUN5) and genes involved in synaptic transmissions such as MEFC2 (39,40), NTNG1 (41) and EPBH1 (Figure 3C and 3D) (42). As shown in Figure 3D, hGDNF treatment also led to the upregulation of genes with secretory function. Particularly, the upregulation of Synaptojanin-1 (SYNJ1), an enzyme whose deficiency has been associated with increased vulnerability of dopaminergic neurons, was found (43).

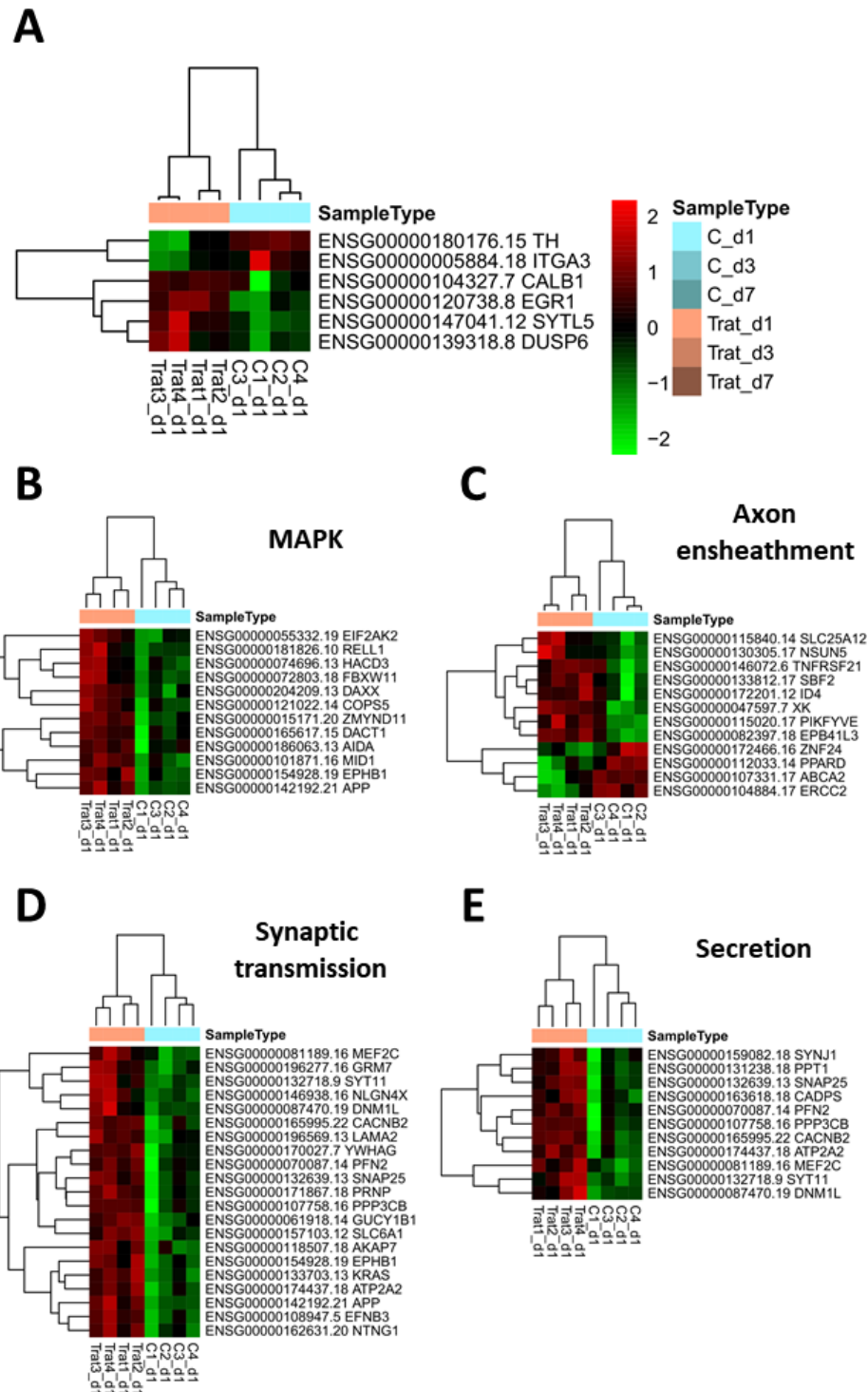


Figure 3. Transcriptional Profiling 1-day post hGDNF-treatment of hiPS-DANs in the Presence and Absence of GDNF Identified Known and Unknown MAPK, Axon ensheathment, Synaptic transmission, and secretion-Related Genes (A) Clustering analysis of differentially expressed genes in both models. (B–E) Heatmap of selected genes related to MAPK signalling (B), Axon ensheathment (C), Synaptic transmission (D), and secretion (E).

3.2.2 Gene expression profile of hiPS-DANs: 7-days post-hGDNF-treatment

The regulation of the transcriptome of hiPS-DANs occurred on day 1 and was followed by a remarkable modulation of the gene expression profile on day 7. In particular, the

CHAPTER 2

transcriptome analysis showed that 7 genes (SEMA3A, SCN5A, TH, DUSP4, SCN1B, FOS and SPRY4) overlap with the data from Gantner *et al* at day 7 (11). Going further, the comparative analysis between different neurological functions at day 1 and day 7 in GDNF-stimulated dopaminergic cells showed the activation of certain relevant molecular events such as the growth of neurites, the quantity of neurons or the growth of axons, among others (Figure 4). These findings agree with the protective effects reported in both rodent and primate models of PD (14,44). In particular, the hGDNF-treatment was able to promote DANs survival and to stimulate regenerative sprouting from spared axons in the partially denervated striatum (14,44).

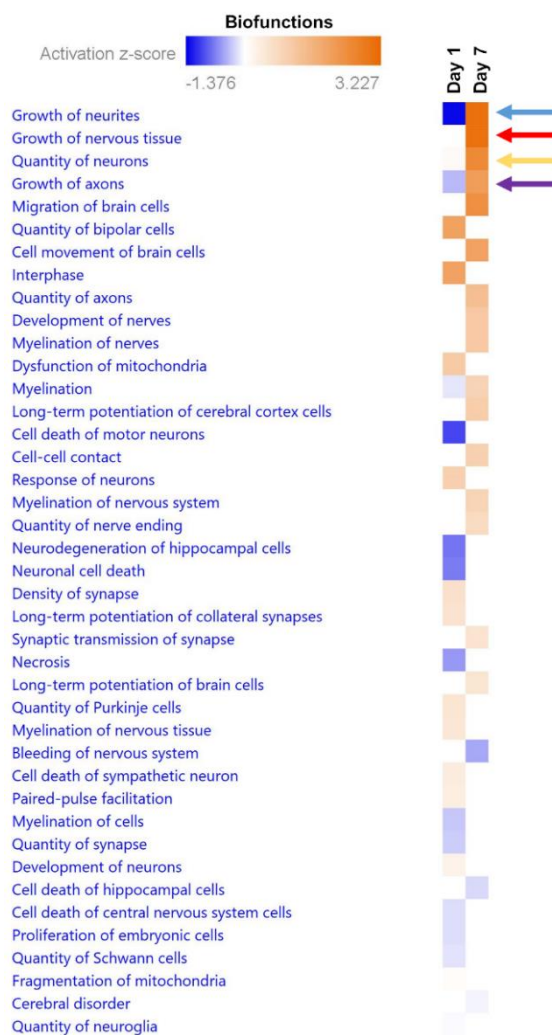


Figure 4. A comparative analysis between deregulated transcriptomes at day 1 and day 7 in hGDNF-stimulated hiPS-DANs based on the activation Z-score. The primary purpose of the activation z-score is to infer the activation states of predicted molecular events. The basis for inference is the relationships in the molecular network that represent experimentally observed gene expression or transcription events, and are associated with a literature-derived regulation direction which can be either “activating” or “inhibiting”.

In addition, the clustering analysis at day 7 showed some differences with those detected at day 1 (Figure 5A-5E). Interestingly, deregulation of SEMA3A gene, whose overexpression has been related to dopaminergic depletion, was found (45). In addition, up-regulation of DUSP4 gene, which promote the neuronal differentiation process (46,47) was observed (Figure 5A). Regarding the expression of TH, the rate-limiting enzyme in dopamine synthesis, we demonstrate that hGDNF treatment contributes to its significant upregulation on hiPS-DANs cultures (Figure 5A) (48). Selective analysis of the upregulated genes revealed many with known roles in DA development and homeostases such as WNT3, EN1, and FGF20 (Figure 5B). The up-regulation of these genes, together with TH up-regulation, reveals how exogenous hGDNF influences DA system function, contributing to the survival of DANs and DA synthesis. It is noteworthy that hGDNF exerts its actions in DANs activating GFR α 1·RET receptor complex. This, in turn, regulates downstream PI3K-AKT and mitogen-activated protein kinase (MAPK)-ERK pathways that regulate transcription of genes related to survival and/or plasticity (11,49). The upregulation of several MAPK-associated genes with known roles on plasticity (DUSP1, MEN1 and APOE) (46,50,51), cell migration and proliferation (MYC, FOS and ITGB1BP1) was also identified in our study (Figure 5C) (52–54), suggesting that hGDNF has an important protective role on DANs mainly via the MAPK-ERK pathway (11). From another perspective, the upregulation of the SOCS-1 gene was also detected supporting the hypothesis that hGDNF can protect from neurodegeneration through the inhibition of neuroinflammation pathways (Figure 5E) (55–57). Collectively, the transcriptional changes induced by hGDNF in DANs cultures throughout the study period (1 and 7 days) seem to be aimed at promoting the survival and plasticity of DA neurons, as well as inducing DA biosynthesis through the regulation of genes TH, WNT3, EN1 and FGF20, involved in DA metabolism.

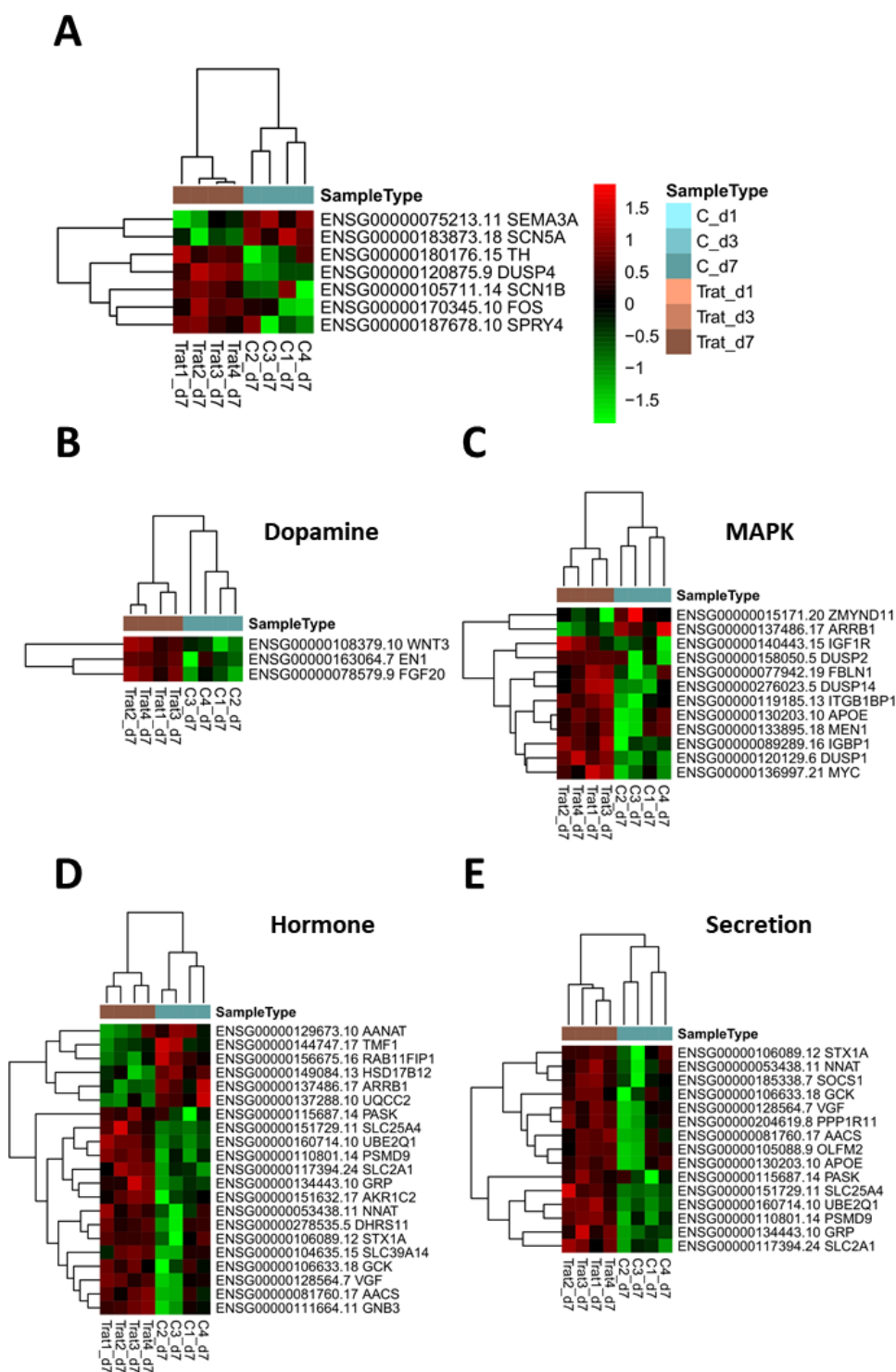


Figure 5. Transcriptional Profiling 7-days post-hGDNF-treatment of hiPS-DANs in the Presence and Absence of GDNF Identified Known and Unknown DA Homeostatic, MAPK, Hormone and Secretion-Related Genes. (A) Clustering analysis of differentially expressed genes in both models. (B–E) Heatmap of selected genes related to dopamine (B), MAPK signalling (C), Hormone (D), and secretion (E).

3.2.3 Gene Set Enrichment Analysis (GSEA) for study validation

Having shown that the transcriptional changes induced by hGDNF in DANs promote the survival and plasticity of DA neurons via the MAPK pathway, we performed a GSEA on the gene sets by Gantner *et al.* to check and confirm our findings (11) (Figure 6). The

enrichment analysis pointed out that MAPK pathway genes and the up-regulated genes found by Gantner *et al.* were significantly enriched in our gene set at day 7. These findings confirm the previous observations and support the potential of hGDNF to modulate the survival of cell grafts based on hiPS-DANs via the MAPK pathway [31].

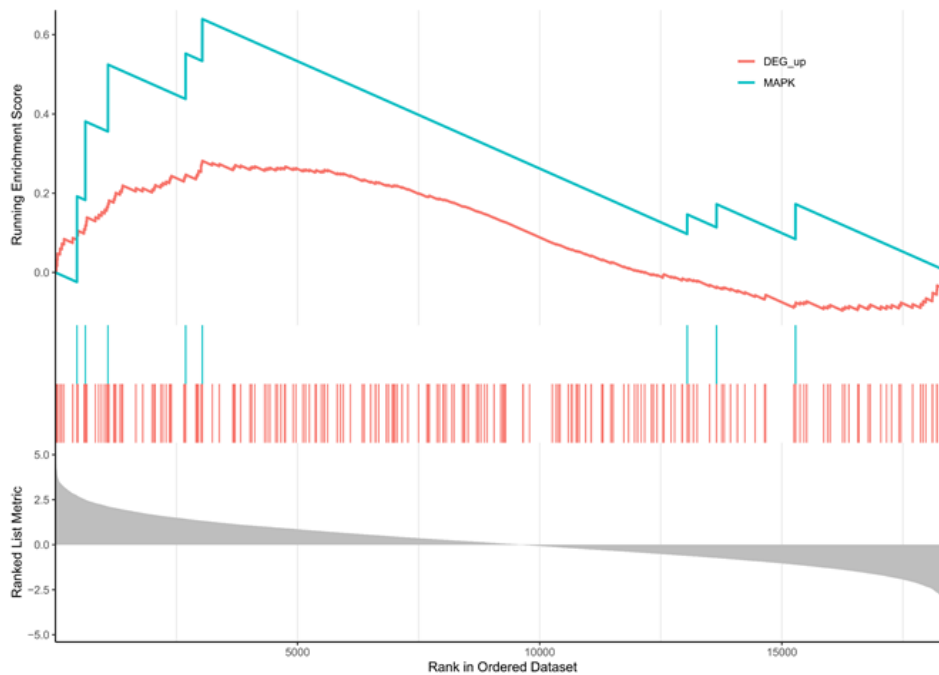


Figure 6. Transcriptional profiling of hMSCs in the presence of hGDNF: GSEA enrichment to compare models. The Running Enrichment score shows that MAPK pathway genes (blue line) and the statistically up-regulated (red line) published by Gantner *et al.* (2020) are enriched in the up-regulated genes of our model.

4. Conclusions

In summary, these findings support the potential of hGDNF to modulate the plasticity and survival of cell grafts based on hiPS-DANs via the MAPK pathway. Therefore, the transcriptional changes that occurred support the role of co-transplantation strategy (hGDNF-DANs), not only to improve its functional integration, but also to enhance the biological functions and the clinical outcome of DANs grafts for the treatment of PD.

5. References

1. Ray Dorsey E, Elbaz A, Nichols E, Abd-Allah F, Abdelalim A, Adsuar JC, et al. Global, regional, and national burden of Parkinson's disease, 1990–2016: a systematic analysis for the Global Burden of Disease Study 2016. *Lancet Neurol.* 2018;17(11):939–53.
2. Mao Q, Qin W zhi, Zhang A, Ye N. Recent advances in dopaminergic strategies for the treatment of Parkinson's disease. *Acta Pharmacol Sin.* 2020 Feb 28;41(4):471–82.
3. Del Rey NLG, Quiroga-Varela A, Garbayo E, Carballo-Carbajal I, Fernández-Santiago R, Monje MHG, et al. Advances in parkinson's disease: 200 years later. *Front Neuroanat.* 2018 Dec 14;12:113.
4. Ford E, Pearlman J, Ruan T, Manion J, Waller M, Neely GG, et al. Human Pluripotent Stem Cells-Based Therapies for Neurodegenerative Diseases: Current Status and Challenges. *Cells.* 2020 Nov 20;9(11).
5. Torres-Ortega PV, Martínez-Valbuena I, Martí-Andrés G, Hanafy AS, Luquin MR, Garbayo E, et al. Nanobiotechnology in Parkinson's Disease. In: *Nanobiotechnology in Neurodegenerative Diseases.* Springer International Publishing; 2019. p. 177–208.
6. Lee TK, Yankee EL. A review on Parkinson's disease treatment. *Neuroimmunol Neuroinflammation.* 2021 Jan 25;8:[Online First].
7. Li H, Han S, Feng J. Delirium after Deep Brain Stimulation in Parkinson's Disease. *Parkinsons Dis.* 2021;2021.
8. C Henchcliffe MP. Repairing the brain: cell replacement using stem cell-based technologies. *J Park Dis.* 2018;8(s1):S131–7.
9. Parmar M, Grealish S, Henchcliffe C. The future of stem cell therapies for Parkinson disease. *Nat Rev Neurosci.* 2020 Jan 6;21(2):103–15.
10. Moriarty N, Pandit A, Dowd E. Encapsulation of primary dopaminergic neurons in a GDNF-loaded collagen hydrogel increases their survival, re-innervation and function after intra-striatal transplantation. *Sci Rep.* 2017 Nov 22;7(1):16033.
11. Gantner CW, de Luzy IR, Kauhausen JA, Moriarty N, Niclis JC, Bye CR, et al. Viral Delivery of GDNF Promotes Functional Integration of Human Stem Cell Grafts in Parkinson's Disease. *Cell Stem Cell.* 2020 Apr 2;26(4):511–526.e5.
12. Brundin P, Karlsson J, Emgård M, Kaminski Schierle GS, Hansson O, Petersén Å,

- et al. Improving the survival of grafted dopaminergic neurons: A review over current approaches. *Cell Transplant*. 2000 Jun 22;9(2):179–95.
13. Saarenpää T, Kogan K, Sidorova Y, Mahato AK, Tascón I, Kaljunen H, et al. Zebrafish GDNF and its co-receptor GFR α 1 activate the human RET receptor and promote the survival of dopaminergic neurons in vitro. *PLoS One*. 2017 May 1;12(5):e0176166.
 14. Garbayo E, Ansorena E, Lana H, Carmona-Abellan M del M, Marcilla I, Lanciego JL, et al. Brain delivery of microencapsulated GDNF induces functional and structural recovery in parkinsonian monkeys. *Biomaterials*. 2016 Dec 1;110:11–23.
 15. Garbayo E, Montero-Menei CN, Ansorena E, Lanciego JL, Aymerich MS, Blanco-Prieto MJ. Effective GDNF brain delivery using microspheres-A promising strategy for Parkinson's disease. *J Control Release*. 2009 Apr 17;135(2):119–26.
 16. Deng X, Liang Y, Lu H, Yang Z, Liu R, Wang J, et al. Co-transplantation of GDNF-overexpressing neural stem cells and fetal dopaminergic neurons mitigates motor symptoms in a rat model of parkinson's disease. *PLoS One*. 2013 Dec 3;8(12):e80880.
 17. Lavin Y, Kobayashi S, Leader A, Amir E ad D, Elefant N, Bigenwald C, et al. Innate Immune Landscape in Early Lung Adenocarcinoma by Paired Single-Cell Analyses. *Cell*. 2017 May 4;169(4):750–765.e17.
 18. Jaitin DA, Kenigsberg E, Keren-Shaul H, Elefant N, Paul F, Zaretsky I, et al. Massively parallel single-cell RNA-seq for marker-free decomposition of tissues into cell types. *Science (80-)*. 2014;343(6172):776–9.
 19. Dobin A, Davis CA, Schlesinger F, Drenkow J, Zaleski C, Jha S, et al. STAR: Ultrafast universal RNA-seq aligner. *Bioinformatics*. 2013 Jan;29(1):15–21.
 20. Liao Y, Smyth GK, Shi W. FeatureCounts: An efficient general purpose program for assigning sequence reads to genomic features. *Bioinformatics*. 2014 Apr 1;30(7):923–30.
 21. Harrow J, Frankish A, Gonzalez JM, Tapanari E, Diekhans M, Kokocinski F, et al. GENCODE: The reference human genome annotation for the ENCODE project. *Genome Res*. 2012 Sep;22(9):1760–74.
 22. Gentleman RC, Carey VJ, Bates DM, Bolstad B, Dettling M, Dudoit S, et al. Bioconductor: open software development for computational biology and bioinformatics. *Genome Biol*. 2004 Sep 15;5(10):1–16.

CHAPTER 2

23. Robinson MD, McCarthy DJ, Smyth GK. edgeR: A Bioconductor package for differential expression analysis of digital gene expression data. *Bioinformatics*. 2009 Nov 11;26(1):139–40.
24. Ritchie ME, Phipson B, Wu D, Hu Y, Law CW, Shi W, et al. Limma powers differential expression analyses for RNA-sequencing and microarray studies. *Nucleic Acids Res*. 2015 Jan 6;43(7):e47.
25. Yu G, Wang LG, Han Y, He QY. ClusterProfiler: An R package for comparing biological themes among gene clusters. *Omi A J Integr Biol*. 2012 May 1;16(5):284–7.
26. Subramanian A, Tamayo P, Mootha VK, Mukherjee S, Ebert BL, Gillette MA, et al. Gene set enrichment analysis: A knowledge-based approach for interpreting genome-wide expression profiles. *Proc Natl Acad Sci U S A*. 2005 Oct 25;102(43):15545–50.
27. Lu B, Atala A. Small Molecules: Controlling Cell Fate and Function. In: *In Situ Tissue Regeneration: Host Cell Recruitment and Biomaterial Design*. Elsevier Inc.; 2016. p. 87–110.
28. Zhao ML, Rabiee A, Kovary KM, Bahrami-Nejad Z, Taylor B, Teruel MN. Regulation of the time when cells commit to terminally differentiate controls the number of differentiated cells. *bioRxiv*. 2019 Dec 30;632570.
29. Ruijtenberg S, van den Heuvel S. Coordinating cell proliferation and differentiation: Antagonism between cell cycle regulators and cell type-specific gene expression. *Cell Cycle*. 2016 Jan 17;15(2):196–212.
30. Kirik D, Georgievska B, Björklund A. Localized striatal delivery of GDNF as a treatment for Parkinson disease. *Nat Neurosci*. 2004 Jan 27;7(2):105–10.
31. Tenenbaum L, Humbert-Claude M. Glial cell line-derived neurotrophic factor gene delivery in parkinson's disease: A delicate balance between neuroprotection, trophic effects, and unwanted compensatory mechanisms. *Front Neuroanat*. 2017 Apr 1;11:29.
32. Brązert M, Kranc W, Celichowski P, Jankowski M, Piotrowska-Kempisty H, Pawelczyk L, et al. Expression of genes involved in neurogenesis, and neuronal precursor cell proliferation and development: Novel pathways of human ovarian granulosa cell differentiation and transdifferentiation capability in vitro. *Mol Med Rep*. 2020;21(4):1749–60.
33. Yuan HH, Chen RJ, Zhu YH, Peng CL, Zhu XR. The neuroprotective effect of

- overexpression of calbindin-D28k in an animal model of Parkinson's disease. *Mol Neurobiol.* 2013;47(1):117–22.
34. Brimblecombe KR, Vietti-Michelina S, Platt NJ, Kastli R, Hnieno A, Gracie CJ, et al. Calbindin-D28K Limits Dopamine Release in Ventral but Not Dorsal Striatum by Regulating Ca²⁺ Availability and Dopamine Transporter Function. *ACS Chem Neurosci.* 2019 Aug 21;10(8):3419–26.
 35. Oh ES, Savonenko A V., King JF, Fangmark Tucker SM, Rudow GL, Xu G, et al. Amyloid precursor protein increases cortical neuron size in transgenic mice. *Neurobiol Aging.* 2009 Aug;30(8):1238–44.
 36. Gakhar-Koppole N, Hundeshagen P, Mandl C, Weyer SW, Allinquant B, Müller U, et al. Activity requires soluble amyloid precursor protein α to promote neurite outgrowth in neural stem cell-derived neurons via activation of the MAPK pathway. *Eur J Neurosci.* 2008 Sep;28(5):871–82.
 37. Bush JO, Soriano P. Ephrin-B1 regulates axon guidance by reverse signaling through a PDZ-dependent mechanism. *Genes Dev.* 2009 Jul 1;23(13):1586–99.
 38. Rudolph J, Gerstmann K, Zimmer G, Steinecke A, Döding A, Bolz J. A dual role of EphB1/ephrin-B3 reverse signaling on migrating striatal and cortical neurons originating in the preoptic area: Should I stay or go away? *Front Cell Neurosci.* 2014 Jul 18;8(JULY):185.
 39. Cho EG, Zaremba JD, McKercher SR, Talantova M, Tu S, Masliah E, et al. MEF2C enhances dopaminergic neuron differentiation of human embryonic stem cells in a parkinsonian rat model. *PLoS One.* 2011 Aug 25;6(8).
 40. Dietrich JB. The MEF2 family and the brain: From molecules to memory. *Cell Tissue Res.* 2013 Feb 9;352(2):179–90.
 41. Matsukawa H, Akiyoshi-Nishimura S, Zhang Q, Luján R, Yamaguchi K, Goto H, et al. Netrin-G/NGL complexes encode functional synaptic diversification. *J Neurosci.* 2014 Nov 19;34(47):15779–92.
 42. Lin L, Lesnick TG, Maraganore DM, Isacson O. Axon guidance and synaptic maintenance: preclinical markers for neurodegenerative disease and therapeutics. *Trends Neurosci.* 2009 Mar;32(3):142–9.
 43. Pan P-Y, Sheehan P, Wang Q, Zhang Y, Wang J, El Gaamouch F, et al. Haploinsufficiency of Parkinsonism Gene SYNJ1 Contributes to Dopamine neuron Vulnerability in Aged Mice. *bioRxiv.* 2017 Dec 13;233585.
 44. Barker RA, Björklund A, Gash DM, Whone A, Van Laar A, Kordower JH, et al.

CHAPTER 2

- GDNF and Parkinson's Disease: Where Next? A Summary from a Recent Workshop. *J Parkinsons Dis.* 2020;10(3):875–91.
45. Yasuhara T, Shingo T, Muraoka K, Kameda M, Agari T, Wenji Y, et al. Toxicity of semaphorin3A for dopaminergic neurons. *Neurosci Lett.* 2005 Jul 1;382(1–2):61–5.
 46. Pérez-Sen R, Queipo MJ, Gil-Redondo JC, Ortega F, Gómez-Villafuertes R, Miras-Portugal MT, et al. Dual-specificity phosphatase regulation in neurons and glial cells. *Int J Mol Sci.* 2019 Apr 2;20(8).
 47. Kim SY, Han YM, Oh M, Kim WK, Oh KJ, Lee SC, et al. DUSP4 regulates neuronal differentiation and calcium homeostasis by modulating ERK1/2 phosphorylation. *Stem Cells Dev.* 2015 Mar 15;24(6):686–700.
 48. White R, Thomas M. Moving Beyond Tyrosine Hydroxylase to Define Dopaminergic Neurons for Use in Cell Replacement Therapies for Parkinson's Disease. *CNS Neurol Disord - Drug Targets.* 2012 Oct 1;11(4):340–9.
 49. Kramer ER, Liss B. GDNF-Ret signaling in midbrain dopaminergic neurons and its implication for Parkinson disease. *FEBS Lett.* 2015 Dec 21;589(24):3760–72.
 50. Zhuang K, Huang C, Leng L, Zheng H, Gao Y, Chen G, et al. Neuron-Specific Menin Deletion Leads to Synaptic Dysfunction and Cognitive Impairment by Modulating p35 Expression. *Cell Rep.* 2018 Jul 17;24(3):701–12.
 51. Kim J, Yoon H, Basak J, Kim J. Apolipoprotein E in synaptic plasticity and alzheimer's disease: Potential cellular and molecular mechanisms. *Mol Cells.* 2014 Nov 1;37(11):833–40.
 52. Wanzel M, Russ AC, Kleine-Kohlbrecher D, Colombo E, Pelicci P-G, Eilers M. A ribosomal protein L23-nucleophosmin circuit coordinates Miz1 function with cell growth. *Nat Cell Biol* 2008 109. 2008 Aug 1;10(9):1051–61.
 53. Fournier H-N, Dupé-Manet S, Bouvard D, Luton F, Degani S, Block MR, et al. Nuclear Translocation of Integrin Cytoplasmic Domain-associated Protein 1 Stimulates Cellular Proliferation. *Mol Biol Cell.* 2005 Apr;16(4):1859.
 54. Molina JR, Adjei AA. The Ras/Raf/MAPK Pathway. *J Thorac Oncol.* 2006 Jan 1;1(1):7–9.
 55. Lofrumento DD, Nicolardi G, Cianciulli A, Nuccio F De, Pesa V La, Carofiglio V, et al. Neuroprotective effects of resveratrol in an MPTP mouse model of Parkinson's-like disease: Possible role of SOCS-1 in reducing pro-inflammatory responses. *Innate Immun.* 2014 Jun 13;20(3):249–60.

56. Tiwari PC, Pal R. The potential role of neuroinflammation and transcription factors in Parkinson disease. *Dialogues Clin Neurosci.* 2017 Mar 1;19(1):71–80.
57. Wang Z, Li S, Wang Y, Zhang X, Chen L, Sun D. GDNF enhances the anti-inflammatory effect of human adipose-derived mesenchymal stem cell-based therapy in renal interstitial fibrosis. *Stem Cell Res.* 2019 Dec 1;41:101605.

**Encapsulation of hMSCs and hGDNF in a novel injectable
nanoreinforced-hydrogel to improve cell replacement therapy in
Parkinson´s Disease**

Pablo V. Torres-Ortega ^(1,2), Daniel Plano ^(1,2), Jacobo Paredes ⁽³⁾, Javier Aldazabal ⁽³⁾,
Rosario Luquin ^(2,4), Carmen Sanmartin ^(1,2), María J. Blanco-Prieto ^(1,2), Elisa Garbayo ^(1,2)

¹ Department of Pharmaceutical Technology and Chemistry, Faculty of Pharmacy and
Nutrition, University of Navarra, C/ Irunlarrea 1, 31008 Pamplona, Spain

² Navarra Institute for Health Research, IdiSNA, C/ Irunlarrea 3, 31008 Pamplona, Spain

³ Tecnun, School of Engineering, University of Navarra, C/ Manuel de Lardizábal 15,
20018 San Sebastián, Spain

⁴ Department of Neurology and Neurosciences, Clínica Universidad de Navarra,
Pamplona, C/ Pío XII 36, 31008 Pamplona, Spain.

*Corresponding authors at: Department of Pharmaceutical Technology and Chemistry,
Faculty of Pharmacy and Nutrition, Universidad de Navarra, C/Irunlarrea 1, 31008
Pamplona, Spain.

E-mail addresses: egarbayo@unav.es (E. Garbayo), mjblanco@unav.es (M.J. Blanco-
Prieto).

Under review

(November 2021)

Abstract

Parkinson's disease (PD) is the most common movement disorder affecting approximately 1–2% of the population \geq 65 years of age. The absence of effective treatments to stop neuronal degeneration and the limited ability of the brain to repair itself after neural damage represents one of the most difficult challenges in medicine. Hyaluronic acid (HA) has been proposed for tissue brain engineering and drug delivery applications, but its poor mechanical strength has hampered its widespread use. Notably, HA can easily be modified to acquire mechanical properties suited to brain engineering applications. Here, we develop a multifunctional drug delivery system where human mesenchymal stem cells (hMSCs) and human glial-derived neurotrophic factor (hGDNF) are included in a nanoparticle-modified HA hydrogel (HG) to form a nanoreinforced vehicle. This approach is intended to design a suitable matrix for cell delivery and controlled drug release for brain administration in PD. To this end, we first evaluated the therapeutic potential of combining hMSCs and hGDNF in the biomaterial by RNA-seq analysis. We found that the hGDNF up-regulate MAPK-associated genes involved in plasticity and neurogenesis. Next, we prepare a guest-host HA-HG that was nanoreinforced with hGDNF-NPs (HA-HG-NPs) and combined/loaded with hMSCs (HA-HG-NPs-hMSCs). The HGs showed shear-thinning and self-healing features. The nanoreinforcement not only enhanced the mechanical properties of HA-HG but also proved a successful approach to protect hGDNF from degradation and achieve its controlled release. Finally, the nanoreinforced HG provide a friendly environment for hMSCs. Therefore, the proposed approach represents a powerful tool for brain tissue engineering.

Keywords

Nanoreinforcement; Shear thinning properties; Self-healing properties; hGDNF; hMSCs; Brain tissue engineering.

1. Introduction

Parkinson's disease (PD) is a progressive neurodegenerative disorder that affects over 1% of the population over the age of 65 (1). Histopathologically, it is characterised by the loss of dopaminergic neurons in the substantia nigra pars compacta followed by a depletion of dopamine levels in the striatum and by the presence of intracytoplasmic inclusions called Lewy bodies (LBs) (2). Currently, dopamine replacement therapy (DRT) is the standard treatment for PD management. However, its use is often associated with significant and sometimes intolerable side effects as the disease progresses, leading to significant declines in quality of life (3). Therefore, a great challenge in the PD field is the development of novel therapies able to prevent the ongoing neurodegeneration and halt disease progression. Cell replacement is being investigated as a therapeutic approach for neurodegenerative diseases (4,5). However, a current limitation of cell therapy is the low cell survival after implantation (6,7). The combination of cells with drug delivery systems such as hydrogels (HGs) able to supply trophic factors could solve this issue and enhance the benefit of cell therapy.

Given the mechanical properties of the brain, which is particularly soft, neuroregenerative strategies must mimic its biochemical and mechanical characteristics (8). HGs are one of the most promising systems in the area of neuronal regeneration due to their tissue-like characteristics, versatility in terms of degradation, ability to release active drugs, and biocompatibility (9). HGs would facilitate cell injection and improve their survival and differentiation by acting as a matrix or scaffold (10). Among natural polymers, hyaluronic acid (HA) is a particularly attractive material for biomedical applications. To date, hyaluronic acid hydrogels (HA-HGs) have been used in various delivery systems in combination with cells or proteins (11). However, the poor mechanical properties of HA limits its clinical applications (12). Fortunately, these properties can be modulated by chemical modifications, guest-host interactions or nanoreinforcement (12–14).

Regarding trophic factors, human glial cell line-derived neurotrophic factor (hGDNF) is the most potent dopaminergic factor described so far, resulting a promising therapeutic agent for PD treatment (15–17). Nonetheless, its short *in vivo* half-life hinders the clinical application of this approach (18,19). The encapsulation of hGDNF in nanoparticles (NPs) may overcome this issue by providing protein protection from degradation and sustained drug release over time. Importantly, the subsequent incorporation of NPs into an HG would provide an additional advantage for the clinical delivery of hGDNF in the striatum

(20,21). In this sense, nanoreinforced HGs have recently emerged as a promising approach to develop tunable shear-thinning and self-healing materials and to achieve a more prolonged drug release (14).

This study proposes a multi-functional drug delivery system for brain tissue engineering, where hGDNF and human mesenchymal stem cells (hMSCs) are combined into a nanoreinforced HG for their simultaneous administration. The therapeutic potential of combining hMSCs with hGDNF was first evaluated by RNA-seq analysis. Then, a guest-host HA-HG nanoreinforced with hGDNF-NPs (HA-HG-NPs) and combined/loaded with stem cells (HA-HG-NPs-hMSCs) was prepared and characterized. The mechanical properties of this HG reveal that it is a strong biomaterial, mechanically compatible with brain tissue and easily injectable. In addition, the developed scaffold can protect hGDNF from degradation and achieve its sustained controlled release over time for the promotion of brain tissue repair. The cytocompatibility studies reveal that the multi-functional HG is a safe system for *in vivo* administration. Therefore, the findings of the present study suggest that biomimetic platform represents an excellent vehicle to provide a controlled release of therapeutic agents and to improve the cell-engraftment for addressing brain repair in PD.

2. Experimental section

2.1 RNA-seq

hMSCs were seeded in 96-well plates (1,000 cells per well) and cultured in hMSCs complete media with or without hGDNF (100 ng/ml) for one week. Bulk RNAseq was performed following MARS-seq protocol adapted for bulk RNAseq (22,23) with minor modifications. Briefly, hMSCs were resuspended in 100 μ l of Lysis/Binding Buffer (Ambion, Waltham, USA), vortexed and stored at -80°C until further processing. Poly-A RNA was reverse-transcribed using poly-dT oligos carrying a 7 nt-index. Pooled samples were subjected to linear amplification by IVT. The resulting aRNA was fragmented and dephosphorylated. Ligation of partial Illumina adaptor sequences (23) was followed by a second reverse-transcription reaction. Full Illumina adaptor sequences were added during final library amplification. RNA-seq libraries quantification was done with Qubit 3.0 Fluorometer (Life Technologies, Waltham, USA) and size profiles were examined using Agilent's 4200 TapeStation System. Libraries were sequenced in an Illumina NextSeq 500 at a sequence depth of 10 million reads per sample.

2.1.2 RNA-Seq Data Analysis

RNA sequencing data analysis was performed using the following workflow: (1) the quality of the samples was verified using FastQC software (<https://www.bioinformatics.babraham.ac.uk/projects/fastqc/>); (2) the alignment of reads to the mouse genome (hg38) was performed using STAR [24]; (3) gene expression quantification using read counts of exonic gene regions was carried out with featureCounts (25); (4) the gene annotation reference was Gencode v38 (26); and (5) differential expression statistical analysis was performed using R/Bioconductor (27).

First, gene expression data was normalized with edgeR (28) and voom (29). After quality assessment and outlier detection using R/Bioconductor (27), a filtering process was performed. Genes with read counts lower than 6 in more than 50% of the samples of all the studied conditions were considered as not expressed in the experiment under study. LIMMA (29) was used to identify the genes with significant differential expression between experimental conditions. Genes were selected as differentially expressed using a p-value cut off $p < 0.01$. Further functional and clustering analyses and graphical representations were performed using R/Bioconductor (25) and clusterProfiler (30). The results were compared with a previously published experiment (31) using Gene Set Enrichment Analysis (GSEA) (30,32).

2.2 Preparation of HA-based HGs

The protocol for HA-HGs preparation was adapted from previous work (12). All chemicals were purchased from Sigma Aldrich (St.Louis, MO, USA) unless otherwise stated.

2.2.1 HA-CD synthesis

Synthesis of *p*-toluensulfonic anhydride (Ts₂O)

16 g of *p*-toluenesulfonyl chloride and 4 g of *p*-toluenesulfonic acid monohydrate were dispersed in 100 mL of methylene chloride (Scharlab, Barcelona, Spain). The solution was stirred overnight and filtered to remove unreacted *p*-toluenesulfonyl chloride. The solvent from the filtered solution was evaporated with the rotavapor and the solid obtained was dried with vacuum overnight.

Synthesis of 6-*O*-monotosyl-6-deoxy-β-cyclodextrin (CD-Tos)

22.39 g of β-cyclodextrin (β-CD) and 9.42 g of Ts₂O were dispersed in 200 mL of deionized water and the suspension was stirred for at least 2 hours. Then, 100 mL of NaOH 2.5 M (Scharlab, Barcelona, Spain) were added to the solution. The unreacted

CHAPTER 2

Ts₂O was removed by filtration and the solution was acidified by the addition of HCl 37% (Scharlab, Barcelona, Spain) until pH 2. The precipitate was filtered under vacuum and the solid obtained was washed with diethylether (3x25 mL) (Scharlab, Barcelona, Spain).

Synthesis of HA-CD

1 g of sodium hyaluronate (Fagron, Barcelona, Spain) was dissolved in 500 mL of deionized water at 80°C. The solution was left under continuous stirring overnight. Then, 0.13 g of CD-Tos were added to the solution. After 62 hours, the product was frozen and lyophilized for 5 days. ¹H-NMR (with D₂O as solvent) spectroscopy was used to confirm the synthesis of HA-CD.

2.2.2 HA-AD synthesis

1 g of HA was slowly dissolved in 400 mL of deionized water. Then, 0.26 mL of triethylamine (TEA) and 0.37 g of adamantane (AD) were added to the solution. The solution was stirred for 62 hours, at room temperature (RT). The precipitate was filtered under vacuum and lyophilized for at least 5 days. ¹H-NMR (with D₂O as a solvent) spectroscopy was used to confirm the synthesis of HA-AD.

2.2.3 Quantification of residual TEA in HA-AD

To quantify the residual amount of TEA, quantitative ¹H-NMR was performed using a known amount of dimethylsulfone as standard. Subsequently, the ratio of the integrated signals was determined and the amount of TEA was calculated and expressed as mg TEA/mg HA-AD.

2.3 Preparation of hGDNF-loaded nanospheres with TROMS

hGDNF was expressed and purified from BHK-21 cells using a Semliki Forest virus (SFV) expressing vector as described before [33]. hGDNF-loaded NPs were prepared by solvent extraction/evaporation method using the Total Recirculation One-Machine System (TROMS). Briefly, the organic solution composed of 2 mL of methylene chloride:acetone (3:1) containing 50 mg of Resomer RG 503H (poly (lactic-co-glycolic acid) (PLGA); M_w: 24,000-38,000 Da) was injected through a needle with an inner gauge diameter of 0.17 mm at a ratio of 35 mL/min into the inner aqueous phase (150 µL). The inner aqueous phase contained 40 µg of hGDNF in 10 mM phosphate, 25 mM sodium chloride (2), pH 7.4, 2.5 mg of HSA and 90 µL of PEG 400. Next, the primary emulsion (W1/O) was recirculated through the system for 1:30 min under a turbulent regime at a flow rate of 35 mL/min. The first emulsion was then injected into 20 mL of the external aqueous phase (W2) composed of 1% polyvinyl alcohol (PVA) (M_w: 13,000-23,000 Da).

The turbulent injection through the needle with an inner gauge diameter of 0.17 mm resulted in the formation of a multiple emulsion (W1/O/W2), which was further homogenized by circulation through the system for 5 min. The W1/O/W2 emulsion was stirred at 300 rpm at RT for at least 2 h to allow solvent evaporation and nanospheres formation. Non-loaded NPs (without hGDNF) were prepared following the same method described above.

2.4 Characterization of nanospheres

2.4.1 Particle size analysis

The mean particle size was determined by Nanoparticle Tracking Analysis (NTA) (Nanosight NS300, Malvern Instruments). All samples were diluted in MilliQ Water to a final volume of 0.5 mL. The ideal measurement concentrations were found by pre-testing the ideal particle per frame value (20–100 particles/frame). The polydispersity index (PDI) was measured by dynamic light scattering (DLS) (Zetasizer Nano, Malvern Instruments). The same samples were used to analyze the surface charge of the NPs by measuring the zeta potential with laser Doppler velocimetry (Zetasizer Nano, Malvern Instruments) at 25 °C. Measurements were conducted in triplicate and the results were presented as the mean \pm standard deviation.

2.4.2 Drug content

The quantity of hGDNF encapsulated in the nanospheres was determined by dissolving 5 mg of freeze-dried loaded particles in 1 mL of dimethyl sulfoxide (DMSO). The amount of hGDNF was measured by ELISA using hGDNF enzyme-linked immunosorbent assay kit from Thermofisher.

2.4.3 In vitro release

To characterize the *in vitro* release profile of hGDNF from PLGA NPs, 3 mg of freeze-dried loaded NPs (n=3) were dissolved in 150 μ l of PBS supplemented with 0.1% HSA and microbiologically protected with 0.02% _{w/w} sodium azide. The incubation was performed with orbital rotation using an Eppendorf multi-rotator. Samples were maintained at 37° C with orbital rotation (15 rpm) for 37 days. The times selected to perform the release profile were 6 hours, 1, 2, 3, 7, 14, 20, 28, 35 and 37 days. At these times tubes containing the samples were centrifuged (25000g, 15 min) and the supernatants were aliquoted and frozen at -20°C. Pellets were resuspended with the same volume of fresh medium. The hGDNF present in the supernatants was quantified by ELISA. Moreover, considering the instability of hGDNF and its possible degradation on

the medium release, the data extracted from supernatant quantification were confirmed by measuring the remaining content of hGDNF within NPs. For this, 3 mg of freeze-dried loaded NPs were dissolved in the above medium and incubated in the same conditions. At 1, 2, 7 and 14 days, samples were centrifuged and the hGDNF entrapped in the pellets was extracted with DMSO. Finally, the hGDNF present in the pellets was quantified by ELISA.

2.4.4 Determination of residual PVA

The residual amount of PVA associated with NPs was quantified by a colourimetric method based on the formation of a blue complex between two adjacent hydroxylic groups in the chain of PVA and an iodine molecule (34). Briefly, 3 mg of freeze-dried NPs were treated with 2 mL of 0.5 M NaOH and incubated for 20 minutes at 40°C to degrade the matrix. Then, each sample was neutralized with 900 μ L of 1 M HCl and the volume was adjusted to 5 mL with ultrapure water. To develop the coloured complex, 3 mL of 0.65 M of a boric acid solution, 0.5 mL of a solution of I₂/KI (0.05 M/0.15 M) and 1.5 mL of ultrapure water were added to each sample. After 15 minutes of incubation at RT, 280 μ L of the obtained solution was loaded in triplicate into a 96-wells plate. Finally, the absorbance intensity was determined at 690 nm using the microplate spectrophotometer iEMS Reader MF (Labsystem). The samples for the regression standard line based on known amounts of PVA were prepared from a PVA stock solution through serial 1:2 dilutions and were treated in the same manner as described above. Each dilution was loaded in triplicate in the same microplate as the samples. The results are presented as the ratio between the calculated residual amount of PVA and the real quantity (considering the yield) of the produced NPs by subtracting the content of cryoprotectant, expressed as a percentage (%w/w, PVA/NPs).

2.5 Preparation of HGs (6 wt % HG, 6 wt % HG-NPs, 6 wt % HA, 6 wt % HG-hMSCs, 6 wt % HG-NPs -hMSCs, and 6 wt % HA-hMSCs)

The HGs were prepared using a polymer concentration of 6%, maintaining a stoichiometric balance of HA-CD and HA-AD (1:1). The total mass of HA-CD and HA-AD for gel formation was determined based on the modification degree of each component according to the equations described by Loebel *et al* (12). The polymeric NPs were incorporated at 30% of the total composition. For 6 wt % HG, the HA-CD and HA-AD were individually dissolved in DMEM and mixed. For 6 wt % HG-NPs, NPs were mixed with HA-CD component, and then the second component (HA-AD) was

incorporated. For the unmodified HG (6 wt% HA), the HA was dissolved in DMEM. The HGs were briefly centrifuged to remove entrapped air and transferred to the back of a syringe for *in vitro* characterization. For cell encapsulation, the 6 wt % HG, 6 wt % HG-NPs or 6 wt % HA solutions were first included into the back of the syringe and then the cell suspension was incorporated to form the 6 wt % HG-hMSCs, 6 wt % HG-NPs - hMSCs and 6 wt % HA-hMSCs, respectively. The blend was continuously mixed until a homogeneous HG was formed.

2.6 Characterization of the HGs (6 wt % HG and 6 wt % HG-NPs)

2.6.1 Rheology characterization

The rheological characterization of all HGs was performed using the rheometer (MCR 301 SN80439479) equipped with a 25 mm plate geometry and 0.850 mm gap. The amplitude sweeps were carried out from 0.1% to 100% at 25 °C and the frequency was kept at 10 s⁻¹. Oscillatory frequency sweep measurements were conducted between 0.15 and 100 rad s⁻¹ with a shear strain of 0.5%. The self-healing properties were carried out by a three-step cyclic strain time sweep. The low strain phase was performed for 0.5 s at 0.5% strain and the high strain phase was conducted for 250 ms at 100% strain. The frequency was 10 Hz for both phases.

2.6.2 Determination of Young's Modulus and Injectability tests

The determination of the Young's module and the injectability was performed using a universal testing machine capable of precisely controlling both the displacement of the crosshead and the force applied. The equipment used was a Zwick/Roell uniaxial testing machine model ZwickiLine Z1.0. The load cell used was a Zwick/Roell Xforce P with a maximum load of 50 N. The software to control the machine and record both the load and the displacement was the Zwick/Roell testXpert III v1.4.

2.6.2.1 Young's Modulus measurement

A spherical indenter was used to determine the elastic modulus. During the test, a force is applied with the indenter against the sample to be studied. During this load, both the force used to “stick” the indenter and the penetration distance at each moment were recorded. Using the theories and mathematical models developed by Hertz for spherical head indenters it is possible, from the load and penetration data, to deduce Young's modulus from the material tested (35). The expression used to deduce this module is as follows (1):

$$E = \frac{3(1-\nu^2)F}{4\sqrt{r}\delta^3} \quad (1)$$

CHAPTER 2

where E corresponds to Young's modulus, ν to Poisson's ratio, F to measured force, r to the radius of the indenting sphere, and δ to indented depth. In this study, a value of 0.5 has been assumed for Poisson's ratio. During all experiments conducted it was guaranteed that both the indented depth and the sphere-sample contact area were within the limits that make this model valid. In the first stage of the experiment, the sphere is approximated to the material surface to be analyzed at a speed of 6 mm/min until it reaches an initial load of 1.5 mN. Once this preload is reached, the ball-surface contact is assumed to have been reached. After this contact, the test itself begins. For this, the moving speed of the sphere is set at 6 mm/min and both the force and the penetration depth are recorded. The test ends when the reached depth is equivalent to 20% of the initial sample thickness. When the test finishes the force vs depth curve is obtained. This curve is adjusted to equation 1 for deducing the Young's modulus of the sample.

2.6.2.2 Injectability tests

For the injectability tests, a setup that allows fixing a syringe vertically in the uniaxial testing machine was designed. Once loaded with the studied material, the syringe is placed in the central hole of the holder. Once placed, the crosshead starts moving downwards to push the syringe plunger.

During experiments, the position of the machine actuator is recorded, as well as the force exerted on the plunger flange. Before starting the test, and to ensure contact between the crosshead and syringe plunger, the crosshead of the testing machine is moved downwards at a speed of 50 mm/min. When reaching a 0.1 N load the existence of push is determined. Once this contact is determined, both the load and the position of the crosshead begin to be recorded. From these tests, the force necessary to extrude the materials studied at different plunger speeds, or flows, is determined.

2.6.3 *In vitro* degradation test of hybrid systems (6 wt % HG-NPs)

The degradation behavior of the 6 wt % HG-NPs at 37°C was characterized using two different methods. First, 300 μ L of 6 wt % HG-NPs were introduced on plastic supports and the samples were immersed in Petri dishes with 1.5 mL of MilliQ Water. At selected times (1, 2 and 7 days), the samples were collected and freeze-dried. Then, the dried samples were weighed (W1). The rate of residual weight (RW) was calculated as $RW = W1/W0 \times 100\%$.

The second strategy used to characterize the 6 wt % HG-NPs degradation was the carbazole assay (12,14,36). Briefly, 100 μ L of HG was added to a 1.5 mL Eppendorf tube

and centrifuged to remove any entrapped air. Then, 400 μL of PBS was then added to the tube ($n = 3$). At 3, 7, 10, and 14 days, the PBS was carefully removed and collected before being replaced with 400 μL of fresh PBS. On day 14, the remaining gel was disrupted using 1 mg/mL hyaluronidase from bovine testes. The standard curve was prepared with different concentrations of glucuronic acid. The total concentration of glucuronic acid in the HGs was determined by disrupting 100 μL of 6 wt % HG-NPs for 14 days. Then, 50 μL of each sample was added to a glass tube followed by 1 mL of ice-cold 25×10^{-3} M sodium tetraborate in concentrated sulfuric acid. Tubes were incubated for 10 min at 100 $^{\circ}\text{C}$ and then were cooled on ice. Next, 30 μL of 0.125 wt % carbazol in absolute ethanol was added and vortexed. The samples were then incubated for 15 min at 100 $^{\circ}\text{C}$. Following incubation, the tubes were allowed to cool to RT and 200 μL of the solution was transferred to a 96-well plate for measurement. The absorbance at 525 nm was read using a plate reader.

2.6.4 *In vitro* release study and bioactivity assay of hGDNF from hybrid systems (6 wt % HG-NPs)

The 6 % (w/v) HG-NPs were prepared according to the protocol previously described and placed on 0.4 μm millicells hanging cell culture insert ($n = 3$, 200 μL each). Then, HGs were submerged in 1 mL of PBS in a 12-well plate (Corning, MA, USA). hGDNF release was measured for a period of 14 days. At each time point, the millicells were transferred to another well with fresh PBS. The aqueous solutions were collected and analyzed by ELISA. For the bioactivity of hGDNF released from the 6 wt % HG-NPs, the biomaterial was placed on a 0.4 μm millicell hanging cell culture insert, from which hGDNF was released in a sustained manner into the PC12 cell culture. After 10 days, the presence of neurites in the PC12 culture was analyzed.

2.6.5 *Scanning electron microscopy*

A Zeiss Sigma Gemini scanning electron microscope (FE-SEM) was used to characterize the 6 wt % HG, 6 wt % HG-NPs, and NPs morphology with an acceleration voltage of 10 kV and different magnifications. Samples were previously prepared, lyophilized and coated with a few nm of Palladium (SC7620 Mini Sputter coater).

2.6.6 *In vitro* cell viability and neural biocompatibility

The cytotoxicity of the biomaterial was evaluated by incubation of hMSCs in contact with the HGs extracts (ISO 10993-5) and after encapsulating the cells in the HGs. The neural compatibility studies in PC12 cells were also conducted under contact with the HGs

CHAPTER 2

extracts (ISO 10993-5) and by direct contact without HG extraction. hMSCs and rat adrenal PC12 cells were purchased from American Type Culture Collection (ATCC). hMSCs cells were cultured in D-MEM supplemented with 20% fetal bovine serum (FBS), 100 µg/mL streptomycin and 100 U/mL penicillin and 10 ng/mL basic FGF. Rat PC12 cells were cultured on collagen I-coated plate (Invitrogen, Waltham, MA) in RPMI medium supplemented with 5% horse heat-inactivated serum, 10% FBS, 100 µg/mL streptomycin and 100 U/mL penicillin. Both cell lines were incubated in a humidified atmosphere with 5% CO₂, at 37 °C.

First, the functionalized 6 wt % HG, the hybrid system (6 wt % HG-NPs) and 6 wt % HA without functionalization were incubated in 4 mL D-MEM culture medium with 0.2 mg/mL of hyaluronidase to extract the different components of the HGs. The samples were extracted with 0,2 mg/mL of hyaluronidase at 37 ± 1 °C for 24 ± 2 hours under magnetic stirring, and then the extracted solution was filtered through 0.22 µm millipore filters for sterilization. PrestoBlue and Live/dead assays were used to evaluate the cytotoxicity of different samples. Briefly, hMSCs cells were seeded in 96-well culture plates at a density of 3×10^3 cells per well. After the attachment of the cells, the culture medium in each well was removed and the cells were treated with the extracted solution from HGs. After the incubation for 24 h and 72 h, Presto Blue and Live/dead assays were performed. For PrestoBlue, 10 µL of the solution was added to each well and the plate was incubate for 3 hours in the dark at 37°C. Finally, the absorbance of each sample was measured at 570 nm as the experimental wavelength and 600 nm as the reference or normalization wavelength. The cell viability was evaluated by the equation (2):

$$\text{Cell viability (\%)} = (OD_{\text{hydrogel extracted solution}} - OD_{\text{blank}}) / (OD_{\text{control}} - OD_{\text{blank}}) \times 100\% \quad (2)$$

For Live/dead assay, cells were incubated for 30 min in the dark at RT.

On the other hand, to study the toxicity after incubating the cells in the HGs, we assemble the hydrogel components with the cells in the back of a syringe, where they are gently mixed. The morphology and viability of encapsulated cells are analyzed with Live/dead after 24 h.

Finally, to study neuronal compatibility, the PC12 cell line was treated with the extracts of the different HGs and by direct contact with them without any type of extraction. For the extract's analysis, the cells were seeded in 96-well culture plates at a density of 3×10^3 cells per well. The cells in contact with HGs were seeded in 24-well culture plates at a density of 2×10^4 cells per well. Cells treated with the extracts were analyzed by PrestoBlue assays at 24 and 72 hours and with Live/dead at 24 hours. On the other hand,

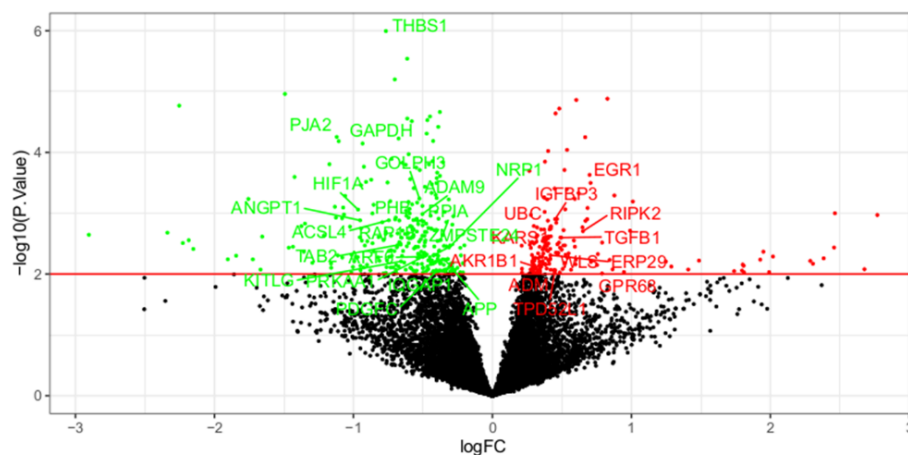
the cellular viability of the cells directly exposed to the different HGs was investigated after 24 hours of incubation by Live/dead assay.

3. Results and discussion

3.1 hGDNF modulates MSCs- gene expression

To assess the therapeutic potential of combining hMSCs with hGDNF in the nanoreinforced HG and to explore the effect of the neurotrophic factor on MSC gene expression profile, RNA-seq was performed. In this regard, the whole-genome profile analysis showed differences in gene expression between treatments and control cells. hGDNF-up-regulated genes were related with gene ontology biological processes such as cell–matrix adhesion, positive regulation of MAPK cascade, ERK1 and ERK2 cascade and positive regulation of secretion by cells, among others (Figure S1. Supporting information). Interestingly, the up-regulation of MAPK-associated genes involved in plasticity and neurogenesis (Erp29, EGR1 and TGF- β) was observed (31,37–39). Moreover, ADM, a gene involved in the regrowth of neuronal processes, and GPR68 gene, with neuroprotective function, were also upregulated (Figure 1A) (40,41). Similarly, Gantner *et al.* reported the potential of hGDNF to promote the integration of human neural grafts through the regulation of different signalling pathways and they showed that several MAPK-associated genes with known roles in plasticity such as EGR1 and SPRY1 were up-regulated (31). Consequently, we performed a gene set enrichment analysis (GSEA) on the gene sets by Gantner *et al.* (31) to check and confirm their findings. The enrichment patterns are summarized in Figure 1B. The MAPK pathway genes and the up- and down-regulated gene set showed a significant enrichment pattern in our gene set thus confirming the previous observations (31). All these findings demonstrate the potential of hGDNF to modulate the plasticity of cell grafts based on hMSCs or hPSCs via the MAPK pathway and support the combination of hGDNF and hMSCs within our nanoreinforced HG.

A



B

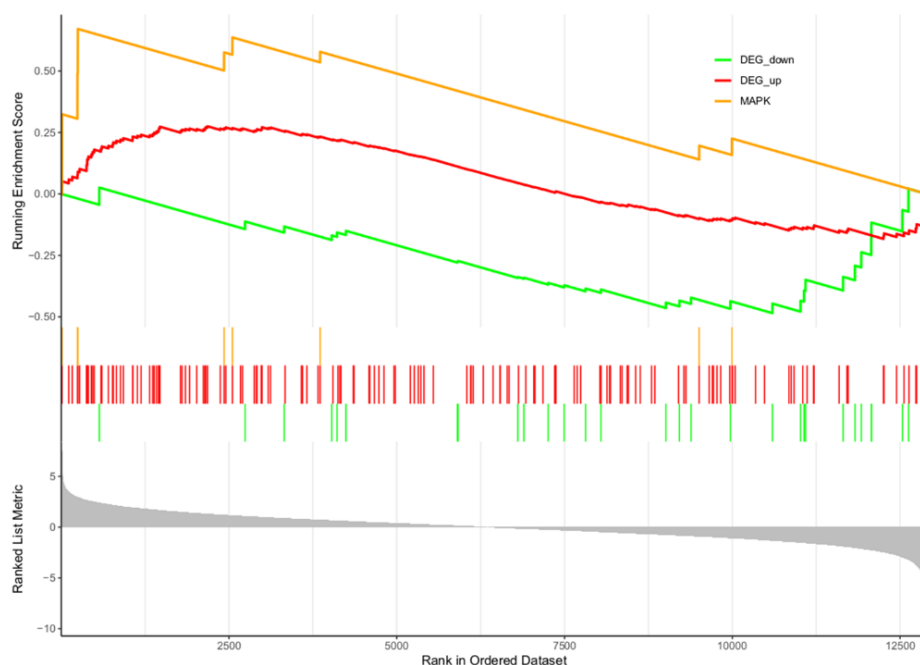


Figure 1. Transcriptional profiling of hMSCs in the presence of hGDNF. A) Volcano plot displaying differential expressed genes between treated and non-treated hMSCs. The red dots represent the up-regulated expressed transcripts. The green dots represent the transcripts whose expression is downregulated. Positive x-values represent up-regulation and negative x-values represent down-regulation. B) GSEA enrichment to compare models. The Running Enrichment score shows that MAPK pathway genes (yellow line) and the statistically up-regulated (red line) and down-regulated genes (green line) published by Gantner *et al.* [31] are enriched in the up and down-regulated genes of our model.

3.2 Synthesis of HA-CD and HA-AD

HA was functionalized with β -CD (host-moiety) and adamantane (guest-moiety) via nucleophilic substitution as previously reported (12). The specific synthetic routes of HA-CD and HA-AD are depicted in Figures 2A and 2B. The preparation steps of the hybrid

system are represented in Figure 2C. The resultant HA-CD and HA-AD were freeze-dried and characterized by $^1\text{H-NMR}$ spectroscopy. HA-CD and HA-AD were recovered as a spongy white solid with yields of $86.5 \pm 3.4 \%$ ($n=4$) for HA-CD and $68.7 \pm 3.8 \%$ for HA-AD ($n=3$). Modification of HA with pendant CD ($10.6 \pm 1.5 \%$) was determined by integration of the signal for the hydrogen on position 1 of CD (H_1); (7 Hs, shaded blue) relative to the signal for *N*-acetyl singlet of HA (3 Hs, shaded red) (Figure S2. Supporting information). Modification of HA ($40.3 \pm 3.5 \%$) with pendant AD was determined by integration of the adamantane hydrogens (15 Hs, shaded blue) relative to the sugar ring of HA (10 Hs, shaded red) (Figure S3. Supporting information). A quantitative $^1\text{H-NMR}$ was performed using a known amount of dimethylsulfone as standard (Figure S4. Supporting information) and the residual amount of TEA from the HA-AD synthesis was determined, resulting in 0.13 mg of TEA/mg HA-AD.

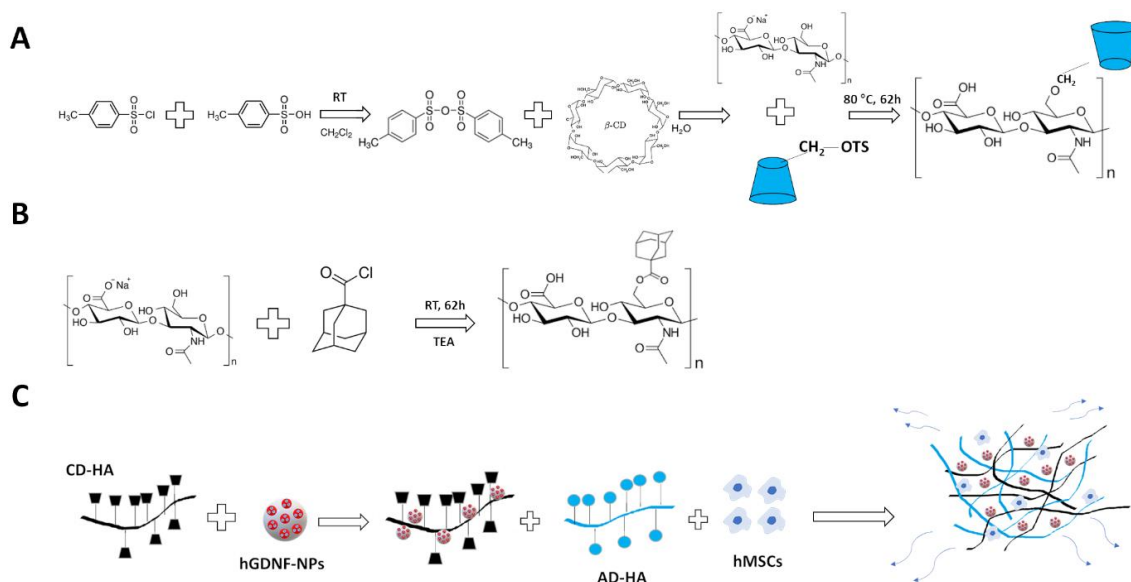


Figure 2. Schematic illustration of the functionalization and synthesis of the hybrid system. A) HA functionalization with β -cyclodextrin through nucleophilic substitution. B) HA functionalization with adamantane through nucleophilic acyl substitution. C) Schematic illustration of the preparation of the hybrid system.

3.3 Preparation and characterization of hGDNF-loaded NPs

Monodisperse spherical particles were successfully obtained using TROMS (Figure 3A). The mean particle size measured by NTA was $208 \pm 26 \text{ nm}$ ($n=4$) (Figure 3B). The PDI average obtained by DLS was 0.13 ± 0.06 ($n=4$). The particle surface charge was analyzed by DLS after the freeze-drying process exhibiting a zeta potential of $-22.8 \pm 3.9 \text{ mV}$ ($n=4$), which represents a stable colloidal system (42). The encapsulation efficacy was $58 \pm 8\%$, which corresponds to a final loading of $0.41 \mu\text{g}$ of GDNF per mg of polymer. The

CHAPTER 2

results were similar to those obtained for other GDNF-loaded MPs and NPs (43,44), but with the advantage of encapsulating hGDNF under milder conditions. SEM analysis showed that hGDNF-PLGA NPs were spherical in shape and confirmed that NP size distribution was uniform (Figure 3C). The release of hGDNF from the NPs was biphasic, with an initial burst release produced within the first 24 hours. After the initial burst produced by the release of hGDNF adsorbed on the particle surface ($19.10 \pm 3.5\%$), a sustained release was observed from day 1 to day 28 (50.6%), caused by drug diffusion through the PLGA. Finally, an increase in the rate of release was observed from day 28 to 40 due to polymer degradation and 96% of the total hGDNF was released within the first 40 days (Figure 3D). These results were confirmed by measuring the remaining hGDNF content within NPs, showing a similar *in vitro* release profile (Figure S5. Supporting information). The percentage of residual PVA in the NPs was $8.6 \pm 0.4\%$, which is several times lower than the values previously reported for PLGA-NPs prepared by a double emulsion method and represented a safe and acceptable quantity (34).

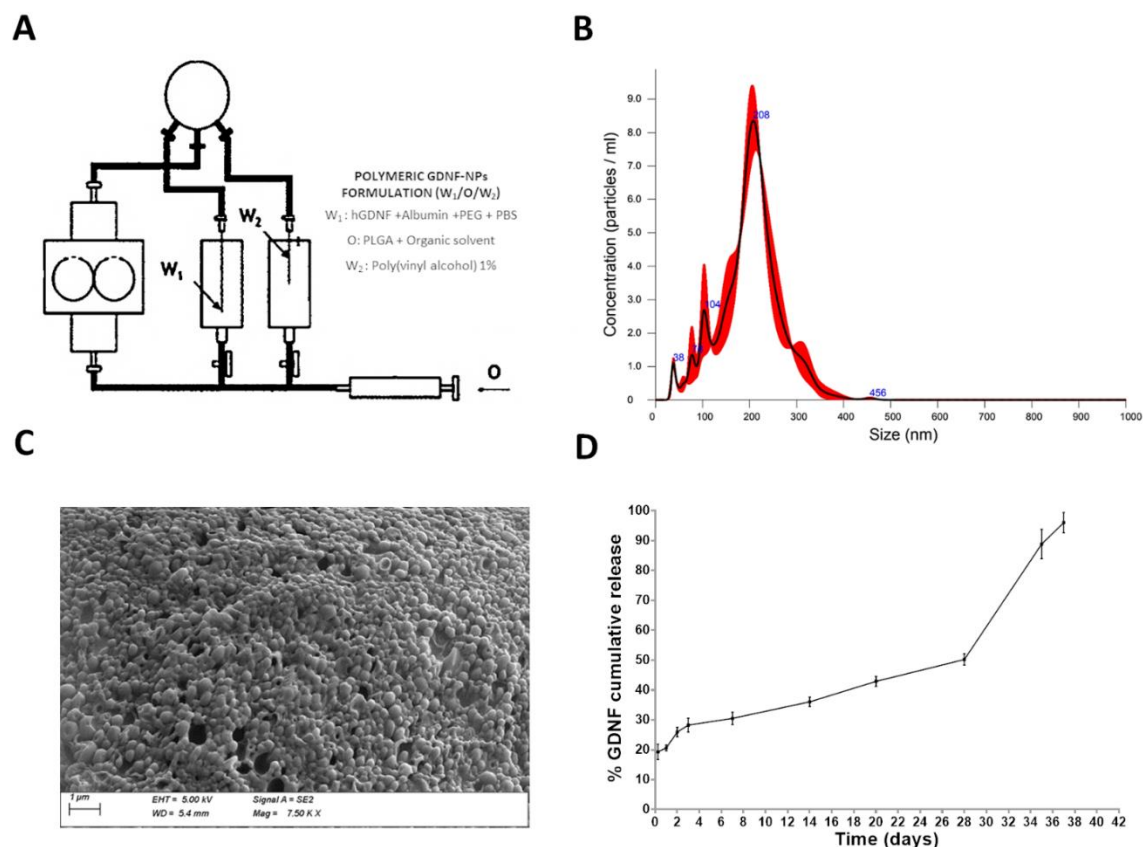


Figure 3. Characterization of GDNF-loaded NPs prepared using TROMS. A) Schematic illustration of TROMS. B) NPs size determined by NTA. C) Scanning Electron Microscopy images showing the morphology of freeze-dried NPs. D) *In vitro* release profile of hGDNF from NPs by determination of the supernatant protein content.

3.4 Preparation and characterization of the HGs (6 wt % HG and 6 wt % HG-NPs)

3.4.1 Hydrogel preparation

The HGs were formed by mixing aqueous solutions of the modified HA (HA-Cd and HA-AD) (6 wt % HG) and PLGA-NPs (6 wt % HG-NPs). Importantly, NPs were non-covalently immobilized in the HA-CD solution before mixing both components with the HA-Ad solution. The supramolecular assembly was instantaneous upon mixing. The NPs incorporation resulted in a homogeneous nanocomposite-HG with a soft and rubbery consistency.

3.4.2 Determination of complex viscosity

The analysis of the complex viscosity from a frequency sweep test is a useful tool for investigating the injectability of HG. This property is one of the most important requirements for minimally invasive surgery, particularly in tissue engineering and drug delivery applications [45]. Additionally, we can also determine if the HG has shear-thinning properties. Importantly, for shear-thinning materials we expect a decrease in viscosity with the increase of the angular frequency (ω) (46). In our case,

the complex viscosity decreases as angular frequencies increase for both the 6 wt % HG and 6 wt % HG-NPs, indicating that both HGs are shear thinning, and are enabled by reversible cross-linking mechanisms (Figure 4A). Therefore, the viscosity profile suggests a high ability for both HGs to be injectable (Figure 4A).

3.4.3 Amplitude sweep test

We then use the storage modulus (G') and loss modulus (G'') to analyze the HG behavior and measure its strength. A slight dominance of G' was observed in the 6 wt % HG indicating that the sample behaves more like viscoelastic solid ($G' > G''$) than viscoelastic liquid ($G'' > G'$). The differences between the two moduli are very similar and it cannot be stated that there is a clear superiority of elastic behavior over viscous behavior. The rheological tests showed a strengthening of the mechanical properties for the HG-NPs as previously demonstrated by embedding PLGA MPs into HA gels (47). It is worth mentioning that the combination of NPs and HG provided a more robust structure than empty HGs, which is demonstrated by a 4-fold increase in the G' value (Figure 4B). The addition of NPs produced an important change in the viscoelastic properties of the sample (Figure 4B), increasing the solid-like character ($G' \gg G''$). This change of behavior suggests that spherical NPs establish stronger interactions with the HA network, obtaining a solid-like material (48–51).

3.4.4 Frequency sweep test

Next, we investigated the behavior of the synthesized HG at both high and low frequencies using a frequency sweep test (52), which gives us an idea of the injection rate at which the HG should be injected. The 6 wt % HG behaves in a manner that is more elastic than viscous at high frequencies. At low frequencies, the results showed the opposite tendency. The 6 wt % HG-NPs show the same phenomenon but with some changes. Therefore, both HGs showed the typical behavior of shear-thinning materials. The values for the latter HG are notably higher and the transition point where the HG goes from a fluid-like (viscous) behavior ($G'' > G'$) to a solid-like (elastic) behavior ($G' > G''$) occurs earlier (Figure 4C). Therefore, these HGs should be slowly administered, since this effect is more important for 6 wt % HG-NPs because they exhibit lower fluency.

3.4.5 Evaluation of thixotropy behavior

To evaluate the self-healing properties of the HGs a three-step oscillation method was performed. The ability of the HGs to recover their mechanical properties was investigated by studying the behavior of G' at high and low strain values. The results were expressed

as a percentage of G' recovery (Figure 4D). The recovery test showed that both HGs showed a fast decrease in G' at high strain values, which were instantly recovered after cessation of the shear and the application of low strain values. This confirms the potential of the developed HGs to recover their mechanical strength upon injection (53). Therefore, the guest-host interactions together with the incorporation of NPs, are an effective strategy to achieve shear-thinning and self-healing HGs.

3.4.6 Determination of the Young's modulus from indentation testing

The biomaterial environment and mechanical properties have great relevance for the clinical success of cell therapies. Therefore, the mechanical properties of the material should be similar to those of brain tissue. In this sense, the brain is a soft tissue, with Young's modulus between 1-14 kPa in humans (54) and biomaterials with stiffness 0.1-20 kPa are preferred to support neuronal cell proliferation (55). The stiffness of both HGs was analyzed by measuring Young's modulus from indentation tests (Figures 4E and F). The developed HGs showed a Young's modulus of 1.22 ± 0.04 kPa (6 wt %) and 1.39 ± 0.08 kPa (6 wt % HG-NPs). These values suggest potential compatibility with brain tissue and a suitable stiffness for neural differentiation (54,55). A higher Young's modulus was observed when the NPs were incorporated into the HG, which demonstrates the relevance of HG reinforcement with nanospheres as an effective strategy to modulate the matrix stiffness for the design of biomaterials for tissue engineering (Figure 4E) (51).

3.4.7 Measurement of hydrogel injection forces

Although the study of storage modulus, loss modulus and the analysis of the shear-thinning and self-healing behavior are suitable predictors of biomaterial injectability, the injection force is the most important parameter to conclude when a material is clinically valid for injection (52). Here, we quantitatively determined the injectability of the prepared HGs through a Hamilton syringe with a 27G needle. Figure 4G is a schematic of the manufactured holder. On the left, the external aspect of the holder is shown. The central area shows both the barrel at the bottom and the plunger at the top. On the right-hand side, the external aspect is displayed.

The force to move the plunger was higher as the injection flow rate increased (Figure 4H). In addition, there was a significant increase in the force required to inject the nanoreinforced material compared to the injection of the material without NPs. At a flow rate of 15 mm/min, the injection force required for a 6 wt % HG was close to 4.3 N while the injection force required for a 6 wt % HG-NPs was close to 4.8 N,

CHAPTER 2

representing an increment of 10%. This difference was increased progressively to 16% for the fastest case studied (60 mm/min) (Figure 4H).

The higher viscosity, storage and loss modulus, and the increment of the stiffness observed for the 6 wt % HG-NPs in the previous analyses involved a higher force to inject the biomaterial. In all cases, the forces were within the valid range for a clinical injection. Thus, materials with injection forces <20 N are potentially injectable at the clinical level (52). The highest force recorded in our study did not exceed 7 N, which indicate that the developed biomaterial is clinically injectable (Figure 4H).

The HGs not only demonstrated good injectability when injected into the air but also when injected into a gelatin gel at 4% (52,56). Thus, the HG injections into the gelatin gel did not increase the force required for its administration, which confirms the excellent injection capability of the developed system (Figure 4I and 4J).

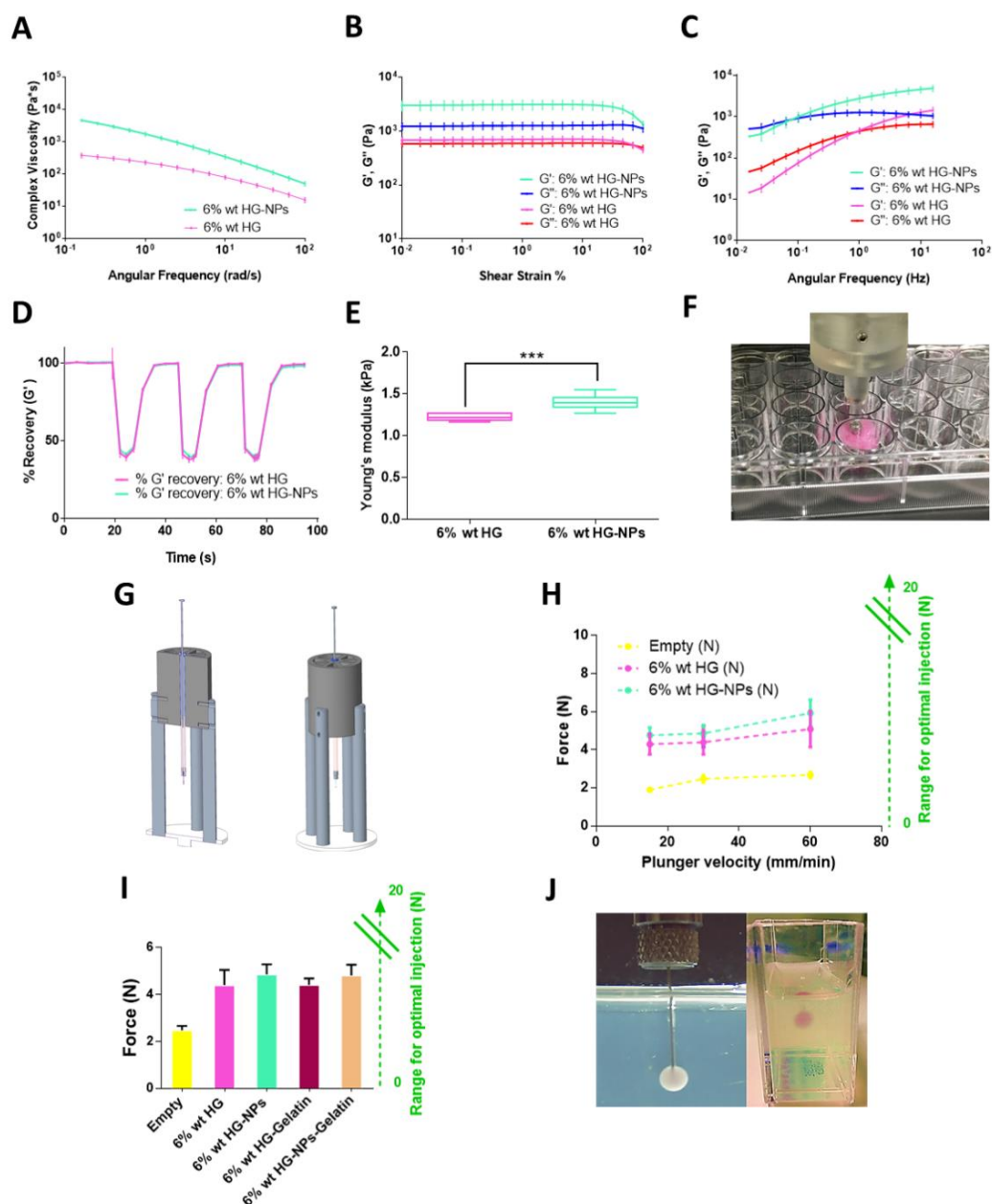


Figure 4. Evaluation of the rheological properties, mechanical stiffness and injectability of the HGs.

A) Determination of complex viscosity through an oscillatory frequency sweep (from 0.15 and 100 rad s^{-1} with a shear strain of 0.5%). B) Oscillatory strain sweep (from 0.1% to 100% and the frequency was kept at 10 s^{-1}). C) Oscillatory frequency sweep (from 0.15 and 100 rad s^{-1} with a shear strain of 0.5%). D) Analysis of thixotropy behavior by three-step cyclic strain time sweep. E) Determination of Young's modulus using an indentation test. Young's modulus was significantly increased by nanoreinforcement (***, $p < 0.001$, unpaired t-test). F) Schematic of the indentation used for the determination of Young's modulus. G) Setup used to perform the injectability study. On the left, a cross-section is shown, and on the right one, the external aspect of the apparatus is shown. H) Determination of HG injection forces. I) Measurement of the force required to inject HGs in air and within 4% gelatine gels at 30 mm/min . J) Representative image of HA-HG-NPs injection on 4% gelatin gel.

3.4.8 Morphological analysis of the multifunctional hydrogels by SEM

The morphological properties of the 6 wt % HG and 6 wt % HG-NPs were analyzed by SEM, which reveals the porosity and nature of the HG structure. All the developed HGs had a homogeneous surface and a porous interior structure. The pore size of all HGs was in the range of 10–20 μm (Figure 5A). The NPs were physically embedded and uniformly dispersed into the HG network in the nanoreinforced HG (Figure 5B). Importantly, the morphological analysis suggests a certain NPs absorption in the HG, which would induce higher friction between components. Therefore, these physical interactions seem to be responsible for the increment of all studied parameters (viscosity, storage modulus, loss modulus and the injection forces) (57,58). These results are consistent with previous studies, where polymeric NPs have been successfully incorporated within the hydrogel network to increase the crosslinked density and to obtain reinforced nanocomposite HGs (14,48,59).

3.4.9 Degradation test of hybrid systems (6 wt % HG-NPs)

The HG degradation influences the release rate of biomolecules from the hybrid system and therefore it is an important parameter to provide a controlled release of hGDNF (60). In this case, the 6 wt % HG-NPs was slowly degraded showing a partial degradation of 42% after one week (Figure S6. Supporting information). Similarly, the carbazole assay demonstrated a linear rate of erosion over a period of 14 days (Figure 5C), which supports the idea that our drug delivery platform could influence drug release kinetics over a few weeks through its linear degradation (61).

3.4.10 In vitro release study and bioactivity assay of hGDNF from hybrid systems (6 wt % HG-NPs)

Despite the proven potential of hGDNF as a treatment for PD, its clinical application has been hampered by safety and efficacy issues associated with GDNF's short *in vivo* half-life (62). As an alternative, hybrid systems such as nanoreinforced HGs may overcome this issue providing protein protection from degradation and sustained drug release over time (63). The release of hGDNF from the 6 wt % HG-NPs occurred in a sustained manner and the cumulative release rate reached $25.4 \pm 4.5\%$ in two weeks. The NPs incorporation into the HG allowed a more sustained release profile, as well as a significant reduction of drug release at two weeks (25% vs 36%) (Figure 5D). It is worth mentioning that the NPs incorporation into the HG considerably reduced the initial release burst from PLGA-NPs. Interestingly, similar results were previously reported with VEGF and

BDNF-MPs embedded in HA-HG (47). This effect may be due to the fact that the HG forms a cross-linked and porous matrix through the proteins that have to diffuse (47). Thus, the nanoreinforcement proved an effective strategy to improve not only the HG robustness but also to achieve a controlled drug release from the HG.

On the other hand, the successful development of a strategy based on hGDNF-NPs embedded within an HA-HG requires the preservation of the biological activity of the neurotrophic factor through all the manufacturing processes. Therefore, the bioactivity of hGDNF released from the 6 wt % HG-NPs was evaluated using a PC-12 neurite outgrowth assay. PC12 cells, which possess the GFR α 1 and RET receptors, change their phenotype and develop neurites after treatment with biologically active hGDNF, which is visualized by the sprouting of neurites (64,65). After 10 days of hGDNF exposure, PC12 cells acquired a phenotype associated with sympathetic neuron-like cells, which includes the inhibition of proliferation and the outgrowth of neurites (Figure 5E). Collectively, these results demonstrate that the neurotrophic factor remains bioactive after its encapsulation and release from the drug delivery platform.

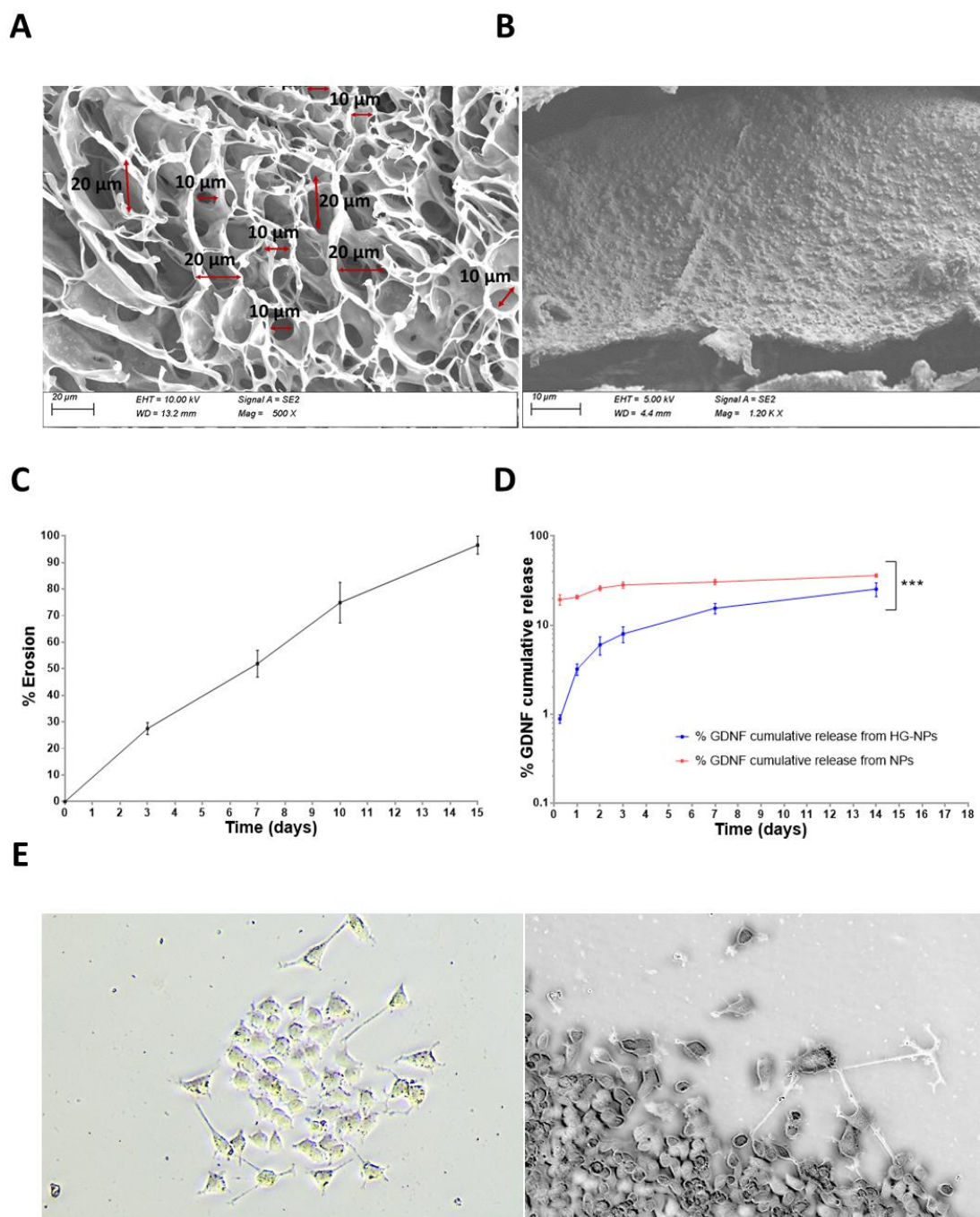


Figure 5. Morphological characterization and *in-vitro* evaluation of 6 wt % HG-NPs. A and B) The SEM analysis of freeze-dried HGs. The HGs showed pores with a size in the range of 10–20 μm (A) and (B) NPs appears physically embedded into HG network (C) *In vitro* erosion of the 6 wt % HG-NPs over a period of 15 days. D) Comparative cumulative release profile of hGDNF: NPs vs 6 wt % HG-NPs. The NPs incorporation into the HG produced a significant reduction of drug release at two weeks (***, $p < 0.001$, paired t-test). E) Analysis of hGDNF activity *in vitro*. The 6 wt % HG-NPs were placed on milicell membranes, from which hGDNF was released in a sustained manner in the PC12 cell culture for 10 days. Then, the presence of neurites in the PC12 culture was analyzed. Representative images were taken with a phase-contrast microscope on day 10. On the left PC12 cells treated with hGDNF are depicted. On the right, the cells treated with 6 wt % HG-NPs are represented. Magnification: 20x.

3.4.11 Cell viability and neural biocompatibility

HA is the major component of the brain extracellular matrix and has a valuable role in neural homeostasis. Precisely, HA influences different cell activities such as cell migration, proliferation and differentiation, among others (66). Nonetheless, due to the introduction of different modifications in the HA and the combination with PLGA-NPs, cell viability and neural biocompatibility were assessed.

From a cell compatibility standpoint, PrestoBlue and Live/dead test revealed that survival rates for modified and nanoreinforced HGs were higher than 90% when compared to extracts of unmodified HA (Figure 6A). For encapsulated cells, Live/dead measurements showed a similar trend without differences in cellular morphology between groups (Figure 6B). These results confirm that the modifications performed in the HA and the incorporation of the NPs did not have a toxic character and therefore, the novel HGs would be safe.

Further, the neural compatibility of the developed nanoreinforced HG was also studied in PC12 cells, a widely characterized neurotoxicology model (67,68). A notable increase in cell proliferation was observed in PC12 treated with the HG extracts at 24 and 72 hours (Figure 6C). The highest proliferation was observed at 24 hours for 6 wt % HG-NPs samples. Importantly, at 72h 6 wt % HG and 6 wt % HG-NPs extracts produced higher proliferation than the control sample of HA extract. The cells directly exposed to the different HGs did not show significant differences in morphology compared to control samples of HA and most of the PC12 cells were alive, indicating good cell compatibility (Figure 6D). These results are in good agreement with previous observations reported on HA-HGs combined with biodegradable NPs, where good biocompatibility with human umbilical cord endothelial cells (HUVECs) was also demonstrated (14).

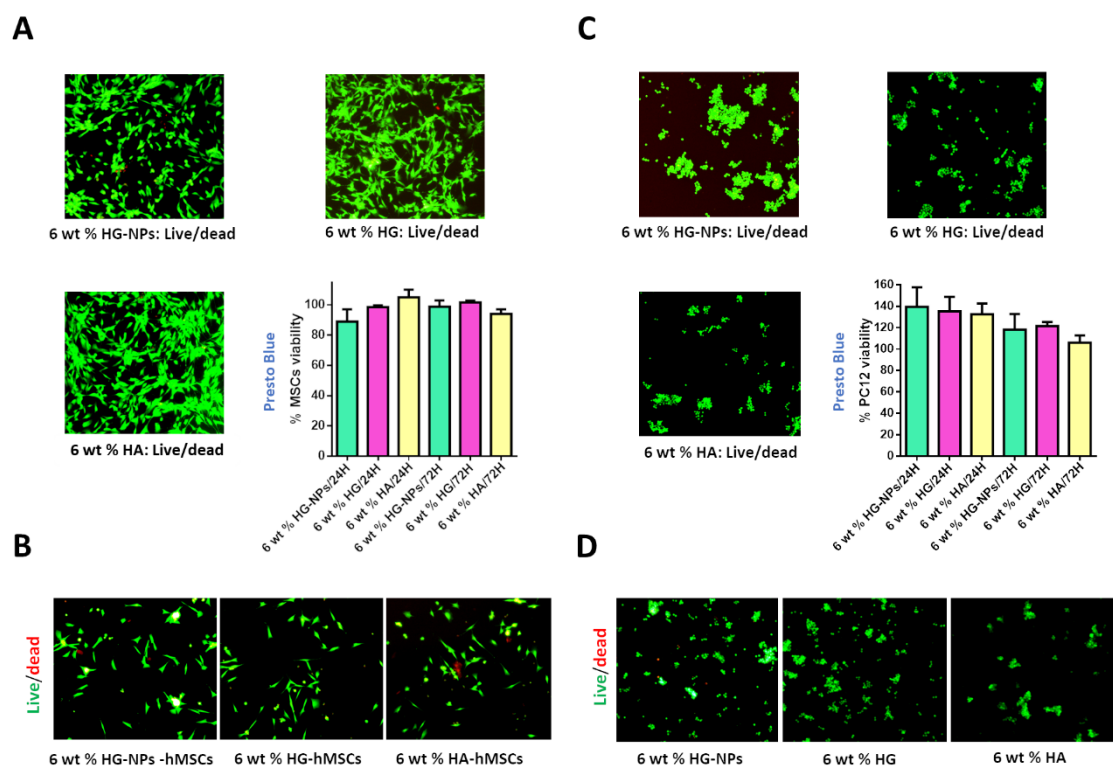


Figure 6. *In vitro* cell viability and neural biocompatibility. A) Live/dead and Presto Blue assay of hMSCs cells treated with extracts according to the ISO 10993-5 for *in vitro* cytotoxicity. B) Live/dead assay of encapsulated MSCs within HGs. C) Live/dead and Presto Blue assay of PC12 cells treated with extracts according to the ISO 10993-5 for *in vitro* cytotoxicity. D) Live/dead assay of encapsulated PC12 within HGs.

4. Conclusions

A nanoreinforced HG for the dual administration of hGDNF and hMSCs has been successfully prepared and characterized. The use of cells, neurotrophic factors and biomaterials in a single therapeutic strategy could have enormous potential in the treatment of neurodegenerative diseases such as PD, where a progressive loss of dopaminergic neurons occurs. Particularly, this work has successfully demonstrated the potential of this GDNF-based therapy to modify pathways related to neural survival and regeneration. Moreover, NPs incorporation in the HG enhanced the mechanical properties of the biomaterial compared to conventional HA gels. In summary, the suitable strength, excellent self-healing properties and good biocompatibility make this nanoreinforced HG a good candidate for drug and cell administration to the brain.

5. Acknowledgements

P. Torres thanks the Spanish Ministry of Education (Programa FPU (FPU17/01212)) and the Government of Navarra (2019_66_NAB9). E. Garbayo is supported by a “Ramon y Cajal Fellowship (RYC2018-025897-I).

6. References

1. Szeto JYY, Walton CC, Rizos A, Martinez-Martin P, Halliday GM, Naismith SL, et al. Dementia in long-term Parkinson's disease patients: a multicentre retrospective study. *npj Park Dis*. 2020 Dec 1;6(1):1–7.
2. Iarkov A, Barreto GE, Grizzell JA, Echeverria V. Strategies for the Treatment of Parkinson's Disease: Beyond Dopamine. *Front Aging Neurosci*. 2020 Jan 31;12:4.
3. Ferrazzoli D, Carter A, Ustun FS, Palamara G, Ortelli P, Maestri R, et al. Dopamine Replacement Therapy, Learning and Reward Prediction in Parkinson's Disease: Implications for Rehabilitation. *Front Behav Neurosci*. 2016 Jun 14;10(JUN).
4. De Gioia R, Biella F, Citterio G, Rizzo F, Abati E, Nizzardo M, et al. Neural Stem Cell Transplantation for Neurodegenerative Diseases. *Int J Mol Sci*. 2020 Apr 28;21(9):3103.
5. Sivandzade F, Cucullo L. Regenerative stem cell therapy for neurodegenerative diseases: An overview. *Int J Mol Sci*. 2021 Feb 2;22(4):1–21.
6. Baldari S, Di Rocco G, Piccoli M, Pozzobon M, Muraca M, Toietta G. Challenges and strategies for improving the regenerative effects of mesenchymal stromal cell-based therapies. *Int J Mol Sci*. 2017 Oct 1;18(10).
7. Marquardt LM, Heilshorn SC. Design of Injectable Materials to Improve Stem Cell Transplantation. *Curr Stem Cell Reports*. 2016;2(3):207–20.
8. Axpe E, Orive G, Franze K, Appel EA. Towards brain-tissue-like biomaterials. *Nat Commun*. 2020 Dec 1;11(1):1–4.
9. Chyzy A, Plonska-Brzezinska ME. Hydrogel Properties and Their Impact on Regenerative Medicine and Tissue Engineering. *Molecules*. 2020 Dec 1;25(24).
10. Zhong J, Chan A, Morad L, Kornblum HI, Guoping Fan, Carmichael ST. Hydrogel matrix to support stem cell survival after brain transplantation in stroke. *Neurorehabil Neural Repair*. 2010;24(7):636–44.
11. Bayer IS. Hyaluronic acid and controlled release: A review. *Molecules*. 2020 Jun 1;25(11).

12. Loebel C, Rodell CB, Chen MH, Burdick JA. Shear-thinning and self-healing hydrogels as injectable therapeutics and for 3D-printing. *Nat Protoc.* 2017;12(8):1521–41.
13. Chimene D, Kaunas R, Gaharwar AK. Hydrogel Bioink Reinforcement for Additive Manufacturing: A Focused Review of Emerging Strategies. *Adv Mater.* 2020;32(1).
14. Steele AN, Stapleton LM, Farry JM, Lucian HJ, Paulsen MJ, Eskandari A, et al. A Biocompatible Therapeutic Catheter-Deliverable Hydrogel for In Situ Tissue Engineering. *Adv Healthc Mater.* 2019 Mar;8(5):1801147.
15. Slevin JT, Gash DM, Smith CD, Gerhardt GA, Kryscio R, Chebrolu H, et al. Unilateral intraputamenal glial cell line-derived neurotrophic factor in patients with Parkinson disease: Response to 1 year of treatment and 1 year of withdrawal. *J Neurosurg.* 2007 Apr;106(4):614–20.
16. Whone A, Luz M, Boca M, Woolley M, Mooney L, Dharia S, et al. Randomized trial of intermittent intraputamenal glial cell line-derived neurotrophic factor in Parkinson’s disease. *Brain.* 2019;142(3):512–25.
17. Gash DM, Gerhardt GA, Bradley LH, Wagner R, Slevin JT. GDNF clinical trials for Parkinson’s disease: a critical human dimension. *Cell Tissue Res.* 2020 Oct 1;382(1):65–70.
18. Gartzandia O, Herrán E, Ruiz-Ortega JA, Miguelez C, Igartua M, Lafuente J V., et al. Intranasal administration of chitosan-coated nanostructured lipid carriers loaded with GDNF improves behavioral and histological recovery in a partial lesion model of Parkinson’s disease. *J Biomed Nanotechnol.* 2016 Dec 1;12(12):2220–30.
19. Wahlberg LU, Emerich DF, Kordower JH, Bell W, Fradet T, Paolone G. Long-term, stable, targeted biodelivery and efficacy of GDNF from encapsulated cells in the rat and Goettingen miniature pig brain. *Curr Res Pharmacol Drug Discov.* 2020 Apr 1;1:19–29.
20. Torres-Ortega PV, Saludas L, Hanafy AS, Garbayo E, Blanco-Prieto MJ. Micro- and nanotechnology approaches to improve Parkinson’s disease therapy. *J Control Release.* 2019 Feb 10;295:201–13.

CHAPTER 2

21. Garbayo E, Montero-Menei CN, Ansorena E, Lanciego JL, Aymerich MS, Blanco-Prieto MJ. Effective GDNF brain delivery using microspheres-A promising strategy for Parkinson's disease. *J Control Release*. 2009 Apr 17;135(2):119–26.
22. Lavin Y, Kobayashi S, Leader A, Amir E ad D, Elefant N, Bigenwald C, et al. Innate Immune Landscape in Early Lung Adenocarcinoma by Paired Single-Cell Analyses. *Cell*. 2017 May 4;169(4):750–765.e17.
23. Jaitin DA, Kenigsberg E, Keren-Shaul H, Elefant N, Paul F, Zaretsky I, et al. Massively parallel single-cell RNA-seq for marker-free decomposition of tissues into cell types. *Science* (80-). 2014;343(6172):776–9.
24. Dobin A, Davis CA, Schlesinger F, Drenkow J, Zaleski C, Jha S, et al. STAR: Ultrafast universal RNA-seq aligner. *Bioinformatics*. 2013 Jan;29(1):15–21.
25. Liao Y, Smyth GK, Shi W. FeatureCounts: An efficient general purpose program for assigning sequence reads to genomic features. *Bioinformatics*. 2014 Apr 1;30(7):923–30.
26. Harrow J, Frankish A, Gonzalez JM, Tapanari E, Diekhans M, Kokocinski F, et al. GENCODE: The reference human genome annotation for the ENCODE project. *Genome Res*. 2012 Sep;22(9):1760–74.
27. Gentleman RC, Carey VJ, Bates DM, Bolstad B, Dettling M, Dudoit S, et al. Bioconductor: open software development for computational biology and bioinformatics. *Genome Biol*. 2004 Sep 15;5(10):1–16.
28. Robinson MD, McCarthy DJ, Smyth GK. edgeR: A Bioconductor package for differential expression analysis of digital gene expression data. *Bioinformatics*. 2009 Nov 11;26(1):139–40.
29. Ritchie ME, Phipson B, Wu D, Hu Y, Law CW, Shi W, et al. Limma powers differential expression analyses for RNA-sequencing and microarray studies. *Nucleic Acids Res*. 2015 Jan 6;43(7):e47.
30. Yu G, Wang LG, Han Y, He QY. ClusterProfiler: An R package for comparing biological themes among gene clusters. *Omi A J Integr Biol*. 2012 May 1;16(5):284–7.
31. Gantner CW, de Luzy IR, Kauhausen JA, Moriarty N, Niclis JC, Bye CR, et al.

- Viral Delivery of GDNF Promotes Functional Integration of Human Stem Cell Grafts in Parkinson's Disease. *Cell Stem Cell*. 2020 Apr 2;26(4):511–526.e5.
32. Subramanian A, Tamayo P, Mootha VK, Mukherjee S, Ebert BL, Gillette MA, et al. Gene set enrichment analysis: A knowledge-based approach for interpreting genome-wide expression profiles. *Proc Natl Acad Sci U S A*. 2005 Oct 25;102(43):15545–50.
 33. Torres-Ortega PV, Smerdou C, Ansorena E, Ballesteros-Briones MC, Martisova E, Garbayo E, et al. Optimization of a GDNF production method based on Semliki Forest virus vector. *Eur J Pharm Sci*. 2021 Apr 1;159:105726.
 34. Zambaux MF, Bonneaux F, Gref R, Maincent P, Dellacherie E, Alonso MJ, et al. Influence of experimental parameters on the characteristics of poly(lactic acid) nanoparticles prepared by a double emulsion method. *J Control Release*. 1998 Jan 2;50(1–3):31–40.
 35. Yoffe EH. Modified Hertz theory for spherical indentation. *Philos Mag A Phys Condens Matter, Struct Defects Mech Prop*. 1984;50(6):813–28.
 36. Burdick JA, Chung C, Jia X, Randolph MA, Langer R. Controlled degradation and mechanical behavior of photopolymerized hyaluronic acid networks. *Biomacromolecules*. 2005 Jan;6(1):386–91.
 37. Caraci F, Gulisano W, Guida CA, Impellizzeri AAR, Drago F, Puzzo D, et al. A key role for TGF- β 1 in hippocampal synaptic plasticity and memory. *Sci Rep*. 2015 Jun 10;5.
 38. Meyers EA, Kessler JA. TGF- β family signaling in neural and neuronal differentiation, development, and function. *Cold Spring Harb Perspect Biol*. 2017;9(8).
 39. Zhang YH, Belegu V, Zou Y, Wang F, Qian BJ, Liu R, et al. Endoplasmic Reticulum Protein 29 Protects Axotomized Neurons from Apoptosis and Promotes Neuronal Regeneration Associated with Erk Signal. *Mol Neurobiol*. 2015 Aug 25;52(1):522–32.
 40. Hobara N, Goda M, Kitamura Y, Sendou T, Gomita Y, Kawasaki H. Adrenomedullin facilitates reinnervation of phenol-injured perivascular nerves in

- the rat mesenteric resistance artery. *Neuroscience*. 2007 Jan 19;144(2):721–30.
41. Wang T, Zhou G, He M, Xu Y, Rusyniak WG, Xu Y, et al. GPR68 Is a Neuroprotective Proton Receptor in Brain Ischemia. *Stroke*. 2020;51(12):3690–700.
 42. Rodríguez-Nogales C, Garbayo E, Martínez-Valbuena I, Sebastián V, Luquin MR, Blanco-Prieto MJ. Development and characterization of polo-like kinase 2 loaded nanoparticles-A novel strategy for (serine-129) phosphorylation of alpha-synuclein. *Int J Pharm*. 2016 Nov 30;514(1):142–9.
 43. Arranz-Romera A, Esteban-Pérez S, Molina-Martínez IT, Bravo-Osuna I, Herrero-Vanrell R. Co-delivery of glial cell-derived neurotrophic factor (GDNF) and tauroursodeoxycholic acid (TUDCA) from PLGA microspheres: potential combination therapy for retinal diseases. *Drug Deliv Transl Res*. 2021 Apr 1;11(2):566–80.
 44. Herrán E, Requejo C, Ruiz-Ortega JA, Aristieta A, Igartua M, Bengoetxea H, et al. Increased antiparkinson efficacy of the combined administration of VEGF- and GDNF-loaded nanospheres in a partial lesion model of Parkinson's disease. *Int J Nanomedicine*. 2014;9(1):2677–87.
 45. Guvendiren M, Lu HD, Burdick JA. Shear-thinning hydrogels for biomedical applications. Vol. 8, *Soft Matter*. The Royal Society of Chemistry; 2012. p. 260–72.
 46. Kaya G, Oytun F. Rheological properties of injectable hyaluronic acid hydrogels for soft tissue engineering applications. *Biointerface Res Appl Chem*. 2021;11(1):8424–30.
 47. Wang Y, Wei YT, Zu ZH, Ju RK, Guo MY, Wang XM, et al. Combination of hyaluronic acid hydrogel scaffold and PLGA microspheres for supporting survival of neural stem cells. *Pharm Res*. 2011;28(6):1406–14.
 48. Zhong S, Yung LYL. Enhanced biological stability of collagen with incorporation of PAMAM dendrimer. *J Biomed Mater Res - Part A*. 2009 Oct 1;91(1):114–22.
 49. Jaiswal MK, Xavier JR, Carrow JK, Desai P, Alge D, Gaharwar AK. Mechanically stiff nanocomposite hydrogels at ultralow nanoparticle content. *ACS Nano*.

- 2016;10(1):246–56.
50. Li Q, Barrett DG, Messersmith PB, Holten-Andersen N. Controlling hydrogel mechanics via bio-inspired polymer-nanoparticle bond dynamics. *ACS Nano*. 2016;10(1):1317–24.
 51. Arno MC, Inam M, Weems AC, Li Z, Binch A LA, Platt CI, et al. Exploiting the role of nanoparticle shape in enhancing hydrogel adhesive and mechanical properties. *Nat Commun*. 2020;11(1).
 52. Chen MH, Wang LL, Chung JJ, Kim YH, Atluri P, Burdick JA. Methods to Assess Shear-Thinning Hydrogels for Application As Injectable Biomaterials. *ACS Biomater Sci Eng*. 2017;3(12):3146–60.
 53. Nair R, Roy Choudhury A. Synthesis and rheological characterization of a novel shear thinning levan gellan hydrogel. *Int J Biol Macromol*. 2020 Sep 15;159:922–30.
 54. Hiscox L V., Johnson CL, Barnhill E, McGarry MDJ, Huston J, Van Beek EJR, et al. Magnetic resonance elastography (MRE) of the human brain: Technique, findings and clinical applications. *Phys Med Biol*. 2016 Nov 15;61(24):R401–37.
 55. Farrukh A, Zhao S, del Campo A. Microenvironments designed to support growth and function of neuronal cells. *Front Mater*. 2018 Nov 2;5:62.
 56. Karimi A, Navidbakhsh M. Material properties in unconfined compression of gelatin hydrogel for skin tissue engineering applications. *Biomed Tech*. 2014 Dec 1;59(6):479–86.
 57. Yang H, Kang W, Wu H, Yu Y, Zhu Z, Wang P, et al. Stability, rheological property and oil-displacement mechanism of a dispersed low-elastic microsphere system for enhanced oil recovery. *RSC Adv*. 2017 Jan 23;7(14):8118–30.
 58. Sprenger S. Epoxy resin composites with surface-modified silicon dioxide nanoparticles: A review. *J Appl Polym Sci*. 2013 Nov 5;130(3):1421–8.
 59. Zhang H, Patel A, Gaharwar AK, Mihaila SM, Iviglia G, Mukundan S, et al. Hyperbranched polyester hydrogels with controlled drug release and cell adhesion properties. *Biomacromolecules*. 2013 May 13;14(5):1299–310.

CHAPTER 2

60. Pérez-Luna V, González-Reynoso O. Encapsulation of Biological Agents in Hydrogels for Therapeutic Applications. *Gels*. 2018 Jul 11;4(3):61.
61. Ucar B, Humpel C. Therapeutic efficacy of glial cell-derived neurotrophic factor loaded collagen scaffolds in ex vivo organotypic brain slice Parkinson's disease models. *Brain Res Bull*. 2019 Jul 1;149:86–95.
62. Garbayo E, Ansorena E, Lana H, Carmona-Abellan M del M, Marcilla I, Lanciego JL, et al. Brain delivery of microencapsulated GDNF induces functional and structural recovery in parkinsonian monkeys. *Biomaterials*. 2016 Dec 1;110:11–23.
63. Madni A, Tahir N, Rehman M, Raza A, Mahmood MA, Khan MI, et al. Hybrid Nano-carriers for Potential Drug Delivery. In: *Advanced Technology for Delivering Therapeutics*. InTech; 2017. p. 54–87.
64. Ansorena E, Casales E, Aranda A, Tamayo E, Garbayo E, Smerdou C, et al. A simple and efficient method for the production of human glycosylated glial cell line-derived neurotrophic factor using a Semliki Forest virus expression system. *Int J Pharm*. 2013;440(1):19–26.
65. Hong Z, Zhang QY, Liu J, Wang ZQ, Zhang Y, Xiao Q, et al. Phosphoproteome study reveals Hsp27 as a novel signaling molecule involved in GDNF-induced neurite outgrowth. *J Proteome Res*. 2009;8(6):2768–87.
66. Jensen G, Holloway JL, Stabenfeldt SE. Hyaluronic Acid Biomaterials for Central Nervous System Regenerative Medicine. *Cells*. 2020 Sep 17;9(9):2113.
67. Heusinkveld HJ, Westerink RHS. Comparison of different in vitro cell models for the assessment of pesticide-induced dopaminergic neurotoxicity. *Toxicol Vitro*. 2017 Dec 1;45:81–8.
68. Perera PGT, Bazaka O, Bazaka K, Appadoo D, Croft RJ, Russell J, et al. Pheochromocytoma (PC 12) as a Model Cell Line for Membrane Permeabilization Studies in the presence of Electromagnetic Fields (EMFs): Recent Advances. *J Neurol Neuromedicine*. 2019;4–1(Pc 12):35–40.

Supporting Information**Encapsulation of hMSCs and hGDNF in a novel injectable nanoreinforced-hydrogel to improve cell replacement therapy in Parkinson´s Disease**

Pablo V. Torres-Ortega ^(1,2), Daniel Plano ^(1,2), Jacobo Paredes ⁽³⁾, Javier Aldazabal ⁽³⁾, Rosario Luquin ^(2,4), Carmen Sanmartin ^(1,2), María J. Blanco-Prieto ^(1,2), Elisa Garbayo ^(1,2)

¹ Department of Pharmaceutical Technology and Chemistry, Faculty of Pharmacy and Nutrition, University of Navarra, C/ Irunlarrea 1, 31008 Pamplona, Spain

² Navarra Institute for Health Research, IdiSNA, C/ Irunlarrea 3, 31008 Pamplona, Spain

³ Tecnun, School of Engineering, University of Navarra, C/ Manuel de Lardizábal 15, 20018 San Sebastián, Spain

⁴ Department of Neurology and Neurosciences, Clínica Universidad de Navarra, Pamplona, C/ Pío XII 36, 31008 Pamplona, Spain.

*Corresponding authors at: Department of Pharmaceutical Technology and Chemistry, Faculty of Pharmacy and Nutrition, Universidad de Navarra, C/Irunlarrea 1, 31008 Pamplona, Spain.

E-mail addresses: egarbayo@unav.es (E. Garbayo), mjblanco@unav.es (M.J. Blanco-Prieto).

CHAPTER 2

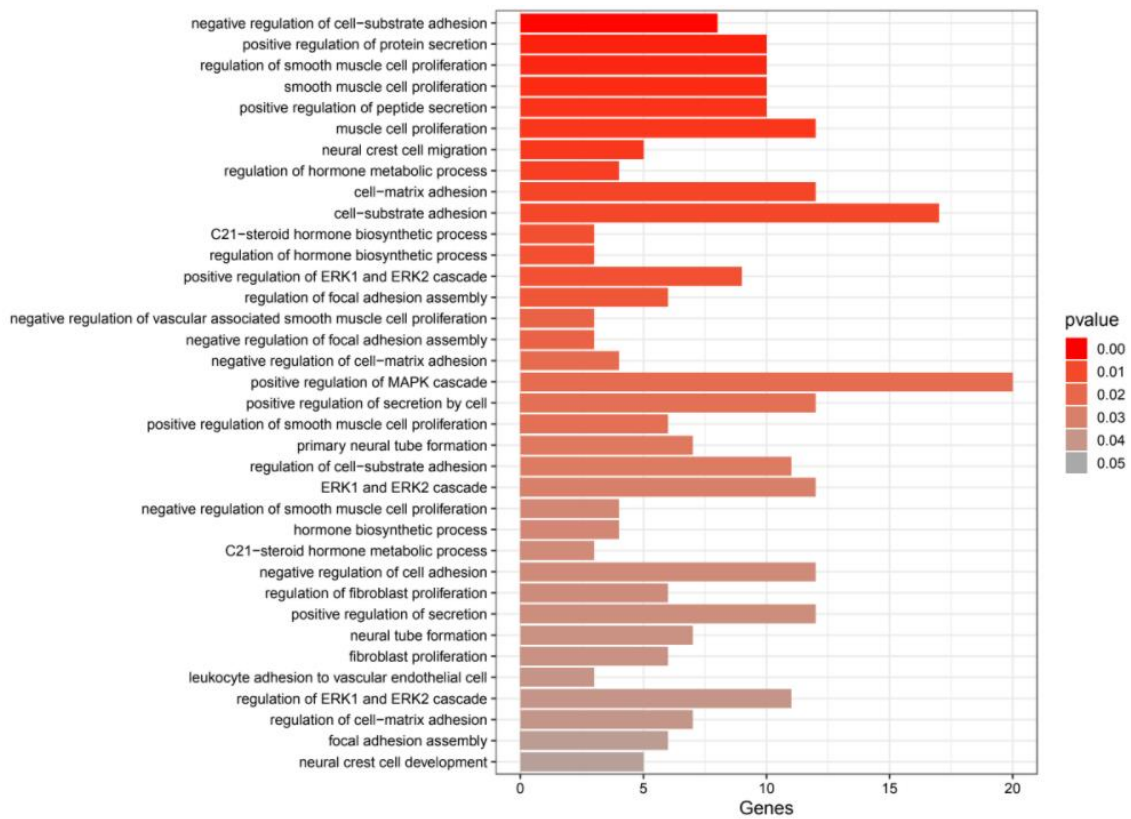


Figure S1. Gene ontology analysis clustering of upregulated genes in hMSCs culture exposed to hGDNF.

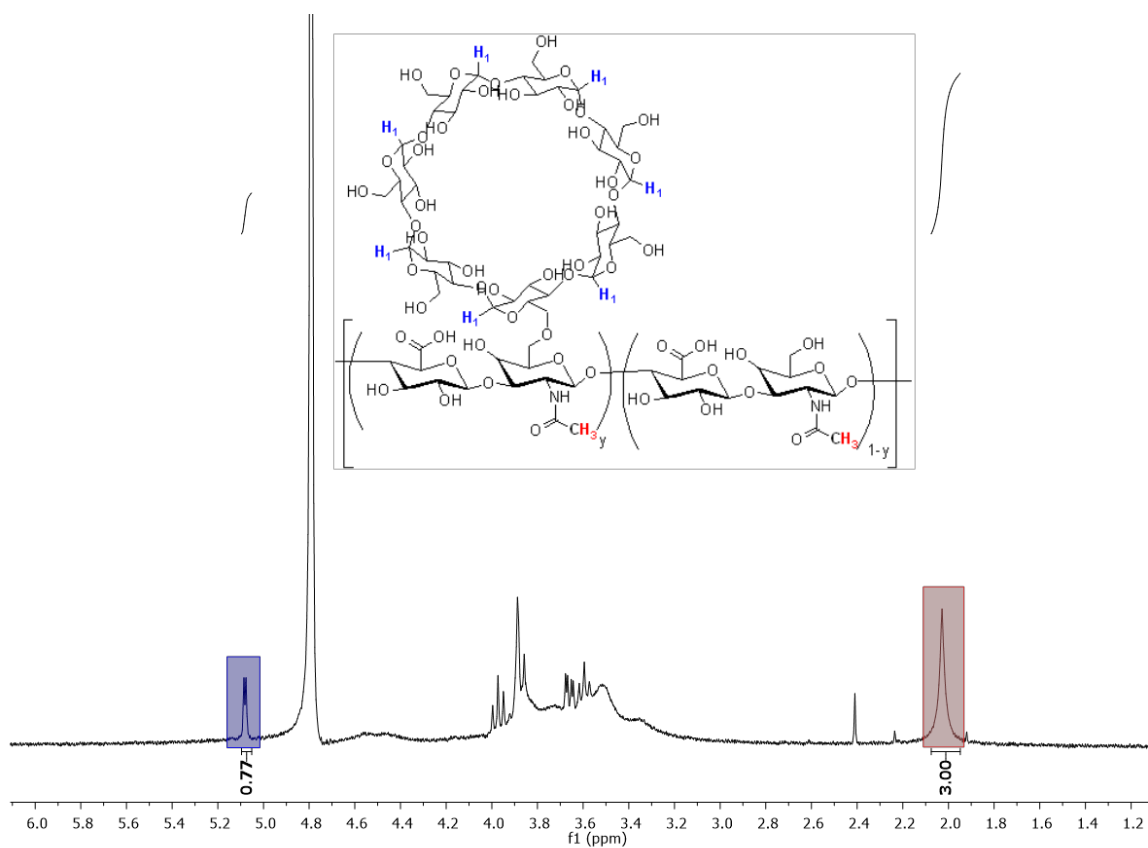


Figure S2. ^1H NMR spectra of hyaluronic acid (HA) modified with cyclodextrin (CD) in D_2O . Modification of HA with pendant CD ($10.6 \pm 1.5\%$) was determined by integration of the signal for the hydrogen on position 1 of CD (7 Hs, shaded blue) relative to the signal for *N*-acetyl singlet of HA (3Hs, shaded red).

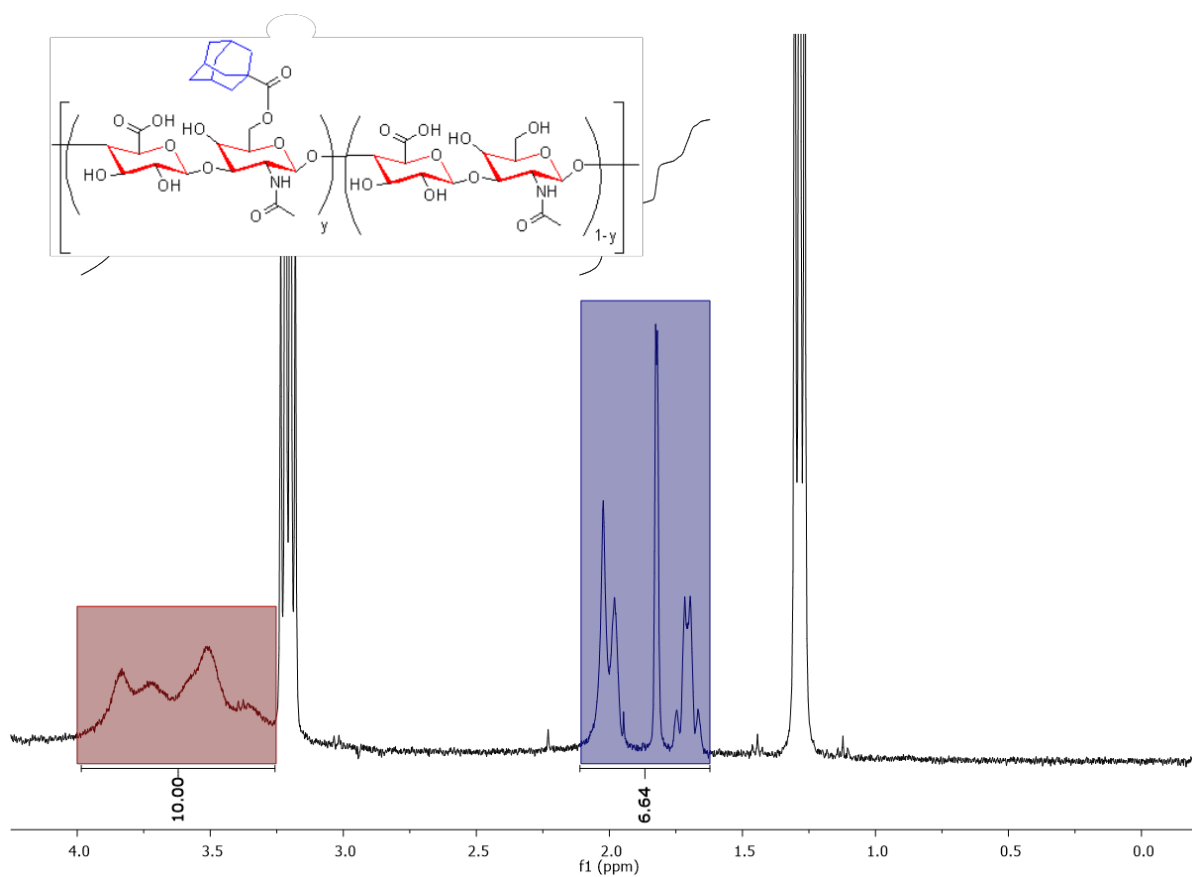


Figure S3. ^1H NMR spectra of HA modified with adamantane (AD) in D_2O . Modification of HA ($40.3 \pm 3.5\%$) with pendant AD was determined by integration of the adamantane hydrogens (15Hs, shaded blue) relative to the sugar ring of HA (10Hs, shaded red).

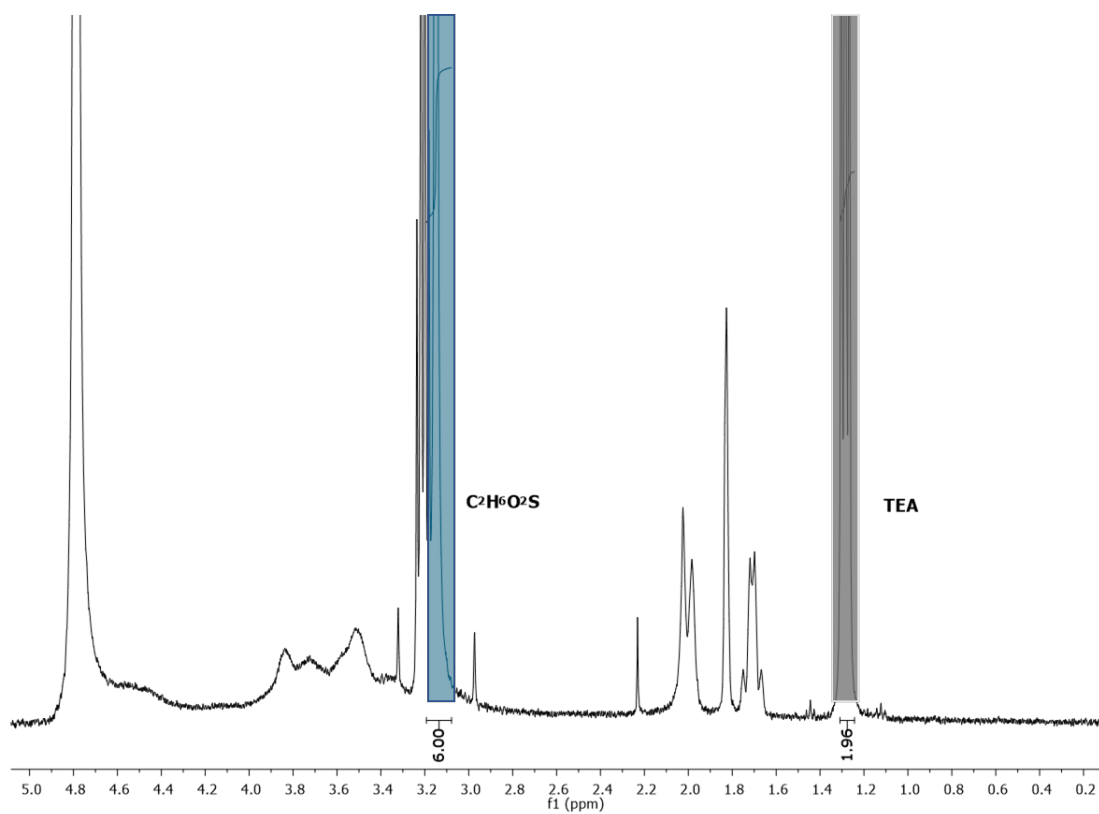


Figure S4. ^1H NMR spectra of HA-AD with dimethylsulfone in D_2O . The residual amount of Triethylamine (TEA) resulting from the HA-AD synthesis was determined by integration of the methyl triplet of TEA (9Hs, shaded grey) relative to the singlet of dimethylsulfone (6Hs, shaded blue).

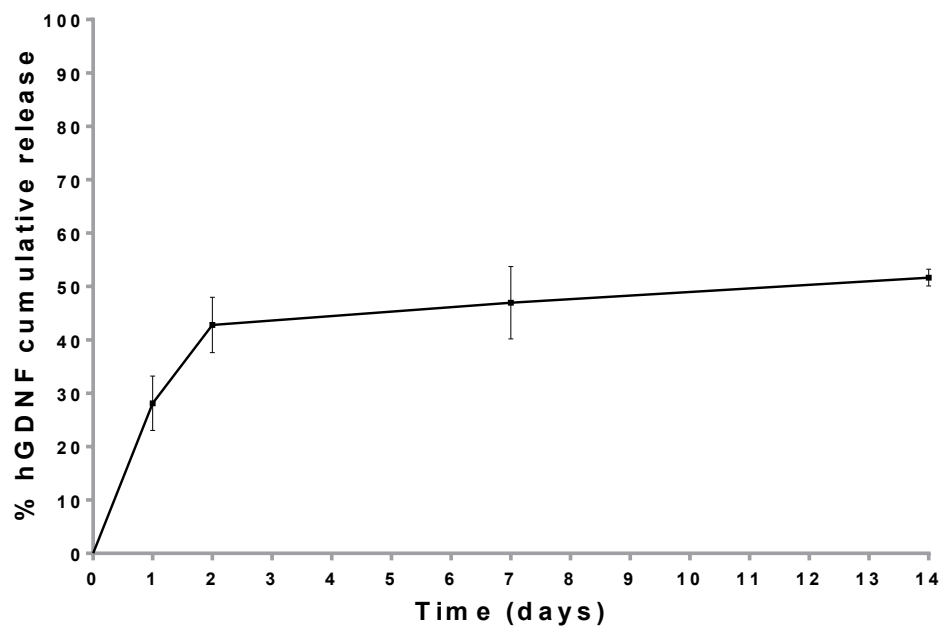


Figure S5. Cumulative release of hGDNF after NPs disruption with DMSO.

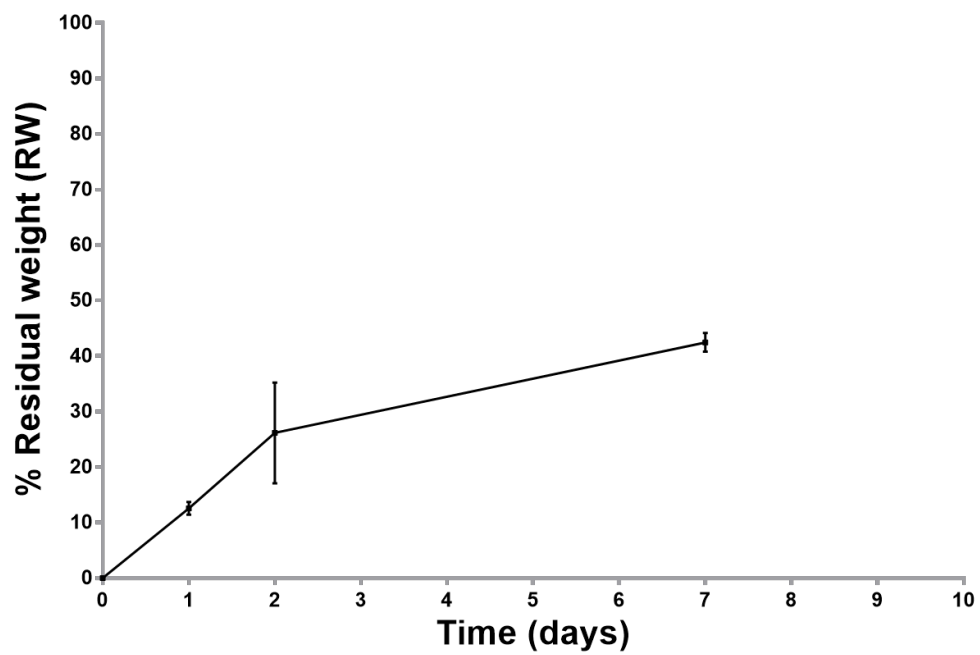


Figure S6. % Residual weight (RW) of 6% wt HG-NPs over seven.

GENERAL **DISCUSSION**

I. PARKINSON'S DISEASE

A summary of Parkinson's disease history

Parkinson's disease (PD) was first described more than 200 years ago as "An involuntary trembling movement, with diminished muscular power, in parts not in action and even when supported; with a propensity to bend the trunk forward and to pass from a walking to a running rhythm: the senses and intelligence are not injured". (1,2). This definition is from the monograph published by James Parkinson "*An Essay on the Shaking Palsy* (1817)" which represents his best-known medical contribution (1,2). In this volume, the characteristic motor symptoms of the disease and the neurological character of this condition were described. Fifty years later, Jean-Martin Charcot provided new scientific evidence that allowed the establishment of the clinical and anatomopathological basis of PD (3). Since then, considerable technological and scientific advances have led to a better understanding of this disease (Figure 1). Many of these advances remain essential in the therapeutic management of PD. One example is the discovery of dopamine as the first effective therapy, which is currently the therapy of choice in the early stages of PD (3,4) (Figure 1). Other milestones, such as the first clinical trials with glial cell line-derived neurotrophic factor (GDNF), the role of α -synuclein as a therapeutic target or the use of immunotherapy for PD represent important attempts to develop new therapies for PD (3,4) (Figure 1). However, even though the symptoms of PD can be managed effectively over a significant period, the challenge to determine the cause of PD and its cure remains.

Parkinson's disease: Epidemiology, Pathophysiology, and Management

As already mentioned, PD was first medically defined by James Parkinson as a neurological syndrome in his work "Essay on the Shaking Palsy". For most of history, PD has been considered a rare disorder (5,6). Nevertheless, in less than two centuries PD has become a common disorder and the fastest growing neurological disorder in the world (6). Importantly, the global burden of PD has doubled in the past two decades (7). The incredibly fast advance of this condition makes it of paramount interest. Like a pandemic, this neurological disorder is spreading over wide geographical areas and is present in all regions of the world (6). The outlook is not encouraging: as the population ages and life expectancy increases, we expect the number of individuals with PD to double again in the next generation (8).

GENERAL DISCUSSION

PD is characterized by the selective loss of dopaminergic neurons (DANs) in the *substantia nigra pars compacta* (SNpc) and the presence of Lewy bodies (LBs). From a therapeutic standpoint, the mainstay of PD management is the pharmacological substitution of dopamine using drugs such as dopamine agonists and levodopa (9). Unfortunately, this scenario cannot be dramatically improved with the available treatments, which are unable to slow down the neurodegenerative process. Therefore, the potential of a promising therapeutic tool where neurotrophic factor (NTFs), stem cells and drug delivery systems (nanoparticles (NPs) and HGs) are combined to bring about significant improvements in PD treatment will be discussed in the following sections.

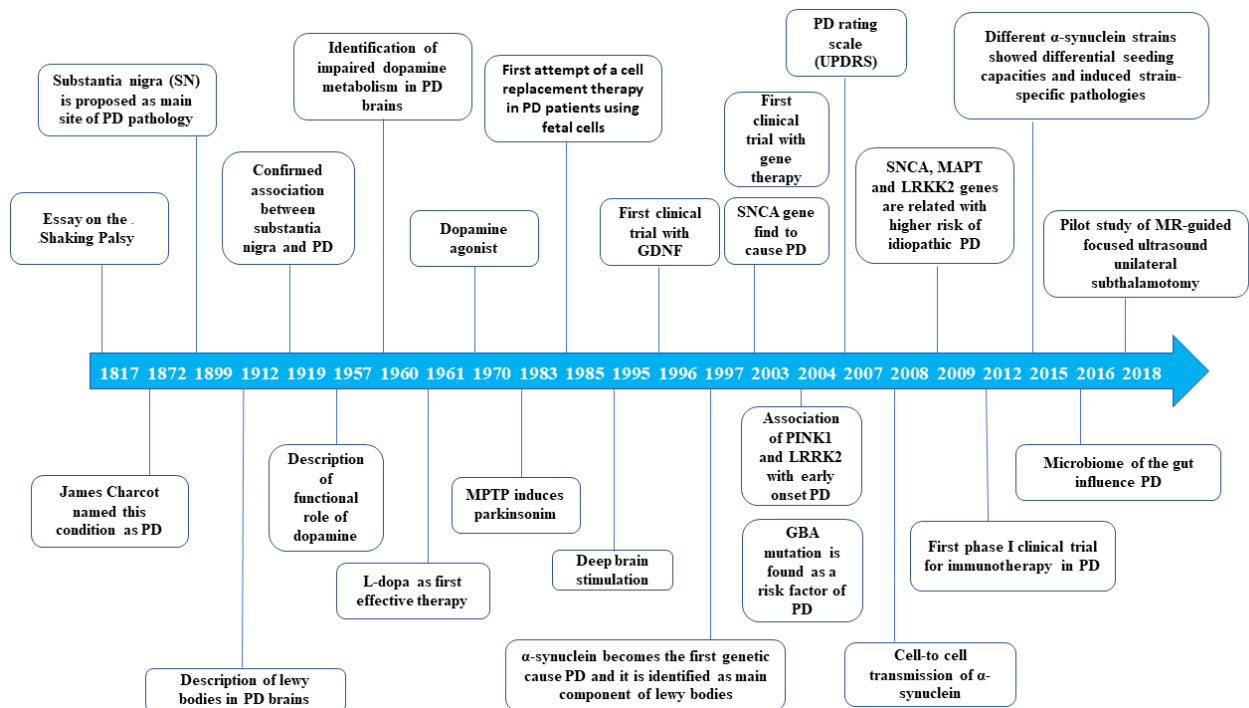


Figure 1. Schematic summary of the most relevant breakthroughs in PD history.

II. NEUROTROPHIC FACTOR THERAPIES FOR PARKINSON'S DISEASE

NTFs are promising candidates for disease-modifying therapies in neurodegenerative disorders. Their functions are not only limited to neuronal protection but also restore neurons, promote neuronal arborization and sprouting of their neurites. They also contribute to the improvement of the functional activity of neurons (10,11). These properties support the efforts that have been made in both academic and industry settings to translate NTFs into drugs for PD treatment (10,11). Furthermore, these proteins have been extensively tested in several preclinical PD models, which have reportedly restored the morphology and function of the degenerated neurons (10,12). However, clinical trial results so far have been somewhat limited and have failed to demonstrate the efficacy of this approach. Several obstacles that may be linked to side effects and poor outcomes have been proposed: inadequate GDNF dosage and delivery regimens, application on late-stage PD patients, and the origin of the NTF (mammalian vs bacterial), among others (10,12,13). For example, high concentrations of NTFs inhibit the formation of functional oligomeric signaling complexes, elicit NTFs and receptor degradation in the short-term or promote the suppression of their receptor expression via various silencing mechanisms in long-term experiments (14,15). Many clinical trials were performed in PD patients under continuous infusion, but continuous overexpression or infusion probably induce negative effects in the DA system, such as downregulation of tyrosine hydroxylase (TH), production of aberrant sprouting and ectopic formation of synapses in the brain (7,10,16). Regarding delivery methods, NTFs have been usually administered systemically or directly into the brain through pumps or gene delivery with viral vectors (13). As already mentioned **in the introduction**, nanotechnology advances offer different alternatives to improve NTF delivery to the brain. Therefore, their use could lead to greater stability of NTFs in the body fluids and to the development of new vehicles able to cross the BBB. In addition, the NP-mediated delivery of NTFs to the brain could improve drug diffusion in the brain and its bioavailability to the target cells (13). Interestingly, the stage of PD at which the NTFs are administered is a key factor that should be examined in depth in future clinical trials (12). It is worth mentioning that PD is caused by progressive neurodegeneration, with the selective loss of most of the dopaminergic neurons of the SNpc within 4–5 years. Ideally, NTFs should be administered immediately after diagnosis, or preferentially even during the presymptomatic period to slow down this

GENERAL DISCUSSION

neurodegeneration (11). However, NTF-based therapies have followed the opposite approach when investigated in clinical trials (11). Therefore, one of the hypotheses to explain the negative results of clinical trials with NTFs is that they were administered in late-stage patients (10,13,17,18). NTF origin can also influence the clinical trial outcomes and therefore, its importance will be discussed in more detail in the next section.

Development of therapeutic proteins: Role of protein expression systems

A mammalian host system is the preferred expression platform for the production of biotherapeutic proteins for humans (10,19). The post-transcriptional metabolic machinery of mammalian cells allows the expression of therapeutic proteins with a glycosylation pattern similar to native human protein (20,21). This results in higher quality and efficacy compared to non-glycosylated proteins produced in bacterial hosts (20,21). Moreover, GDNF of bacterial origin has lower stability and activity than GDNF produced in mammalian cells (13,22,23). This is demonstrated among others in a recent study that found that hGDNF from *E. coli* was less functional in the phosphorylation and MAPK signaling experiments than hGDNF from zebrafish (24). The lack of post-translational modifications of the protein or a lower percentage of correctly folded protein from the *E. coli* expression system could be the reason. The failed clinical trials investigating the use of hGDNF to treat PD patients used “r-metHuGDNF”, which is a recombinant protein expressed in *E. coli* (25,26). This topic is reviewed **in Chapter 1** of this doctoral thesis. This chapter discusses the advantages of the expression of therapeutic proteins in mammalian cells and proposes an efficient methodology for producing highly glycosylated hGDNF like the endogenous one (Figure 2). In our system, the mammalian cell line BHK-21 was used. BHK-21 cells have been largely used for the production of several recombinant proteins that are currently present in the market (i.e. coagulation factors VIIa and VIII) (27–29). These are highly complex recombinant proteins requiring post-translational modifications that can be provided by these eukaryotic cells (30). Indeed, our group has previously published some studies in which purified recombinant GDNF obtained from BHK-21 cells was microencapsulated in PLGA microparticles and administered to rats and monkeys. No anti-GDNF antibodies were detected in the serum of both treated animals, suggesting that the glycosylation pattern was close to the endogenous protein (31–33). Moreover, in additional studies from our group hGDNF was produced in electroporated BHK-21 cells using a Semliki Forest virus (SFV) expression vector. This recombinant hGDNF was highly glycosylated,

containing both N- and O-linked glycosylation sites, and was active, confirming its proper folding (33). Going further, some studies have reported a higher protein expression using biphasic temperature protocols (34–36). Therefore, in chapter 1 of this thesis, we increased the incubation temperature during the shut-off period from 33°C to 37°C to induce a higher expression of hGDNF. It has also been described that the cell culture conditions can influence the glycosylation pattern of recombinant proteins (37–39). By contrast, a study from Helder J. Cruz *et al.* (40) demonstrated that metabolic shifts do not influence the glycosylation patterns of a recombinant fusion protein expressed in BHK cells. They showed that the recombinant protein did not modify its glycosylation pattern when the composition of the culture medium was changed (40). Taking all these data into account and the fact that we are employing the same temperature during post shut-off period and the same culture medium used for Ansorena et al (33), it is very unlikely that the composition or the structure of the glycans of the hGDNF will be significantly impacted by the small change in the incubation temperature. Also noteworthy is that the proper folding of the protein is a necessary condition for hGDNF binding with the receptors that mediate its activity (family receptor $\alpha 1$ (GFR $\alpha 1$), and the RET receptor protein tyrosine kinase) (41,42). Importantly, we demonstrate the bioactivity of hGDNF using a PC-12 neurite outgrowth bioassay. These cells, which possess the GFR $\alpha 1$ and RET receptors, change their phenotype and develop neurites in the presence of biologically active hGDNF (33,42). In this regard, misfolding proteins cannot bind to these receptors and thus, cannot induce the change of PC-12 phenotype. In our work, purified hGDNF induce neurite outgrowth in PC12 cells, being proof of its suitable folding and biological activity. Moreover, our protocol led to the production of almost 3-fold more hGDNF when compared to the previously described method (33).

GENERAL DISCUSSION

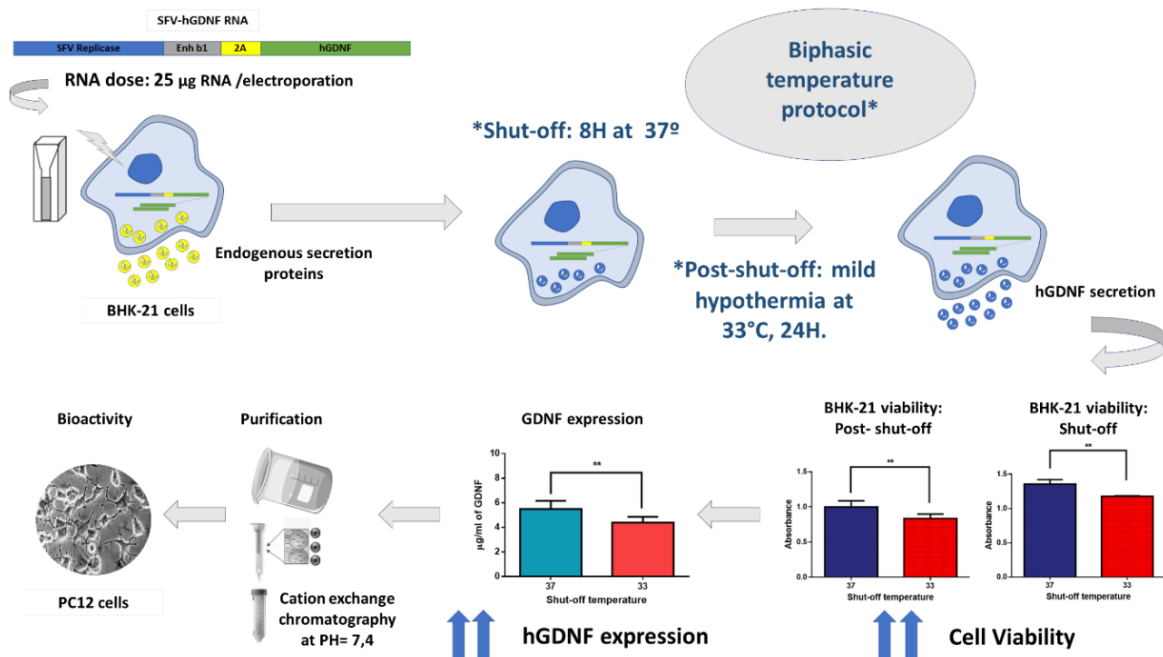


Figure 2. Schematic illustration of GDNF production method based on Semliki Forest virus vector.

hGDNF and Parkinson's Disease: Is hGDNF enough?

hGDNF is the most extensively investigated NTF in the context of PD. The therapeutic efficacy of hGDNF in mild and moderate neurotoxic animal models of PD has been extensively demonstrated (17). However, hGDNF showed weak neuroprotection when the nigrostriatal pathway lesion was severe and in α -synuclein overexpression models (11). This lack of effectiveness could be attributable to the factors described in the above section (**Neurotrophic factor therapies for Parkinson's Disease**). In addition, the downregulation of RET and transcription factor Nurr1 could dramatically reduce the therapeutic efficacy of hGDNF in models based on α -synuclein overexpression (11,43). In contrast, a later study showed that the gene expression of the α -synuclein gene was not increased in sporadic PD and that, at least at the transcriptional level, GDNF signalling molecules such as Nurr1 and RET were not affected in sporadic PD (44). Moreover, α -synuclein overexpression was not correlated with the downregulation of Nurr1 and RET. Therefore, the accumulation of α -synuclein would not block GDNF signaling in PD (44).

Despite the unclear results in clinical studies, experts maintain that hGDNF remains a highly promising drug for the treatment of PD progression (45). Preclinical data are sufficiently robust, and we may not have been able to unlock the full potential of this protein in the context of human disease (45). In this field, novel alternatives such as new delivery systems (NPs and HGs) and hGDNF combination with stem cell-based therapies

should be explored to exploit the real potential of this neurotrophic factor for PD. These strategies are addressed in **Chapter 2** of this thesis and will be discussed in detail in the next sections.

III. CELL THERAPY FOR BRAIN REGENERATION

Cell replacement therapies for Parkinson's Disease: how could cell transplantation help?

PD is characterized by a combination of motor and non-motor symptoms that gradually appears as a consequence of the selective death of DANs from the SNpc and the abnormal accumulation and aggregation of α -synuclein in the form of Lewy bodies (LBs) (46). Dopamine replacement therapy using levodopa and surgical treatment based on deep brain stimulation can only reduce the symptoms but cannot halt the disease progression. Due to the selective degeneration of DANs, cell transplant-based treatments provide an enormous potential for PD management (47). Since 1979, many studies have examined the potential of cell-based therapies to restore dopamine in the striatum and ameliorate PD motor deficits (48–53). Overall, transplantation of fetal ventral midbrain tissue into the striatum of PD patients has provided the proof of principle that cell therapies can provide long-term clinical benefits (46). However, inconsistent results and side effects such as graft-induced dyskinesias were reported (46). Moreover, the fetal material showed notable limitations such as the high variability and the lack of possibility for its standardization to be transplanted (46,49,54). The phenotypic instability of the cells after passaging and the poor proliferation and survival observed after grafting the cells in the brain also contributed to the inconsistent results (55). Furthermore, from the ethical standpoint, the use of human embryonic stem cells as a cell source supposes the destruction of embryos and their use is not ethically sustainable. The ethical dilemma and the limitations of embryonic stem cell research have resulted in further investigations on alternative cell sources. Subsequently, two cell types have been proposed: DANs derived from human induced pluripotent stem cells (hiPS-DANs) and mesenchymal stem cells (MSCs) (47,48,56).

hiPS are particularly attractive as a unique source of DANs. Furthermore, they represent a practical and ethically acceptable stem cell population (57). These cells are obtained from adult cells that have been genetically reprogrammed to a state similar to embryonic stem cells. The hiPS can be induced by introducing four transcription factors such as Sox2, Oct3/4, Klf-4, and c-Myc (58). Subsequently, hiPS cells can be differentiated into

GENERAL DISCUSSION

DAns (hiPS-DAns) (59). The efficacy of hiPS-DAns transplantation has been demonstrated on several PD animal models. One study showed that hiPS-DAns grafts were successfully implanted in parkinsonian monkeys and showed remarkable improvements in PD scores, but a relatively low maturation rate was found and only $33.3 \pm 24.4\%$ of surviving cells expressed TH (60). In another study, an increase in the number of surviving TH⁺ neurons in the grafts was found using hiPS-DAns derived from a major histocompatibility complex (MHC) homozygous cynomolgus (61). In this regard, the poor survival of grafted neurons and the limited dopaminergic reinnervation in the host striatum remains a challenge (62). Importantly, the clinical application of hiPS is also limited due to its tumorigenicity (63). For this reason, scientists are developing new procedures for direct reprogramming that avoid the pluripotent state and reduce the tumor-initiating capacities.

For PD studies, MSCs have been isolated from various neonatal and adult tissues highlighting bone marrow, adipose tissue, or umbilical cord (55,64,65). Regarding the mechanism of action of MSCs, several hypotheses have been proposed. First, human MSCs secretion includes protective neurotrophic factors, anti-apoptotic factors, growth factors, and cytokines into a damaged or inflamed area (55,66–68). Secondly, MSCs modulate hematopoiesis regulation and tissue regeneration by their paracrine signaling and multipotency, respectively (69). Thirdly, MSCs have the potential to independently migrate to the damaged area when introduced into the human body by different routes of administration (70,71). Furthermore, MSCs present low teratoma risk, low immunogenicity, a suitable profile for autologous transplantation (72), and their use is not limited by ethical issues (70,71). Currently, several clinical trials using MSCs for PD treatment are in progress (55), although low cell survival and engraftment have been reported (73,74). For example, a recent study has explored the survival of green fluorescent protein (GFP)-MSCs after its injection into the SN of mice (73). The MSC-GFP-luciferase signal decreased by nearly 50% five days post-injection (73). Importantly, cell survival after transplantation is crucial for the efficacy of MSCs therapies and depends on a combination of mechanical, cellular, and host factors that must be carefully addressed (74,75).

In summary, although hiPS-Dans and MSCs are promising candidates for cell-based approaches in PD, stem cell therapy is still in development, and the ideal scenario for clinical transplantation should be explored in the near future (76). Among other aspects,

novel approaches to enhance stem cell viability after transplantation are required to promote the efficacy of cell replacement therapies for PD (74).

Cell and neurotrophic based therapies for brain regeneration (hiPS-DANs-hGDNF and hMSCs-hGDNF)

Recently, the ability of hGDNF to promote the functional integration of DANs grafts has received great attention. A study published by Khazaei *et al* (77) showed that modulation of Notch signaling by hGDNF in transplanted hiPS-DANs increased their neuronal fate and improved their electrical integration independently of an effect on cell survival (77). Furthermore, a recently published study demonstrated the ability of hGDNF to increase the survival, plasticity, and functional integration of hiPS-DANs grafts, in a post-transplantation-time dependent manner (78). Additionally, some recent studies have also demonstrated that the combination of hMSCs and hGDNF has a positive impact on motor recovery and dopaminergic function in the striatum of different PD models (6-hydroxydopamine (6-OHDA), 1-Methyl-4-phenyl-1,2,3,6-tetrahydropyridine (MPTP), lactacystin and lipopolysaccharide (LPS) PD models) (79–84). Going a step further, a recent study showed that hGDNF is not only able to induce a positive effect on the viability and neural-like cell differentiation capacity of MSCs but could also contribute to the therapeutic effectiveness of MSCs-GDNF grafts in a 6-OHDA-lesioned mouse model (85). Therefore, we next investigate the ability of hGDNF to modulate gene expression in hiPS-DANs and hMSCs and its potential to regulate mechanisms involved in the survival and plasticity of these cells.

The ability of hGDNF to modulate gene expression in hiPS-DANs was analyzed by RNA-seq in the first part of **chapter 2**. The study of transcriptomic data revealed a remarkable potential of hGDNF to induce dynamic changes in the gene expression profile of hiPS-DANs. Gene modulation was observed both at day 1 and 7 post-hGDNF-treatment, with important changes between days 1 and 7. In addition to a remarkable regulation of the transcriptome of hiPS-DANs, there was a positive regulation of functions directly involved in neuronal survival and development. Specifically, a significant activation in the neurite outgrowth biofunction was observed during hGDNF stimulation. Figure 3 shows that hGDNF regulates the expression of different genes that promote the activation of neurite outgrowth and how their activation is increased after 7 days of treatment with hGDNF. In addition, hGDNF stimulation leads to the activation of many other important functions such as nerve tissue growth, number of neurons and axonal growth, among

GENERAL DISCUSSION

others. These findings strongly support the neuroprotective role of hGDNF and its ability to stimulate the regenerative sprouting from spared axons in the partially denervated striatum of rodent and primate models of PD (17,32).

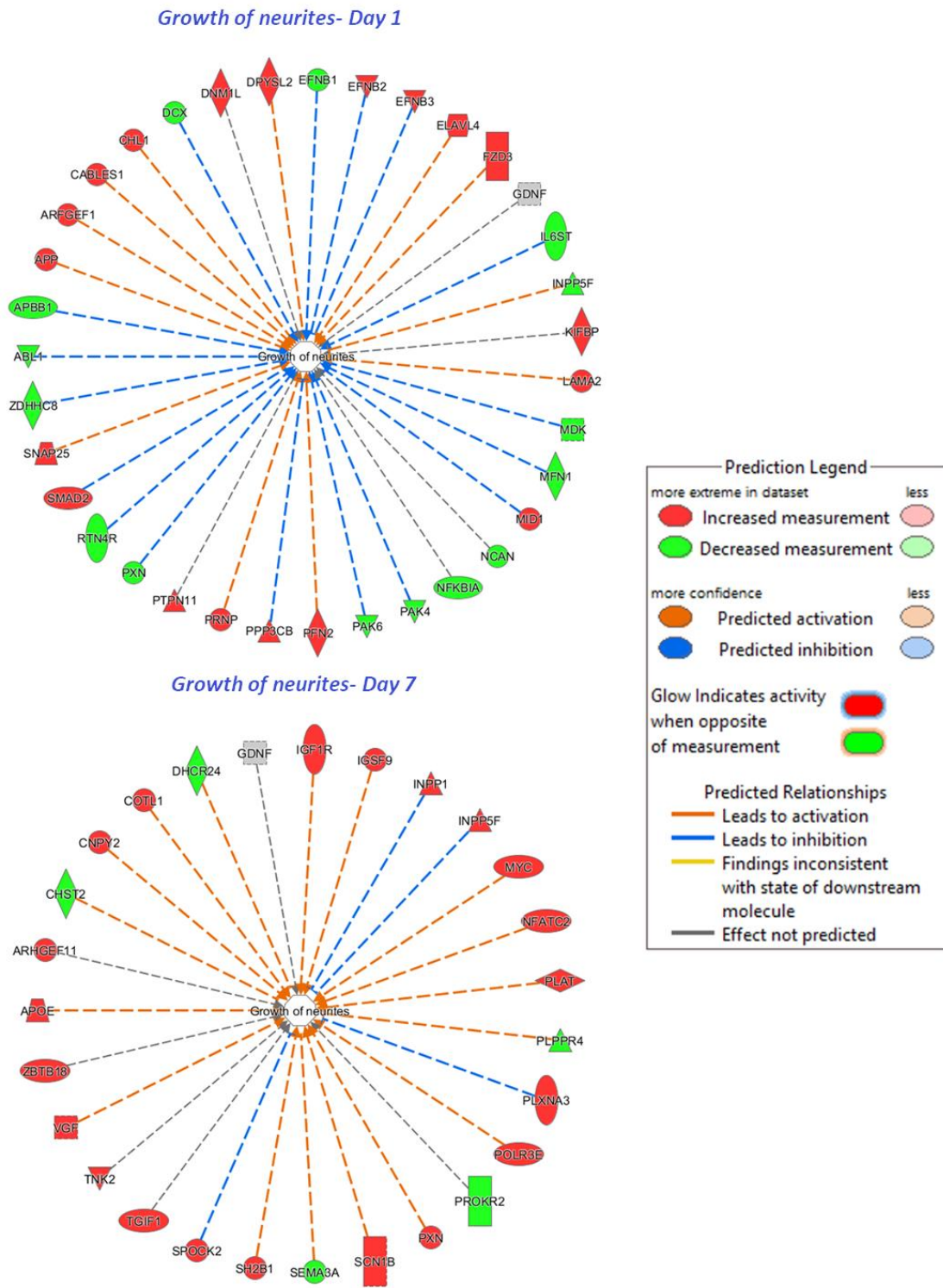


Figure 3. Comparative activation of growth of neurites between deregulated transcriptomes at day 1 and day 7 in GDNF-stimulated hiPS-DANs.

Furthermore, as described in this thesis, GDNF effects on the plasticity and survival of cell grafts could be derived from the modulation exerted by this neurotrophic factor on

GENERAL DISCUSSION

the hiPS-DAnS via the MAPK pathway. Interestingly, the positive effects were not limited to this, because hGDNF also contributed to the significant upregulation of TH expression on hiPS-DAnS cultures (86). Importantly, we have confirmed the ability of hGDNF to promote the survival and plasticity of DA neurons, as well as to induce DA biosynthesis through the regulation of TH, WNT3, EN1 and FGF20 genes involved in DA metabolism. Therefore, our findings agree with previous studies, where hGDNF promoted the functional integration of DAn grafts and enhanced the DA system function (78,87).

In the second part of **chapter 2**, the ability of hGDNF to modulate gene expression in hMSCs was also analyzed by RNA-seq. The transcriptomic data showed relevant changes in the gene expression profile of GDNF-treated hMSCs although the transcriptomic modulation was much less pronounced than in the case of hiPS-DAnS. The hGDNF up-regulated genes were related with gene ontology biological processes such as cell–matrix adhesion, positive regulation of MAPK cascade, ERK1 and ERK2 cascade and positive regulation of secretion by cells, among others. Interestingly, the up-regulation of ADM and GPR68 offer evidence in favor of the hGDNF role to stimulate neuronal remodeling process and neuroprotective functions (88,89).

As stated before, GDNF effects on MSCs survival could be also modulated via the MAPK pathway. Specifically, the upregulation of several specific MAPK-associated genes involved in cell survival (Erp29, EGR1 and TGF- β) was identified in our study (90,91). According to the scientific literature, hGDNF bind to GFR α 1 and mediate the activation of RET or the neural cell adhesion molecule (NCAM) (92–94). In our experiment, hMSCs expressed GFR1 and NCAM, but we did not detect RET expression. Therefore, the hGDNF treatment can lead to MAPK pathway activation via GFR α 1/NCAM signaling, independently of the presence of RET in hMSCs (94–96) (Figure 4). Collectively, these observations support the potential of hGDNF to enhance hMSC survival and differentiation via the MAPK pathway.

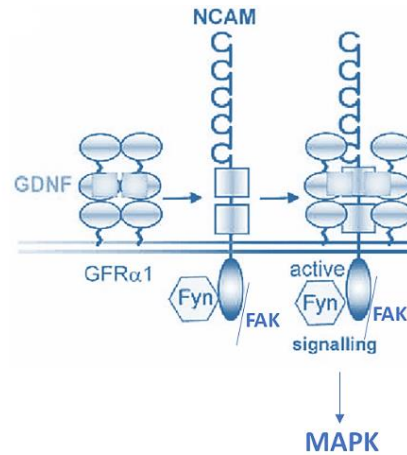


Figure 4. Non-RET signaling for hGDNF. GDNF/GFR alpha-1 stimulates NCAM leading to the activation MAPK signaling cascade. Adapted from Sariola *et al.*,2003 (94).

Therefore, the beneficial changes observed in the transcriptomic profile of hiPS-DANs and hMSCs treated with hGDNF support their combination within our nanoreinforced HG. Finally, a novel approach to enhance the survival and integration of stem cell transplants in PD will be discussed in more detail in the following section.

IV. DRUG DELIVERY SYSTEMS FOR CELL AND NEUROTROPHIC BASED THERAPIES

Nanoparticle-hydrogel system for hGDNF and hMSCs delivery

Cell replacement strategies for PD are mainly limited by the low cell survival of transplanted cells and the lack of a desired regenerative action on neuronal circuits. A promising alternative to improve this scenario is based on the development of biomaterials capable of combining growth/differentiation factors and stem cells in a unique multifunctional system. This approach is aimed to form a matrix that enhances stem cell engraftment as well as the effective delivery of neuroprotective factors that exert a neuroprotective effect in PD. Currently, the unique mechanical properties of HG-based systems postulate them as ideal candidates to develop suitable vehicles for brain tissue engineering. However, there are some essential requirements that HGs must meet for brain regeneration, which are summarized in Figure 5 (97).

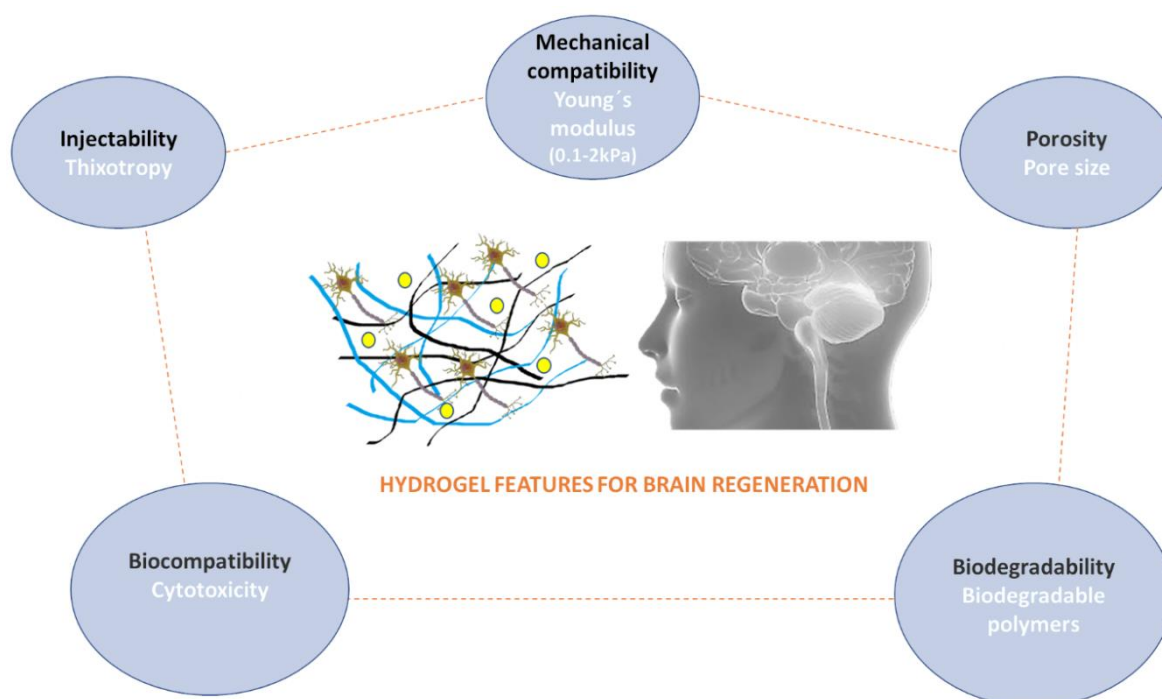


Figure 5. Schematic overview depicting the desired features of HGs systems for brain regeneration.

At present only a dozen HGs have been investigated in the context of PD to promote neuronal differentiation *in vitro* and to use in the delivery of drugs and stem cells into the brain (Table 1). Since HGs can provide spatial and temporal release of therapeutic agents, they have been proposed for dopamine administration (98). When this neurotransmitter was included in a dextran/gelatin HG, it was released for 2 weeks in hemiparkinsonian

rats achieving significant behavioral improvements (98). Furthermore, methacrylamide modified gelatin HGs has also been used for dopamine administration, demonstrating an enhancement of the neural differentiation *in vitro* (99). Among the limited examples of approaches in the HG field, thermosensitive injectable HGs and synthetic materials such as PuraMatrix have also been proposed to deliver drugs into the brain. A thermosensitive injectable HG based on the combination of poly (amidoamine) (PAA) and Poly(N-isopropyl acrylamide) NIPAM polymers was effective in achieving striatal activin B release in a mouse PD model and in inducing long-term dopaminergic fibre protection in the striatum (100). In another study, dopaminergic axon guidance has been stimulated by semaphorin 3C released from PuraMatrix-HGs (101).

In addition, going one step further, HGs have not only been investigated for the encapsulation of different drugs but also the delivery of NTFs alone or in combination with stem cells (Table 1).

GENERAL DISCUSSION

Table 1. Investigated HGs designed to promote neuronal differentiation and for the delivery of drugs and stem cells for PD therapy.

Hydrogel Material	Encapsulated drug	Encapsulated cell	Study of mechanical properties	Results	Ref
Dextran/gelatin	Dopamine	---	---	-Dopamine release for 2 weeks. -Significant behavioural improvement in hemiparkinsonism rats.	98
Gelatin methacrylate	Dopamine	---	---	-Highly porous environment that supports neural stem cells grown <i>in vitro</i> . -Enhancement of neuron gene expression of TUJ1 and MAP2.	99
PNIPAM-PAA	Activin B	---	-Frequency-dependent viscoelastic behavior. -Shear-thinning behavior.	-Sustained release of activin B in the brain. -Induction of long-term protection of striatal dopaminergic fibres in a mouse model of PD.	100
PuraMatrix	Semaphorin 3C	---	---	<i>In vitro</i> stimulation of dopaminergic axon guidance.	101
Collagen	GDNF	DAns	---	-Enhancement of DAns graft survival. -Striatal re-innervation in a rat model of PD.	103,104
Poly(l-lactic acid)/xyloglucan	GDNF	DAns	-Determination of composition at which the elastic modulus matched the modulus of the rodent brain (1.0–3.0 kPa).	-Graft improvement of transplanted DAns in a mouse model of PD.	105
Laminin	GDNF	DAns	---	-Sustained release of GDNF and enhancement of graft plasticity. -Significant improvements in motor deficits at 6 months in a mice model of PD.	106
HA-Laminin	---	---	-Solid-like behavior. - $G' \gg G''$	Neurite extension in injured brains of rats.	111

Abbreviations: PNIPAM-PAA, Poly(N-isopropylacrylamide)-poly(amidoamine); GDNF, glial cell line-derived neurotrophic factor; DAns, Dopaminergic neurons; PD, Parkinson's disease; HA, Hyaluronic acid.

Specifically, hGDNF has been successfully loaded in collagen (102–104) or composites of poly(l-lactic acid)/xyloglucan scaffolds (105). The intra-striatal administration of a GDNF-enriched collagen HG demonstrated a significant enhancement of DAns graft survival and the striatal re-innervation in a rat model of PD (103,104). Interestingly, the functionalization of poly(l-lactic acid)/xyloglucan HG with hGDNF was also a useful approach to improve the engraftment of transplanted DAns in a mouse PD model

(105). More recently, a new laminin matrix functionalized with hGDNF has been found to enhance the human neural grafts into the brain of parkinsonian mice (106). Encouragingly, these studies showed that HG-based approaches offer a promising matrix, which provides a friendly environment and suitable protection to deliver drugs and to increase cell graft survival after transplantation. However, after careful evaluation of the above studies, we find few details regarding the mechanical properties of the investigated HGs. This point is essential to evaluate whether the biomaterials comply with the main requirements for brain applications. Therefore, a special emphasis was paid in this thesis to the mechanical characterization of the developed biomaterial (Chapter 2). Thus, the mechanical properties of the prepared scaffold will be discussed in detail in the following paragraphs.

In this thesis, we proposed an easy and reproducible process to manufacture a nanoreinforced-HG as an ideal matrix to protect stem cells from the different stresses that they can suffer during transplantation. In addition, HG was supplemented with hGDNF-loaded NPs to facilitate graft integration and functional recovery. The HG was fabricated with HA due to its biodegradable nature. Interestingly, HA has been extensively studied in terms of neuroregeneration (97,107,108) and its derived HGs are porous and with low immunogenicity. This natural compound was functionalized with CD and AD to improve its mechanical properties and to establish a guest-host interaction that would allow the HG assembly and reassembly after its injection (109). Generally, HGs can be prepared from interactions of different nature. In this regard, a general disadvantage of covalent cross-linking HGs is the non-reversible character of their interactions. On the other hand, structures derived from non-covalent interactions (physical interactions, including hydrogen bonds, electrostatic and hydrophobic attraction) presents injectability issues as a consequence of the prolonged time required to recover their structures after administration (109,110). In contrast, the guest-host HG that we propose offers precise control over the assembly, shear-thinning and reassembly processes (109). Going one step further, hGDNF-loaded biodegradable polymeric particles were incorporated with a two-fold aim: 1) to mechanically reinforce the HG and 2) to ensure the protection and sustained release of hGDNF. According to the requirements depicted in Figure 5, our nanoreinforced HG showed a thixotropy behaviour. In previous studies, Li *et al* (100) developed an activin B-loaded HG using PNIPAM and PAA polymers. They obtained a novel HG with self-healing properties but with lower storage moduli (G') (100) than that

GENERAL DISCUSSION

reported in our study ($< 10^3\text{Pa}$ vs $> 10^3\text{Pa}$). Another approach that has been investigated is the use of an HA-HG modified with laminin (111). This HG exhibited a solid-like behavior, but a lower mechanical stiffness than that obtained in our study. Importantly, the biomaterial environment and mechanical properties have great relevance for the clinical success of cell therapies. Therefore, the mechanical properties of the material should be similar to those of brain tissue. In this sense, the brain is a soft tissue, with Young's modulus between 1-14 kPa in humans (112,113). Additionally, it has been reported that low stiffness scaffolds (0.1-2kPa) promote stem cell differentiation into neurons (114–116). In **chapter 2**, we hypothesized that NPs incorporation could improve the mechanical properties of the system. In our case, the HG modifications and the NPs inclusion were effective to obtain a mechanical reinforcement. The Young's modulus of our biomaterial was 1.39 ± 0.08 kPa. This is the first report where a nanoreinforcement approach has been successfully used to improve the mechanical stiffness of HA-HGs for brain administration. In consonance with previous studies, the Young's modulus value is compatible with neuronal differentiation and brain tissue (114–116). Interestingly, the mechanical improvement of our scaffold was accompanied by an excellent injectability through small diameter needles (27G). The values were below 7 N, being 20N the limit force for clinical injections (117). Notably, SEM images showed a porous structure scaffold and an adequate mesh pore size to favor hMSCs survival (118–120). On the other hand, the developed system showed an excellent ability to slow down hGDNF release compared to NPs alone, and additionally, it was able to maintain the activity of the therapeutic protein. Furthermore, these modifications did not compromise the HG compatibility with hMSCs and PC12 cells, suggesting an adequate safety profile for *in vivo* administration. Therefore, this multifunctional scaffold fulfilled each of the requirements depicted in Figure 5.

Reported studies considering HGs enriched with stem cells have proven their interest in many different tissue engineering applications, including neural tissues, blood vessels, cardiac tissue, liver and cartilage (121,122). Nevertheless, the field is in its infancy and the work included in this thesis has some challenges and limitations that need to be addressed. For instance, many aspects related to the industrial production of these advanced biomaterials should be considered. For example, the addition of drugs or cells to the HGs required a large and careful homogenization process that can be complex and time-consuming (123). However, it represents a key parameter for maintaining the

viability and function of encapsulated therapeutic agents (123). Therefore, new systems able to combine bioactive molecules and HGs while maintaining their activity will be crucial for the clinical future of HG-based therapies.

Besides this, further studies are necessary to assess the brain compatibility and the *in vivo* efficacy of the system. Furthermore, this thesis has addressed the compatibility of the developed system with hMSCs cells. Additionally, it would be interesting to test its combination with hiPS-DANs. Meanwhile, a recent study has reported a similar strategy with an HG-based therapy where hiPS-DANs and hGDNF have been combined to be administered in PD mice. The sustained administration of hGDNF improved the graft plasticity and promoted significant improvements in motor deficits at 6 months (106). Therefore, this study supports the potential of combining hGDNF and hiPS-DANs grafts in a single HG for PD therapy. Moreover, having seen the therapeutic potential of combining hGDNF with hiPS-DANs and hMSCs, and observed that these cells act through different mechanisms, we might consider that combining both stem cells into a single therapy could improve the efficacy of cell replacement therapies for PD.

Interestingly, 3D printing technologies in combination with stem cells and drugs can provide an attractive solution to develop complex tissue-engineered *in vitro* 3D models for preclinical drug screening (123,124). In line with this, HGs have been proposed as a natural choice of bioink materials for cellular 3D bioprinting (123). Furthermore, HGs can provide a highly hydrated and permeable 3D polymeric structure that promote cellular anchorage and metabolic activities (125). Preliminary results with our nanoreinforced HG have shown that our biomaterial presents good printability and a stable post-printed

GENERAL DISCUSSION

morphology (Figure 6). Hence, further studies should explore in-depth its real potential as bioink.

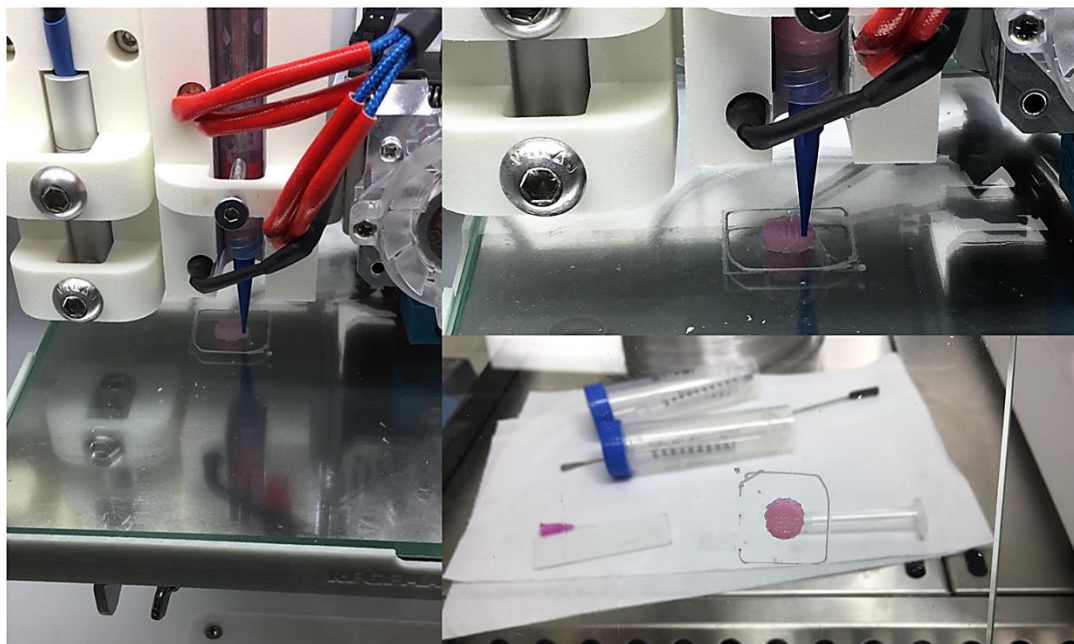


Figure 6. 3D bioprinting of nanoreinforced HG with Regemat 3D.

In summary, the excellent features of the biomaterial developed in this work, together with the demonstrated potential of hGDNF to promote the survival and integration of hMSCs or hiPS-DANs, provide a powerful therapy with unique properties to treat PD. Finally, it is worth mentioning that there are no ongoing clinical trials combining cell therapies (clinical trial identifiers: NCT02452723, NCT03119636, NCT02184546, NCT03684122, NCT03550183, NCT04064983, NCT04506073) with hGDNF treatment (NCT04167540, NCT01621581). However, we envision that a combination of biomaterials and NTFs, together with cells, might lead to a breakthrough in the development of an effective therapy capable of alleviating neuronal degeneration and halting disease progression.

References

1. Goldman JG, Goetz CG. History of Parkinson's disease. *Handb Clin Neurol.* 2007 Jan 1;83:107–28.
2. Parkinson J. An essay on the shaking palsy. 1817. *J Neuropsychiatry Clin Neurosci.* 2002 Mar;14(2).
3. Del Rey NLG, Quiroga-Varela A, Garbayo E, Carballo-Carbajal I, Fernández-

- Santiago R, Monje MHG, et al. Advances in parkinson's disease: 200 years later. *Front Neuroanat.* 2018 Dec 14;12:113.
4. Charvin D, Medori R, Hauser RA, Rascol O. Therapeutic strategies for Parkinson disease: beyond dopaminergic drugs. *Nat Rev Drug Discov* 2018 1711. 2018 Sep 28;17(11):804–22.
 5. Morris AD. James Parkinson His Life and Times. James Parkinson His Life and Times. Birkhäuser Boston; 1989.
 6. Dorsey ER, Sherer T, Okun MS, Bloem BR. The emerging evidence of the Parkinson pandemic. *J Parkinsons Dis.* 2018;8(s1):S3–8.
 7. Georgievska B, Kirik D, Björklund A. Overexpression of glial cell line-derived neurotrophic factor using a lentiviral vector induces time- and dose-dependent downregulation of tyrosine hydroxylase in the intact nigrostriatal dopamine system. *J Neurosci.* 2004 Jul 21;24(29):6437–45.
 8. Ray Dorsey E, Elbaz A, Nichols E, Abd-Allah F, Abdelalim A, Adsuar JC, et al. Global, regional, and national burden of Parkinson's disease, 1990–2016: a systematic analysis for the Global Burden of Disease Study 2016. *Lancet Neurol.* 2018;17(11):939–53.
 9. Barker R, Farrell. Stem cells and regenerative therapies for Parkinson's disease. *Degener Neurol Neuromuscul Dis.* 2012 Jul;2:79.
 10. Sidorova YA, Saarma M. Can Growth Factors Cure Parkinson's Disease? *Trends Pharmacol Sci.* 2020 Dec 1;41(12):909–22.
 11. Chmielarz P, Saarma M. Neurotrophic factors for disease-modifying treatments of Parkinson's disease: gaps between basic science and clinical studies. *Pharmacol Reports.* 2020 Oct 1;72(5):1195–217.
 12. Nasrolahi A, Mahmoudi J, Akbarzadeh A, Karimipour M, Sadigh-Eteghad S, Salehi R, et al. Neurotrophic factors hold promise for the future of Parkinson's disease treatment: Is there a light at the end of the tunnel? *Rev Neurosci.* 2018 Jul 26;29(5):475–89.

GENERAL DISCUSSION

13. Bondarenko O, Saarma M. Neurotrophic Factors in Parkinson's Disease: Clinical Trials, Open Challenges and Nanoparticle-Mediated Delivery to the Brain. *Front Cell Neurosci.* 2021 Jun 2;15:178.
14. Schlee S, Carmillo P, Whitty A. Quantitative analysis of the activation mechanism of the multicomponent growth-factor receptor Ret. *Nat Chem Biol.* 2006 Oct 1;2(11):636–44.
15. Sommerfeld MT, Schweigreiter R, Barde YA, Hoppe E. Down-regulation of the neurotrophin receptor TrkB following ligand binding. Evidence for an involvement of the proteasome and differential regulation of TrkA and TrkB. *J Biol Chem.* 2000 Mar 24;275(12):8982–90.
16. Georgievska B, Kirik D, Björklund A. Aberrant sprouting and downregulation of tyrosine hydroxylase in lesioned nigrostriatal dopamine neurons induced by long-lasting overexpression of glial cell line derived neurotrophic factor in the striatum by lentiviral gene transfer. *Exp Neurol.* 2002 Oct 1;177(2):461–74.
17. Barker RA, Björklund A, Gash DM, Whone A, Van Laar A, Kordower JH, et al. GDNF and Parkinson's Disease: Where Next? A Summary from a Recent Workshop. *J Parkinsons Dis.* 2020;10(3):875–91.
18. Quintino L, Avallone M, Brännstrom E, Kavanagh P, Lockowandt M, Garcia Jareño P, et al. GDNF-mediated rescue of the nigrostriatal system depends on the degree of degeneration. *Gene Ther.* 2019 Feb 1;26(1–2):57–64.
19. Torres-Ortega PV, Smerdou C, Ansorena E, Ballesteros-Briones MC, Martisova E, Garbayo E, et al. Optimization of a GDNF production method based on Semliki Forest virus vector. *Eur J Pharm Sci.* 2021 Apr 1;159:105726.
20. Verma R, Boleti E, George AJ. Antibody engineering: Comparison of bacterial, yeast, insect and mammalian expression systems. *J Immunol Methods.* 1998 Jul;216(1–2):165–81.
21. Jefferis R. Glycosylation of Recombinant Antibody Therapeutics. *Biotechnol Prog.* 2008 Sep 5;21(1):11–6.

22. Grondin R, Littrell OM, Zhang Z, Ai Y, Huettl P, Pomerleau F, et al. GDNF revisited: A novel mammalian cell-derived variant form of GDNF increases dopamine turnover and improves brain biodistribution. *Neuropharmacology*. 2019 Mar 15;147:28–36.
23. Piccinini E, Kalkkinen N, Saarma M, Runeberg-Roos P. Glial cell line-derived neurotrophic factor: Characterization of mammalian posttranslational modifications. *Ann Med*. 2013 Feb;45(1):66–73.
24. Saarenpää T, Kogan K, Sidorova Y, Mahato AK, Tascón I, Kaljunen H, et al. Zebrafish GDNF and its co-receptor GFR α 1 activate the human RET receptor and promote the survival of dopaminergic neurons in vitro. *PLoS One*. 2017 May 1;12(5):e0176166.
25. Gill SS, Patel NK, Hotton GR, O’Sullivan K, McCarter R, Bunnage M, et al. Direct brain infusion of glial cell line-derived neurotrophic factor in Parkinson disease. *Nat Med*. 2003 May 31;9(5):589–95.
26. Nutt JG, Burchiel KJ, Comella CL, Jankovic J, Lang AE, Laws ER, et al. Randomized, double-blind trial of glial cell line-derived neurotrophic factor (GDNF) in PD. *Neurology*. 2003 Jan;60(1):69–73.
27. Dumont J, Euwart D, Mei B, Estes S, Kshirsagar R. Human cell lines for biopharmaceutical manufacturing: history, status, and future perspectives. *Crit Rev Biotechnol*. 2016 Nov 1;36(6):1110–22.
28. Swiech K, Picanço-Castro V, Covas DT. Production of recombinant coagulation factors: Are humans the best host cells? *Bioengineered*. 2017;8(5):462–70.
29. Mirzaahmadi S, Asaadi-Tehrani G, Bandehpour M, Davoudi N, Tahmasbi L, Hosseinzadeh N, et al. Expression of Recombinant Human Coagulation Factor VII by the Lizard *Leishmania* Expression System. *J Biomed Biotechnol*. 2011;2011:1–8.
30. Butler M, Spearman M. The choice of mammalian cell host and possibilities for glycosylation engineering. *Curr Opin Biotechnol*. 2014;30:107–12.

GENERAL DISCUSSION

31. Garbayo E, Montero-Menei CN, Ansorena E, Lanciego JL, Aymerich MS, Blanco-Prieto MJ. Effective GDNF brain delivery using microspheres-A promising strategy for Parkinson's disease. *J Control Release*. 2009 Apr 17;135(2):119–26.
32. Garbayo E, Ansorena E, Lana H, Carmona-Abellan M del M, Marcilla I, Lanciego JL, et al. Brain delivery of microencapsulated GDNF induces functional and structural recovery in parkinsonian monkeys. *Biomaterials*. 2016 Dec 1;110:11–23.
33. Ansorena E, Casales E, Aranda A, Tamayo E, Garbayo E, Smerdou C, et al. A simple and efficient method for the production of human glycosylated glial cell line-derived neurotrophic factor using a Semliki Forest virus expression system. *Int J Pharm*. 2013;440(1):19–26.
34. Lin CY, Huang Z, Wen W, Wu A, Wang C, Niu L. Enhancing protein expression in HEK-293 cells by lowering culture temperature. *PLoS One*. 2015;10(4).
35. Kaisermayer C, Reinhart D, Gili A, Chang M, Aberg PM, Castan A, et al. Biphasic cultivation strategy to avoid Epo-Fc aggregation and optimize protein expression. *J Biotechnol*. 2016 Jun 10;227:3–9.
36. Becerra S, Berrios J, Osses N, Altamirano C. Exploring the effect of mild hypothermia on CHO cell productivity. Vol. 60, *Biochemical Engineering Journal*. Elsevier; 2012. p. 1–8.
37. Pažitná L, Nemčovič M, Pakanová Z, Baráth P, Aliev T, Dolgikh D, et al. Influence of media composition on recombinant monoclonal IgA1 glycosylation analysed by lectin-based protein microarray and MALDI-MS. *J Biotechnol*. 2020 May 20;314–315:34–40.
38. Nam JH, Zhang F, Ermonval M, Linhardt RJ, Sharfstein ST. The effects of culture conditions on the glycosylation of secreted human placental alkaline phosphatase produced in Chinese hamster ovary cells. *Biotechnol Bioeng*. 2008 Aug 15;100(6):1178–92.
39. Ehret J, Zimmermann M, Eichhorn T, Zimmer A. Impact of cell culture media additives on IgG glycosylation produced in Chinese hamster ovary cells.

- Biotechnol Bioeng. 2019 Apr 1;116(4):816–30.
40. Cruz HJ, Peixoto CM, Nimtz M, Alves PM, Dias EM, Moreira JL, et al. Metabolic shifts do not influence the glycosylation patterns of a recombinant fusion protein expressed in BHK cells. *Biotechnol Bioeng.* 2000;69(2):129–39.
 41. Cintrón-Colón AF, Almeida-Alves G, Boynton AM, Spitsbergen JM. GDNF synthesis, signaling, and retrograde transport in motor neurons. *Cell Tissue Res.* 2020 Oct 8;382(1):47–56.
 42. Wang LM, Zhang Q, Zhang Q, Zhu W, He C, Lu CL, et al. Identification of the Key Amino Acids of Glial Cell Line-derived Neurotrophic Factor Family Receptor $\alpha 1$ Involved in Its Biological Function. *J Biol Chem.* 2004 Jan 2;279(1):109–16.
 43. Decressac M, Kadkhodaei B, Mattsson B, Laguna A, Perlmann T, Björklund A. α -synuclein-induced down-regulation of Nurr1 disrupts GDNF signaling in nigral dopamine neurons. *Sci Transl Med.* 2012 Dec 5;4(163).
 44. Su X, Fischer DL, Li X, Bankiewicz K, Sortwell CE, Federoff HJ. Alpha-Synuclein mRNA Is Not Increased in Sporadic PD and Alpha-Synuclein Accumulation Does Not Block GDNF Signaling in Parkinson's Disease and Disease Models. *Mol Ther.* 2017 Oct 4;25(10):2231–5.
 45. Manfredsson FP, Polinski NK, Subramanian T, Boulis N, Wakeman DR, Mandel RJ. The Future of GDNF in Parkinson's Disease. *Front Aging Neurosci.* 2020 Dec 7;12:388.
 46. Fan Y, Winanto, Ng SY. Replacing what's lost: A new era of stem cell therapy for Parkinson's disease. *Transl Neurodegener.* 2020 Jan 7;9(1).
 47. Han F. Stem Cell Therapy for Parkinson's Disease. In: *Challenges in Parkinson's Disease.* InTech; 2016.
 48. Yasuhara T, Kameda M, Sasaki T, Tajiri N, Date I. Cell Therapy for Parkinson's Disease. *Cell Transplant.* 2017 Sep 1;26(9):1551–9.
 49. Harris JP, Burrell JC, Struzyna LA, Chen HI, Serruya MD, Wolf JA, et al. Emerging regenerative medicine and tissue engineering strategies for Parkinson's

GENERAL DISCUSSION

- disease. *npj Park Dis* 2020 61. 2020 Jan 8;6(1):1–14.
50. Li W, Englund E, Widner H, Mattsson B, Van Westen D, Lätt J, et al. Extensive graft-derived dopaminergic innervation is maintained 24 years after transplantation in the degenerating parkinsonian brain. *Proc Natl Acad Sci U S A*. 2016 Jun 7;113(23):6544–9.
 51. Hallett PJ, Cooper O, Sadi D, Robertson H, Mendez I, Isacson O. Long-Term Health of Dopaminergic Neuron Transplants in Parkinson’s Disease Patients. *Cell Rep*. 2014 Jun 26;7(6):1755–61.
 52. Barker RA, Drouin-Ouellet J, Parmar M. Cell-based therapies for Parkinson disease-past insights and future potential. *Nat Rev Neurol*. 2015 Sep 7;11(9):492–503.
 53. Björklund A, Lindvall O. Cell replacement therapies for central nervous system disorders. *Nat Neurosci*. 2000 Jun;3(6):537–44.
 54. Parmar M, Grealish S, Henchcliffe C. The future of stem cell therapies for Parkinson disease. *Nat Rev Neurosci*. 2020 Jan 6;21(2):103–15.
 55. Fričová D, Korchak JA, Zubair AC. Challenges and translational considerations of mesenchymal stem/stromal cell therapy for Parkinson’s disease. *npj Regen Med*. 2020 Dec 1;5(1).
 56. Sivandzade F, Cucullo L. Regenerative stem cell therapy for neurodegenerative diseases: An overview. *Int J Mol Sci*. 2021 Feb 2;22(4):1–21.
 57. Kim TW, Koo SY, Studer L. Pluripotent Stem Cell Therapies for Parkinson Disease: Present Challenges and Future Opportunities. *Front Cell Dev Biol*. 2020 Aug 6;8:729.
 58. Takahashi K, Tanabe K, Ohnuki M, Narita M, Ichisaka T, Tomoda K, et al. Induction of Pluripotent Stem Cells from Adult Human Fibroblasts by Defined Factors. *Cell*. 2007 Nov 30;131(5):861–72.
 59. Cai J, Yang M, Poremsky E, Kidd S, Schneider JS, Iacovitti L. Dopaminergic neurons derived from human induced pluripotent stem cells survive and integrate

- into 6-OHDA-lesioned rats. *Stem Cells Dev.* 2010 Jul 1;19(7):1017–23.
60. Kikuchi T, Morizane A, Doi D, Magotani H, Onoe H, Hayashi T, et al. Human iPSC cell-derived dopaminergic neurons function in a primate Parkinson's disease model. *Nature.* 2017 Aug;548(7669):592–6.
 61. Morizane A, Kikuchi T, Hayashi T, Mizuma H, Takara S, Doi H, et al. MHC matching improves engraftment of iPSC-derived neurons in non-human primates. *Nat Commun.* 2017 Aug 30;8(1):1–12.
 62. Liu Z, Cheung HH. Stem cell-based therapies for parkinson disease. *Int J Mol Sci.* 2020 Nov 1;21(21):1–17.
 63. Neveen A S. Mesenchymal Stem Cell Based Therapy for Parkinson's Disease. *Int J Stem Cell Res Ther.* 2019 Sep 23;6(1).
 64. Chi H, Guan Y, Li F, Chen Z. The Effect of Human Umbilical Cord Mesenchymal Stromal Cells in Protection of Dopaminergic Neurons from Apoptosis by Reducing Oxidative Stress in the Early Stage of a 6-OHDA-Induced Parkinson's Disease Model. *Cell Transplant.* 2019 Nov 28;28(1_suppl):87S–99S.
 65. Reyhani S, Abbaspanah B, Mousavi SH. Umbilical cord-derived mesenchymal stem cells in neurodegenerative disorders: From literature to clinical practice. *Regen Med.* 2020 Jun 1;15(4):1561–78.
 66. C B, E H. Adult stem cell therapies for neurological disorders: benefits beyond neuronal replacement? *J Neurosci Res.* 2009 May 15;87(7):1509–21.
 67. Nagatsu T, Mogi M, Ichinose H, Togari A. Cytokines in Parkinson's disease. *J Neural Transm Suppl.* 2000;(58):143–51.
 68. MG T, MS G. Neuroinflammation in Parkinson's disease: its role in neuronal death and implications for therapeutic intervention. *Neurobiol Dis.* 2010 Mar;37(3):510–8.
 69. Caplan AI. Adult mesenchymal stem cells: When, where, and how. *Stem Cells Int.* 2015;2015.

GENERAL DISCUSSION

70. Boika A, Aleinikava N, Chyzhyk V, Zafranskaya M, Nizheharodava D, Ponomarev V. Mesenchymal stem cells in Parkinson's disease: Motor and nonmotor symptoms in the early posttransplant period. *Surg Neurol Int.* 2020 Nov 11;11.
71. Hellmann MA, Panet H, Barhum Y, Melamed E, Offen D. Increased survival and migration of engrafted mesenchymal bone marrow stem cells in 6-hydroxydopamine-lesioned rodents. *Neurosci Lett.* 2006 Mar 6;395(2):124–8.
72. Guo X, Tang L, Tang X. Current Developments in Cell Replacement Therapy for Parkinson's Disease. *Neuroscience.* 2021 May 21;463:370–82.
73. Muñoz MF, Argüelles S, Guzman-Chozas M, Guillén-Sanz R, Franco JM, Pintor-Toro JA, et al. Cell tracking, survival, and differentiation capacity of adipose-derived stem cells after engraftment in rat tissue. *J Cell Physiol.* 2018 Oct 1;233(10):6317–28.
74. Baldari S, Di Rocco G, Piccoli M, Pozzobon M, Muraca M, Toietta G. Challenges and strategies for improving the regenerative effects of mesenchymal stromal cell-based therapies. *Int J Mol Sci.* 2017 Oct 1;18(10).
75. Lee S, Choi E, Cha MJ, Hwang KC. Cell adhesion and long-term survival of transplanted mesenchymal stem cells: A prerequisite for cell therapy. *Oxid Med Cell Longev.* 2015;2015.
76. Marquardt LM, Heilshorn SC. Design of Injectable Materials to Improve Stem Cell Transplantation. *Curr Stem Cell Reports.* 2016;2(3):207–20.
77. Khazaei M, Ahuja CS, Nakashima H, Nagoshi N, Li L, Wang J, et al. GDNF rescues the fate of neural progenitor grafts by attenuating Notch signals in the injured spinal cord in rodents. *Sci Transl Med.* 2020 Jan 8;12(525).
78. Gantner CW, de Luzy IR, Kauhausen JA, Moriarty N, Niclis JC, Bye CR, et al. Viral Delivery of GDNF Promotes Functional Integration of Human Stem Cell Grafts in Parkinson's Disease. *Cell Stem Cell.* 2020 Apr 2;26(4):511–526.e5.
79. Wang J, Hu WW, Jiang Z, Feng MJ. Advances in treatment of neurodegenerative

- diseases: Perspectives for combination of stem cells with neurotrophic factors. *World J Stem Cells*. 2020 May 26;12(5):323–38.
80. Moloney TC, Rooney GE, Barry FP, Howard L, Dowd E. Potential of rat bone marrow-derived mesenchymal stem cells as vehicles for delivery of neurotrophins to the Parkinsonian rat brain. *Brain Res*. 2010 Nov 4;1359:33–43.
 81. Glavaski-Joksimovic A, Virag T, Mangatu TA, McGrogan M, Wang XS, Bohn MC. Glial cell line-derived neurotrophic factor-secreting genetically modified human bone marrow-derived mesenchymal stem cells promote recovery in a rat model of Parkinson's disease. *J Neurosci Res*. 2010 Sep;88(12):2669–81.
 82. Wu J, Yu W, Chen Y, Su Y, Ding Z, Ren H, et al. Intrastratial transplantation of GDNF-engineered BMSCs and its neuroprotection in lactacystin-induced parkinsonian rat model. *Neurochem Res*. 2010 Mar;35(3):495–502.
 83. Ren Z, Wang J, Wang S, Zou C, Li X, Guan Y, et al. Autologous transplantation of GDNF-expressing mesenchymal stem cells protects against MPTP-induced damage in cynomolgus monkeys. *Sci Rep*. 2013 Sep 27;3(1):1–11.
 84. Hoban DB, Howard L, Dowd E. GDNF-secreting mesenchymal stem cells provide localized neuroprotection in an inflammation-driven rat model of Parkinson's disease. *Neuroscience*. 2015 Sep 1;303:402–11.
 85. Sun S, Zhang Q, Li M, Gao P, Huang K, Beejadhursing R, et al. GDNF Promotes Survival and Therapeutic Efficacy of Human Adipose-Derived Mesenchymal Stem Cells in a Mouse Model of Parkinson's Disease. *Cell Transplant*. 2020 Apr 15;29.
 86. White R, Thomas M. Moving Beyond Tyrosine Hydroxylase to Define Dopaminergic Neurons for Use in Cell Replacement Therapies for Parkinson's Disease. *CNS Neurol Disord - Drug Targets*. 2012 Oct 1;11(4):340–9.
 87. Mätlik K, Võikar V, Vilenius C, Kuleskaya N, Andressoo J-O. Two-fold elevation of endogenous GDNF levels in mice improves motor coordination without causing side-effects. *Sci Rep*. 2018 Dec 8;8(1):11861.

GENERAL DISCUSSION

88. Hobara N, Goda M, Kitamura Y, Sendou T, Gomita Y, Kawasaki H. Adrenomedullin facilitates reinnervation of phenol-injured perivascular nerves in the rat mesenteric resistance artery. *Neuroscience*. 2007 Jan 19;144(2):721–30.
89. Wang T, Zhou G, He M, Xu Y, Rusyniak WG, Xu Y, et al. GPR68 Is a Neuroprotective Proton Receptor in Brain Ischemia. *Stroke*. 2020;51(12):3690–700.
90. Wei Z, Liu HT. MAPK signal pathways in the regulation of cell proliferation in mammalian cells. Vol. 12, *Cell Research*. Nature Publishing Group; 2002. p. 9–18.
91. Zhang Y, Alexander PB, Wang XF. TGF- β family signaling in the control of cell proliferation and survival. *Cold Spring Harb Perspect Biol*. 2017 Apr 1;9(4).
92. Ledda F, Paratcha G, Sandoval-Guzmán T, Ibáñez CF. GDNF and GFR α 1 promote formation of neuronal synapses by ligand-induced cell adhesion. *Nat Neurosci*. 2007 Feb 18;10(3):293–300.
93. Xiao N, Lin Y, Cao H, Sirjani D, Giaccia AJ, Koong AC, et al. Neurotrophic factor GDNF promotes survival of salivary stem cells. *J Clin Invest*. 2014 Aug 1;124(8):3364–77.
94. Sariola H, Saarma M. Novel functions and signalling pathways for GDNF. *J Cell Sci*. 2003 Oct 1;116(19):3855–62.
95. Irala D, Bonafina A, Fontanet PA, Alsina FC, Paratcha G, Ledda F. The GDNF-GFR α 1 complex promotes the development of hippocampal dendritic arbors and spines via NCAM. *Dev*. 2016 Nov 15;143(22):4224–35.
96. Paratcha G, Ledda F. GDNF and GFR α : a versatile molecular complex for developing neurons. *Trends Neurosci*. 2008 Aug 1;31(8):384–91.
97. Kornev VA, Grebenik EA, Solovieva AB, Dmitriev RI, Timashev PS. Hydrogel-assisted neuroregeneration approaches towards brain injury therapy: A state-of-the-art review. *Comput Struct Biotechnol J*. 2018 Jan 1;16:488–502.
98. Senthilkumar KS, Saravanan KS, Chandra G, Sindhu KM, Jayakrishnan A,

- Mohanakumar KP. Unilateral implantation of dopamine-loaded biodegradable hydrogel in the striatum attenuates motor abnormalities in the 6-hydroxydopamine model of hemi-parkinsonism. *Behav Brain Res.* 2007 Nov 22;184(1):11–8.
99. Zhou X, Cui H, Nowicki M, Miao S, Lee SJ, Masood F, et al. Three-Dimensional-Bioprinted Dopamine-Based Matrix for Promoting Neural Regeneration. *ACS Appl Mater Interfaces.* 2018 Mar 14;10(10):8993–9001.
100. Li J, Darabi M, Gu J, Shi J, Xue J, Huang L, et al. A drug delivery hydrogel system based on activin B for Parkinson’s disease. *Biomaterials.* 2016 Sep 1;102:72–86.
101. Carballo-Molina OA, Sánchez-Navarro A, López-Ornelas A, Lara-Rodarte R, Salazar P, Campos-Romo A, et al. Semaphorin 3C Released from a Biocompatible Hydrogel Guides and Promotes Axonal Growth of Rodent and Human Dopaminergic Neurons. *Tissue Eng Part A.* 2016;22(11–12):850–61.
102. Ucar B, Humpel C. Therapeutic efficacy of glial cell-derived neurotrophic factor loaded collagen scaffolds in ex vivo organotypic brain slice Parkinson’s disease models. *Brain Res Bull.* 2019 Jul 1;149:86–95.
103. Moriarty N, Pandit A, Dowd E. Encapsulation of primary dopaminergic neurons in a GDNF-loaded collagen hydrogel increases their survival, re-innervation and function after intra-striatal transplantation. *Sci Rep.* 2017 Nov 22;7(1):16033.
104. Moriarty N, Cabré S, Alamilla V, Pandit A, Dowd E. Encapsulation of young donor age dopaminergic grafts in a GDNF-loaded collagen hydrogel further increases their survival, reinnervation, and functional efficacy after intrastriatal transplantation in hemi-Parkinsonian rats. *Eur J Neurosci.* 2019 Feb;49(4):487–96.
105. Wang TY, Bruggeman KF, Kauhausen JA, Rodriguez AL, Nisbet DR, Parish CL. Functionalized composite scaffolds improve the engraftment of transplanted dopaminergic progenitors in a mouse model of Parkinson’s disease. *Biomaterials.* 2016 Jan;74:89–98.
106. Hunt CPJ, Penna V, Gantner CW, Moriarty N, Wang Y, Franks S, et al. Tissue Programmed Hydrogels Functionalized with GDNF Improve Human Neural Grafts in Parkinson’s Disease. *Adv Funct Mater.* 2021;2105301.

GENERAL DISCUSSION

107. Wei YT, Tian WM, Yu X, Cui FZ, Hou SP, Xu QY, et al. Hyaluronic acid hydrogels with IKVAV peptides for tissue repair and axonal regeneration in an injured rat brain. *Biomed Mater*. 2007 Sep;2(3):S142–6.
108. Ma J, Tian W-M, Hou S-P, Xu Q-Y, Spector M, Cui F-Z. An experimental test of stroke recovery by implanting a hyaluronic acid hydrogel carrying a Nogo receptor antibody in a rat model. *Biomed Mater*. 2007 Dec;2(4):233–40.
109. Loebel C, Rodell CB, Chen MH, Burdick JA. Shear-thinning and self-healing hydrogels as injectable therapeutics and for 3D-printing. *Nat Protoc*. 2017;12(8):1521–41.
110. Steele AN, Stapleton LM, Farry JM, Lucian HJ, Paulsen MJ, Eskandari A, et al. A Biocompatible Therapeutic Catheter-Deliverable Hydrogel for In Situ Tissue Engineering. *Adv Healthc Mater*. 2019 Mar;8(5):1801147.
111. Hou S, Xu Q, Tian W, Cui F, Cai Q, Ma J, et al. The repair of brain lesion by implantation of hyaluronic acid hydrogels modified with laminin. *J Neurosci Methods*. 2005 Oct 15;148(1):60–70.
112. Seidlits SK, Khaing ZZ, Petersen RR, Nickels JD, Vanscoy JE, Shear JB, et al. The effects of hyaluronic acid hydrogels with tunable mechanical properties on neural progenitor cell differentiation. *Biomaterials*. 2010 May 1;31(14):3930–40.
113. Hiscox L V., Johnson CL, Barnhill E, McGarry MDJ, Huston J, Van Beek EJR, et al. Magnetic resonance elastography (MRE) of the human brain: Technique, findings and clinical applications. *Phys Med Biol*. 2016 Nov 15;61(24):R401–37.
114. Farrukh A, Zhao S, del Campo A. Microenvironments designed to support growth and function of neuronal cells. *Front Mater*. 2018 Nov 2;5:62.
115. Engler AJ, Sen S, Sweeney HL, Discher DE. Matrix Elasticity Directs Stem Cell Lineage Specification. *Cell*. 2006 Aug 25;126(4):677–89.
116. Ali S, Wall IB, Mason C, Pelling AE, Veraitch FS. The effect of Young's modulus on the neuronal differentiation of mouse embryonic stem cells. *Acta Biomater*. 2015 Oct 1;25:253–67.

117. Chen MH, Wang LL, Chung JJ, Kim YH, Atluri P, Burdick JA. Methods to Assess Shear-Thinning Hydrogels for Application As Injectable Biomaterials. *ACS Biomater Sci Eng.* 2017;3(12):3146–60.
118. Bružauskaitė I, Bironaitė D, Bagdonas E, Bernotienė E. Scaffolds and cells for tissue regeneration: different scaffold pore sizes—different cell effects. *Cytotechnology.* 2016 May 1;68(3):355–69.
119. Mohand-Kaci F, Assoul N, Martelly I, Allaire E, Zidi M. Optimized Hyaluronic Acid–Hydrogel Design and Culture Conditions for Preservation of Mesenchymal Stem Cell Properties. *Tissue Eng Part C Methods.* 2013 Apr;19(4):288–98.
120. El-Sherbiny IM, Yacoub MH. Hydrogel scaffolds for tissue engineering: Progress and challenges. *Glob Cardiol Sci Pract.* 2013 Sep;2013(3):38.
121. Willerth SM, Sakiyama-Elbert SE. Combining Stem Cells and Biomaterial Scaffolds for Constructing Tissues and Cell Delivery. *StemJournal.* 2019 Jan 1;1(1):1–25.
122. Tsou YH, Khoneisser J, Huang PC, Xu X. Hydrogel as a bioactive material to regulate stem cell fate. *Bioact Mater.* 2016 Sep 1;1(1):39–55.
123. Catoira MC, González-Payo J, Fusaro L, Ramella M, Boccafoschi F. Natural hydrogels R&D process: technical and regulatory aspects for industrial implementation. *J Mater Sci Mater Med.* 2020 Aug 1;31(8).
124. Nie J, Gao Q, Fu J, He Y. Grafting of 3D Bioprinting to In Vitro Drug Screening: A Review. *Adv Healthc Mater.* 2020 Apr 1;9(7).
125. Bian L. Functional hydrogel bioink, a key challenge of 3D cellular bioprinting. *APL Bioeng.* 2020 Sep 1;4(3):30401.

CONCLUSIONS

The main objective of this thesis was to design and develop an advanced multifunctional drug delivery system that combines glial cell line-derived neurotrophic factor and stem cells in a nanoparticle-modified hydrogel for application in Parkinson's Disease. Based on all the studies performed, the following can be concluded:

1. The glial cell line-derived neurotrophic factor was successfully expressed and purified using a production method based on Semliki Forest virus vector. The previously published expression method was modified using a biphasic protocol that increases cell culture temperature during the shut-off period. Under the optimized conditions, the production of a highly pure glycosylated glial cell line-derived neurotrophic factor was almost 3-fold more efficient compared to the previously published method. Moreover, a PC-12 neurite outgrowth bioassay demonstrated the proper folding and bioactivity of the purified protein.
2. Beneficial changes were observed in the transcriptomic profile of dopaminergic neurons derived from human induced pluripotent stem cells and human mesenchymal stem cells treated with the glial cell line-derived neurotrophic factor. Transcriptional changes related to cell survival, plasticity and dopamine biosynthesis were found in dopaminergic neurons derived from human induced pluripotent stem cells. Additionally, the upregulation of genes involved in plasticity, neurogenesis, the neuronal remodelling process and neuroprotective functions were found in human mesenchymal stem cells treated with the neurotrophic factor. All these findings support the combination of glial cell line-derived neurotrophic factor and these stem cells within our nanoreinforced HG.
3. Poly (lactic-co-glycolic acid) nanoparticles were successfully prepared using TROMS® technology, obtaining a homogeneous population with a mean size of 208 ± 26 nm and a negative Z potential. The neurotrophic factor was successfully encapsulated into poly (lactic-co-glycolic acid) nanoparticles obtaining high encapsulation efficiencies. The polymeric nanoparticles provided a gradual sustained released of the glial cell line-derived neurotrophic factor for 40 days. Moreover, the neurotrophic factor maintained its bioactivity during the entire encapsulation process.

CONCLUSIONS

4. A multifunctional hydrogel made up of hyaluronic acid modified with β -cyclodextrin and adamantane and reinforced with poly (lactic-co-glycolic acid) nanoparticles was successfully designed for potential brain delivery of the glial cell line-derived neurotrophic factor and stem cells. The developed hydrogels showed a Young's modulus which supports their use in brain tissue engineering applications and the neural differentiation of stem cells. Moreover, the synthesized hydrogels showed good injectability. The incorporation of the nanoparticles in the hydrogel enhanced the mechanical properties of the biomaterial compared to conventional hyaluronic acid hydrogels.
5. The incorporation of nanoparticles in the hydrogel allowed a more sustained drug release profile compared to the neurotrophic factor release from nanoparticles not included in the hydrogel. The glial cell line-derived neurotrophic factor remained bioactive after its incorporation into the hydrogel and, therefore, the nanoreinforcement also proved to be a successful approach to protect the neurotrophic factor from degradation.
6. The modifications made in the hyaluronic acid and the incorporation of the nanoparticles did not have a toxic character and the novel hydrogels demonstrated good compatibility with hMSCs and PC12 cells.

ANNEXES

ANNEX 1

Hybrid Nanosystems

Pablo Vicente Torres-Ortega^{a,b} Laura Saludas,^{a,b} Jon Eneko Idoyaga,^a Carlos Rodríguez-Nogales,^{a,b} Elisa Garbayo^{a,b} and María José Blanco-Prieto^{a,b}

^a Department of Pharmaceutical Technology and Chemistry, Faculty of Pharmacy and Nutrition, Universidad de Navarra, C/Irunlarrea 1, 31008 Pamplona, Spain

^b Instituto de Investigación Sanitaria de Navarra, IdiSNA, C/Irunlarrea 3, 31008 Pamplona, Spain

mjblanco@unav.es, egarbayo@unav.es

DOI: 10.1201/9781003119326-8

Nanoparticles for Brain Drug Delivery. Chapter 6.

Edited by Carla Vitorino, Andreia Jorge and Alberto Pais Copyright © 2021 Jenny Stanford Publishing Pte. Ltd.

ISBN 978-981-4877-31-2 (Hardcover), 978-1-003-11932-6 (eBook)

www.jennystanford.com

Abstract

Treatments aiming to stop the progression of brain-related disorders are often nonspecific and focused on the resolution of short-term symptoms. Moreover, the delivery of therapeutics across the blood-brain barrier represents another limiting challenge in the treatment of these diseases. Hybrid nanosystems (HNs), defined as the combination of inorganic and organic compounds in a single nanocarrier, offer a new generation of multifunctional nanoparticles with superior biological and structural properties. HNs could contribute not only to the design of more effective therapies for brain disorders but also to the development of new theragnostic strategies that combine therapeutic and diagnostic functions in a single system.

This chapter aims to give an overview of the enormous possibilities offered by HNs providing better diagnostic imaging agents, biosensors to detect specific biomarkers and enhanced targeted therapies for brain disorders. The focus lies on HNs made of an organic component in which an inorganic compound is loaded, and on formulations constituted by an inorganic core functionalized with an organic element. The main limitations, future perspectives and the necessity to evaluate its potential on more relevant *in vivo* models are also discussed. Specifically, HNs based on inorganic nanomaterials loaded within organic matrices are playing an important role in brain cancers. Metals as imaging agents and cytotoxic drugs have been predominantly combined for simultaneous imaging and treatment of glioma. Furthermore, an enhanced NP tumor accumulation can be obtained by the application of an external magnetic field directed to the tumor site due to the inherent magnetic properties of these systems. HNs constituted by an inorganic core coated with functional molecules have also allowed the development of promising diagnostic and theragnostic tools for the application in brain tumors. On the other hand, HNs could contribute to stop the progression of diseases such as Parkinson's or Alzheimer's diseases, as well as provide new techniques that would make possible an earlier diagnosis of these neurodegenerative pathologies.

Finally, HNs are currently being investigated for the visualization and treatment of ischemic areas of the brain with the aim of achieving an effective reduction of the brain infarcted regions. The evidence found in a large number of studies confirm that HNs are one of the most promising approaches in the quest for new diagnostic and therapeutic alternatives in brain-related disorders.

